

Miniaturised nucleic acid analysis systems: purification, amplification and real-time detection

Zur Erlangung des akademischen Grades eines

Dr.rer.nat

vom Fachbereich Bio- und Chemieingenieurwesen der Universität

Dortmund

genehmigte Dissertation

vorgelegt von

M.-Eng. Lin Chen

aus

Shanghai, P. R. China

Tag der mündlichen Prüfung: 21.09.2007

1. Gutachter: Prof. Dr. Andreas Schmid

2. Gutachter: Prof. Dr. Holger Zorn

3. Gutachter: Prof. Dr. Philip J. R. Day

Dortmund 2007

Content

Content	1
Abstract	5
Kurzfassung	7
Chapter 1 Introduction: Systems for Miniaturised Nucleic Acid Analysis	9
1.1 Miniaturised Total Analysis System (μ -TAS)	9
1.1.1 History and Development	10
1.1.2 Microfabrication Techniques.....	12
1.1.2.1 Silicon and Glass	12
1.1.2.1.1 Mask Fabrication	13
1.1.2.1.2 Patterning and Channel Etching.....	14
1.1.2.1.3 Microchip Bonding	14
1.1.2.2 Polymer	15
1.1.2.2.1 PDMS microchips (Casting).....	15
1.1.2.2.2 PMMA microchips (Injecting Moulding).....	16
1.1.2.2.3 Direct Microfabrication of Polymer Microchips	17
1.2 Integration of Components in μ -TAS	17
1.2.1 Sample Pre-treatment	17
1.2.1.1 Sample Separation and Purification from Sample Matrix.....	17
1.2.1.2 Sample Pre-concentration	18
1.2.1.3 Sample Derivation	18
1.2.2 Sample Manipulation	18
1.2.2.1 Hydrodynamic Flow for Sample Manipulation	18
1.2.2.2 Electrodynamic Flow for Sample Manipulation.....	19
1.2.3 Reaction	20
1.2.4 Separation	20
1.2.4.1 Electrophoresis.....	20
1.2.4.2 Chromatography.....	21
1.2.4.3 Other Separation Methods.....	22

1.2.5	Detection.....	22
1.2.5.1	Fluorescence Detection.....	23
1.2.5.2	Electrochemical Detection.....	24
1.2.5.3	Chemiluminescence & Electrochemiluminescence Detection ..	24
1.2.5.4	Mass Spectrometry.....	25
1.2.5.5	Other Detection Methods.....	25
1.3	Miniaturised Nucleic Acid Analysis	25
1.3.1	Miniaturised Isotachopheresis (ITP) for Nucleic Acid Purification ..	27
1.3.1	Miniaturised Isotachopheresis (ITP) for Nucleic Acid Purification ..	28
1.3.2	Miniaturised Whole Genome Amplification	29
1.3.2.1	Whole Genome Amplification.....	29
1.3.2.2	WGA on Miniaturised Systems	32
1.3.3	Bidirectional Shunting PCR with Real-time Detection.....	33
1.3.3.1	Polymerase Chain Reaction (PCR).....	33
1.3.3.1.1	Principle	33
1.3.3.1.2	Components for PCR	37
1.3.3.1.3	Real-time PCR.....	39
1.3.3.2	Miniaturised PCR.....	44
1.4	Research Aims.....	47
Chapter 2 Experimental Section.....		51
2.1	Miniaturised ITP for Nucleic Acid Purification	51
2.1.1	ITP Microchip Fabrication.....	51
2.1.2	Instrumentation.....	51
2.1.3	Separation Conditions.....	54
2.1.4	Reagents and Materials.....	54
2.1.5	Yeast Cell Lysis.....	55
2.2	Miniaturised WGA	56
2.2.1	Microchip Fabrication	56
2.2.2	Reagents and Materials.....	56
2.2.3	Microchip Silanisation.....	57

2.2.4	WGA on Microchips	57
2.2.5	WGA Product Analysis	58
2.2.6	Real-time Quantitative PCR	58
2.2.7	Single-Nucleotide Polymorphisms (SNPs) Analysis	58
2.3	Bidirectional Shunting PCR with Real-time Detection.....	59
2.3.1	Device Assembly and Operation	59
2.3.2	Silanisation	60
2.3.3	Silanisation Effect Testing.....	60
2.3.4	Microchip Gel Electrophoresis.....	61
2.3.5	Real-time Detection of Bidirectional Shunting PCR.....	61
Chapter 3	Results and Discussion	63
3.1	Miniaturised ITP for Nucleic Acid Purification.....	63
3.1.1	Electrolyte System.....	63
3.1.2	Miniaturised ITP for DNA samples.....	64
3.1.3	Miniaturised ITP for RNA sample.....	68
3.1.4	Miniaturised ITP for a mixture of DNA and protein.....	70
3.1.5	Miniaturised ITP for cell lysates.....	71
3.1.6	Conclusions and outlooks.....	73
3.2	Miniaturised WGA	74
3.2.1	Denaturation	74
3.2.2	DNA amplification product sizing	75
3.2.3	Silanisation effect	76
3.2.4	Real-time monitoring of on-chip MDA.....	77
3.2.5	Quantitative real-time PCR	78
3.2.6	Single-nucleotide polymorphism genotyping.....	79
3.2.7	Specificity of WGA synthesis	80
3.2.7	Conclusions and outlooks.....	81
3.3	Bidirectional shunting PCR with real-time detection	83
3.3.1	Temperature calibration.....	83
3.3.2	Bidirectional Thermocycling	85

3.3.3	Silanisation surface modification.....	88
3.3.4	Real-time PCR of human genomic DNA	90
3.3.5	Conclusions and outlooks	94
Chapter 4	Conclusions.....	96
References		99
Acknowledgments		111
Curriculum Vitae		112

Abstract

The design and implementation of miniaturised systems for analysis of nucleic acids from various biological samples has undergone extensive development. Several advances have been made particularly with the integration of nucleic acid amplification and detection, where amplification is most often polymerase chain reaction (PCR). Sample preparation remains a major obstacle for achieving a quantitative analysis employing full miniaturised integration. Miniaturised devices for nucleic acid sample preparation, amplification and detection have to be further developed in order to achieve a fully integrated system, which ultimately can perform single cells genomic analysis with sample-in-answer-out ability.

In this thesis, three miniaturised systems have been presented, which can be used for purification and preconcentration of DNA, pre-amplification and long-term storage of DNA, and amplification with real-time detection of DNA, respectively. The first miniaturised system applies isotachopheresis for pretreatment of DNA, where the DNA sample can be purified and concentrated using a discontinuous electrolyte system. Both qualitative and quantitative information can be acquired simultaneously. The second miniaturised system employs simple isothermal multiple displacement amplification, (MDA) for whole genome amplification (WGA) of human genomic DNA. The miniaturised WGA process showed a high efficiency of 95.8%, and the fidelity of the amplified products is extremely high as suggested by single-nucleotide polymorphisms analysis. For the last system, we developed a bidirectional shunting PCR microdevice equipped with real-time fluorescence detection, which allows higher flexibility and fast thermocycling by combining both advantages of stationary PCR and continuous-flow PCR. Real-time monitoring of RNase P PCR amplification from lower concentration human genomic DNA down to ~24 copy numbers or 12 cells was achieved.

The three systems described in this thesis can be readily adapted to current reported miniaturised platforms. Such a fully integrated device capable of quantitative nucleic acid analysis remains an enigma, and with further development will represent significant importance for the development of point-of-care device.

Kurzfassung

Das Design und die Implementierung miniaturisierter Systeme für die Analyse von Nukleinsäuren aus verschiedenen biologischen Proben haben eine beträchtliche Entwicklung erlebt. Fortschritte wurden insbesondere bei der Integration der Nukleinsäure-Vervielfältigung und –Detektion gemacht, wobei die Vervielfältigung meistens auf der Polymerase-Kettenreaktion (*Polymerase Chain Reaction*, PCR) beruht. Die Probenvorbereitung bleibt ein Haupthemmnis bei dem Versuch, eine quantitative Analyse mit vollständig miniaturisierten Systemen zu verwirklichen. Miniaturisierte Geräte für die Probenvorbereitung, Vervielfältigung und Detektion von Nukleinsäuren müssen weiter entwickelt werden, um ein vollständig integriertes System zu verwirklichen, das letztendlich in der Lage ist, die Genomanalyse einzelner Zellen mit „sample-in-answer-out“-Fähigkeit durchzuführen.

In dieser Arbeit werden drei miniaturisierte Systeme präsentiert, die jeweils für die DNA-Aufreinigung und –Vorkonzentrierung, deren Vor-Vervielfältigung und Langzeit-Speicherung bzw. der Vervielfältigung mit Echtzeitdetektion von DNA verwendet werden können. Das erste miniaturisierte System nutzt die Isotachophorese zur Vorbehandlung der DNA, bei der die DNA-Probe in einem diskontinuierlichen Elektrolytsystem gereinigt und aufkonzentriert werden kann. Dabei können sowohl qualitative als auch quantitative Informationen simultan aufgenommen werden. Das zweite miniaturisierte System verwendet die simple Methode der isothermischen *Multiplen Displacement Amplification* (MDA) für die Vervielfältigung des gesamten Genoms (*Whole Genome Amplification*, WGA) der humanen, genomischen DNA. Der miniaturisierte WGA-Prozess zeigte eine hohe Effizienz von 95,8% und die Wiedergabetreue des vervielfachten Produkts ist extrem hoch, was durch die Ergebnisse einer *Single Nucleotide Polymorphism* (SNP) Analyse angedeutet wurde. Für des letzte System entwickelten wir ein kleines bidirektionales shunting-PCR-Instrument, in dem die injizierte DNA durch eine temperierte Zone

mehrfach hin und her verschoben wird. Ausgestattet mit einem Fluoreszenz Detektor, erreicht man eine höhere Flexibilität und schnelle Temperaturzyklen, und kombiniert so die Vorteile der stationären PCR und der Durchfluss-PCR. Eine Echtzeitdetektion der RNase-P-PCR-Vervielfältigung von niedrig konzentrierter, humaner genomischer DNA mit einem Minimum von ~24 Kopien oder 12 Zellen wurde erreicht.

Die drei in dieser Arbeit beschriebenen Systeme können direkt an aktuelle miniaturisierte Aufbauten angepasst werden. Ein solches vollständig integriertes, zur quantitativen Nukleinsäure-Analyse fähiges Gerät bleibt ein Mysterium, und zusammen mit weiteren Verbesserungen wäre es von großer Bedeutung für die Entwicklung von point-of-care Geräten.

Chapter 1

Introduction:

Systems for Miniaturised Nucleic Acid Analysis

1.1 Miniaturised Total Analysis System (μ -TAS)

Analytical chemistry is an important tool for biotechnology and particularly for genomics and proteomic research. Nowadays, there is a vast demand for high throughput analysis, e.g. DNA sequencing and protein expression studies. However, to make these demands become reality, several deficiencies must be overcome, including analytical time, cost and throughput. Unfortunately, most current bioassays are labour intensive, since they are conducted in specific labs, where the samples are subjected to different analytical procedures (e.g. purification, amplification and detection/analysis) and furthermore, it takes a couple of hours even days to obtain the final results. In addition, the whole analysis process is performed in discrete and in spatially separated equipment which makes analysis both time-consuming and labour intensive, whilst hugely increasing the risk of contamination.

To resolve these problems, scientists are seeking portable devices or platforms containing all the necessary analytical components, which are able to perform all the required process in a continuous way. Such a device should have sample-in-answer-out ability, and only need minimal sample input, if possible even without the intervention of the user. With these in mind, a concept of miniaturised total analysis system (μ -TAS) was proposed. The technique is capable of high throughput analysis and automation, therefore it will reduce analysis time and cost at the same time. Furthermore, the integration of various technologies will not only reduce the cost, but also reduce the cost and the risk of being contamination.

1.1.1 History and Development

The concept of μ -TAS is first introduced by Manz *et al.* in the early 1990s.¹⁻⁴ The initial idea was to combine several steps necessary for sample analysis (e.g. sample handling, sample preparation, sample separation and detection) into a single device. It was soon recognised that such integration would significantly improve the analytical performance of chemical sensors in many perspectives, including speed, resolution, sample consumption, sample handling and others. In 1992, this concept was demonstrated with the first fabricated capillary electrophoresis (CE) microdevices formed from silicon and glass. In the middle of 1990s, μ -TAS began to attract attention, but was limited to the research groups with access to the clean room fabrication. The early applications of μ -TAS are mainly focused on the integration of CE into silicon and glass substrates.^{3, 5-9} This is mainly due to the unique property of the electro-osmotic flow (EOF) generated during CE separation, which ingeniously and gently avoids the need of external high pressure to transport a fluid inside a small channel and subsequent back pressure problems. The microchip CE was successfully applied to the separation of amino acids, which showed high efficiency compared to conventional CE instrument. Furthermore, sample injection and separation procedures can be easily optimized by switching and/or adjusting voltage. In 1994, Ramsey's Group produced intensive studies to enhance the performance of microchip CE by improving the injection methods.¹⁰

From mid-1990s, new methods and protocols have been developed, and the field of application has broadened. In 1995, Mathies achieved high-speed DNA sequencing by using capillary gel electrophoresis on a microchip, which has shown several potential applications of μ -TAS.¹¹ The same group has also integrated nucleic acid amplification technique with subsequent CE separation. The amplified products can be directly injected into main CE separation channel for subsequent genetic analysis, thus greatly reducing the whole analysis time.¹² The microfluidic devices have also be applied to cell analysis owing to the similar dimensions that microfluidic channels

possess relative to those of cells, which facilitates handling, incubation, transportation, manipulation, lysis and analysis of cells.¹³ In the late 1990s, due to the high fabrication costs of glass and silicon substrates, scientists started to look for other alternatives. . Several polymer-based miniaturised devices have been reported and they required lower fabrication costs and relatively simple fabrication processes, therefore they are suitable for massive production and disposable use.¹⁴⁻¹⁶ Polymer-based miniaturised devices have triggered another rapid development in the μ -TAS arena. The diversity of μ -TAS has been further explored in the late 1990s after several popular biotechnologies including nucleic acid amplification and extraction, were developed into miniaturised formats.¹⁷ The multiple channel CE separations in parallel have also been realized on miniaturised chip format. This has revealed the practical applications of μ -TAS in genetic analysis.¹⁸⁻²⁰ In 1999, commercial microchip CE instrument (Bioanalyzer 2100, Agilent) was introduced to the market by Agilent, which can be used for DNA, RNA and protein analysis. After that, several companies also brought their miniaturised device into the market. In 2001, a journal named “Lab on a chip” released by Royal Society of Chemistry. This journal is specific dedicated to μ -TAS area, serving as an academic forum to facilitate the development. Instead of a single-channel format, microfluidic devices with high-throughput capacity were also developed using multi-layer elastic polymers for sample manipulation, thus allowing thousands of samples to be analysed with defined volumes between the nL ~ pL level.²¹ Most recently, a fully integrated microchip for genetic analysis with sample-in-answer-out ability was reported, which has brought a prototype of μ -TAS into reality.²² Nowadays, the applications of μ -TAS are extremely diverse, and cover nearly all the analytical science areas by adaptation or integration of various analytical methods.²³⁻²⁶ The important events during the development of μ -TAS are listed in Table 1-1.

Table 1-1 Important events during the development of μ -TAS

Year	Events	Remark	Ref.
1990	A miniaturised open-tubular liquid chromatograph on a silicon chip	μ -TAS concept was first proposed	1-4
1993	Glass microchip with straight channel for CE separation of amino acids	CE showed its advantages in miniaturised system	3, 5-9
1995	Glass microchip for high speed DNA sequencing	Miniaturised system for genetic analysis	11
1996	Integration of PCR and CE on a single microchip	Integrated system broadened the applications of μ -TAS	12
1997	Microfluidic devices for cell analysis	μ -TAS for complex analytes	13
1998	Polymer-based microchip	Polymer-based microchip is suitable for massive production and single use	14-16
1998	Continuous-flow PCR	Greatly reduced thermocycling time	17
1999	Glass-based microchip with 12 channels for separation of DNA, RNA, protein and cells	The first commercial microchip instrument Bioanalyzer 2100	
2001	“Lab on a chip” Journal released	The first academic journal dedicated to μ -TAS	
2002	384-lane microchip electrophoresis	Ultra high throughput genetic analysis	20
2002	Multi-layer microchip for sample volume and movement control	Parallel control enable high throughput reaction and analysis	21
2006	Fully integrated glass microchip for genetic analysis	Prototype of μ -TAS with sample-in-answer-out ability	22

1.1.2 Microfabrication Techniques

To date, the fabrication methods for μ -TAS can be classified into two categories: silicon and glass-based substrates, and polymer-based substrates.

1.1.2.1 Silicon and Glass

In its early stage, most of the methods used in μ -TAS devices were developed from the silicon microprocessors industry, which made silicon a popular substrate. It

generally consists of three steps: mask fabrication, patterning and channel etching and microchip bonding. A standard fabrication procedure is briefly described in Figure 1-1.

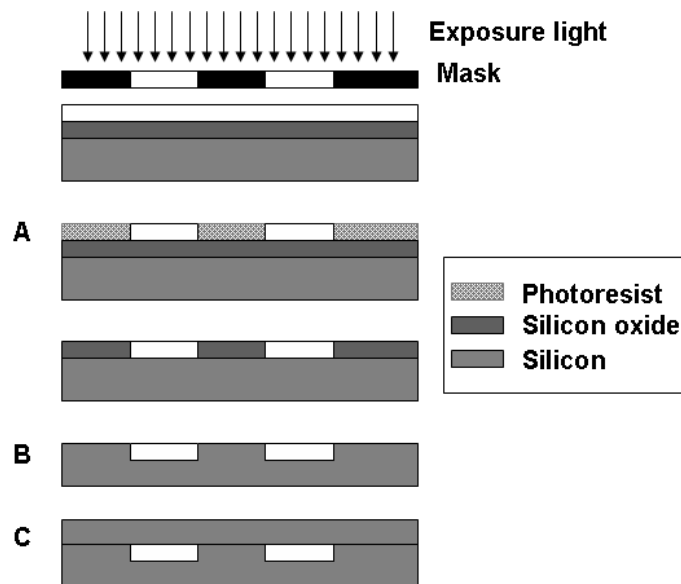


Figure 1-1 Silicon microchip fabrication steps

A: patterning of photoresist layer, B: silicon etching, C: bonding

1.1.2.1.1 Mask Fabrication

Generally, the mask design is done with the aid of adequate software such as AutoCAD. The pattern is then photo-lithographically transferred onto an optically flat glass wafer coated first with an absorbing metal layer and then a photoresist layer. There are two types of photoresist, positive (becomes soluble after in developing after UV-light exposure) and negative (becoming insoluble after in developing after UV-light exposure). After development of the photoresist layer and a post-bake for hardening, the absorbing metal layer is etched where the photoresist is removed to obtain the desired pattern.

1.1.2.1.2 Patterning and Channel Etching

A silicon wafer was first coated with a protective layer of silicon oxide and then a photoresist layer. The pattern is lithographically transferred onto the photoresist layer by exposing the wafer to UV-light through the mask. The photoresist is then developed and the silicon oxide layer is etched away. The silicon wafer is then etched to form a channel profile. For the etching of silicon substrate, there are two major methods: wet etching and dry etching. Wet etching uses acidic solutions such as mixing concentrated hydrofluoric acid (HF) and nitric acid (HNO₃), or alkaline solution of KOH, NaOH or NH₄OH, while dry etching is achieved by physical and chemical reaction between reactive species present in a gas/vapour environment and silicon substrate.

1.1.2.1.3 Microchip Bonding

The patterned substrate has to be bonded to another flat substrate in order to form a complete channel. The bonding technique commonly used is a thermal fusion process. After alignment, the two substrates are placed into an oven and undergo heating that will slowly bring the temperature above the softening of silicon (normally above 600 °C), and after cooling, a permanent sealing is formed

In principle, glass microfabrication is very similar to silicon microfabrication. Glass substrates are commonly coated with chromium to serve as the protective layer for etching. Only wet etching technique exists for glass, with typical etching solutions comprising hydrofluoric acid and ammonium fluoride. Since glass has an amorphous, non-crystalline, structure etching is always isotropic, limiting the aspect ratios obtainable. The most common bonding technique for glass is thermal bonding. It requires application of temperatures around 600° C for several hours. Only recently alternative low temperature methods have been developed which are based on the formation of an additional bonding layer between the two glass plates. It can be epoxy, sodium silicate, or a thin layer of HF resulting in temporary dissolution of the

glass boundaries and subsequent re-hardening. Drawbacks include that the channel surfaces are also altered, as in the epoxy and sodium silicate methods, or that high pressures are required, as in the HF method.

Silicon microfabrication with dry etching technologies and simple bonding techniques allows for the fabrication of sophisticated microstructures. However, applications for silicon microstructures in microfluidics and diagnostics are limited due to its mechanical properties (electric conductor, opaque). In contrast, glass microstructures (electric insulator, optically transparent) are suitable for a much wider range of applications but microfabrication is hampered by the lack of established simple bonding techniques.

1.1.2.2 Polymer

As described above, the microfabrication processes for silicon and glass-based microdevices are complex and time consuming. Therefore, fabrication cost is expensive, which makes the devices far away from single-use. Late in the 1990s, to cover a broader range of applications, scientists shifted their favourite substrate to several polymers such as poly(dimethylsiloxane) (PDMS)²⁷⁻²⁹, poly(methylmethacrylate) (PMMA)¹⁴ and polycarbonate (PC)¹⁶ due to their ease of fabrication and other specific properties. There are two major techniques for polymer microfabrication: replication, where a master containing a mirror image of the desired pattern is required for repeated use as a mould, and direct microfabrication, where each device is produced piece by piece.

1.1.2.2.1 PDMS microchips (Casting)

The fabrication process for PDMS-based microdevices generally uses casting. In this method, the PDMS pre-polymer and curing agent are first mixed at a certain ratio, and after thoroughly stirring and degassing, the solution is poured over the master (silicon or SU-8), to produce a precise replica of the surface. The master covered with PDMS will then be heated to 60 ~ 80 °C for 1 ~ 2 hours to facilitate the curing process. The

PDMS will become rigid due to three dimensional cross-linking. The cured PDMS is transparent and colourless, which meets the requirements for optical detection. PDMS can also be easily peeled off from the master and the PDMS replica can readily form reversible bonding to other substrate or itself by pressing them against each other. In most cases, a strong irreversible bonding is required. Such a bonding can be achieved by using an oxygen plasma treatment or UV irradiation. The fabrication process for a PDMS-based microdevice is shown in Figure 1-2.

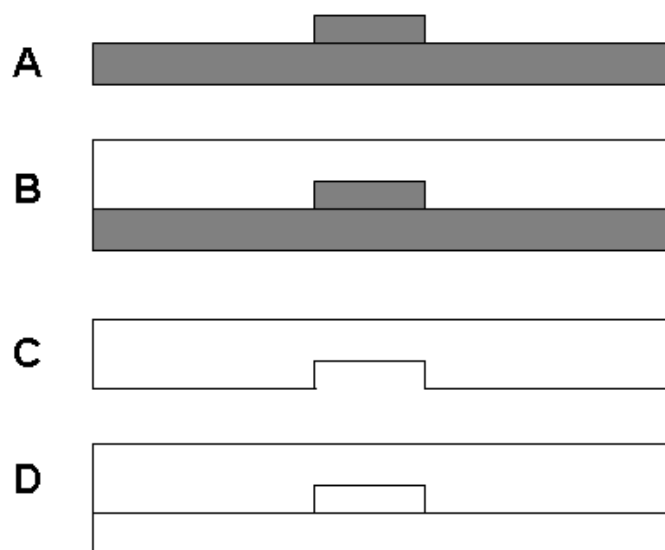


Figure 1-2 The fabrication process for PDMS-based microdevice. A: master, B: PDMS mixture is poured over the master, C: cured PDMS replica, D: PDMS bonded to another substrate

1.1.2.2.2 PMMA microchips (Injecting Moulding)

Injection moulding is suitable for mass production of polymer-based microdevices. A thermoplastic material (e.g. PMMA) is heated to its melting temperature (T_m) and injected into a thermostable mould and then cooled down below the thermoplastic glass transition temperature (T_g) to obtain a substrate replica. After that, the replica is bonded to another substrate to form a complete channel.

1.1.2.2.3 Direct Microfabrication of Polymer Microchips

Direct microfabrication often utilizes mechanical machining or laser ablation techniques to form the shape of the electrophoresis channels in polymeric substrates. Each part of the microchip must be fabricated separately, which makes for uneconomical mass production, and additionally, rough surfaces are also an obstruction to high-resolution separation.

1.2 Integration of Components in μ -TAS

Integrated devices incorporating multiple fluidic, electronic and mechanical components are one of the most important features for μ -TAS.^{30,31} The different parts on such a device play critical roles to allow samples to undergo all the necessary stages to obtain the useful analytical information through continuous flow. The advantages of such integration are numerous, including portability, contamination-free, fast analysis speed and less reagent consumption. Several important components with different functionality are listed below.

1.2.1 Sample Pre-treatment

Integration of sample pre-treatment into a miniaturised system is one of the main remaining obstacles for the full realisation of μ -TAS.³² The challenge is made more complex by the enormous variation in samples to be analyzed. Moreover, the pre-treatment technique has to be compatible with the downstream analysis device to which it is coupled in terms of time, reagent and power consumption as well as sample volume and not to forget the ‘meaningfulness’ of the bioassay. Chip-based sample pre-treatment is normally compromised from several parts.

1.2.1.1 Sample Separation and Purification from Sample Matrix.

Real-world samples generally contain large amounts of organic and inorganic particles, which must be removed to avoid fouling and disruption during bioanalysis.

In bioanalytical applications, interesting and informative analytes are often within a cell, and must be extracted from the cell lysates. In all cases, samples are required to be separated from a complex background matrix in a purification step.

1.2.1.2 Sample Pre-concentration

If the sample is only available in trace amounts, which is nearly always the case in bioanalytical applications, pre-concentration is a necessary step to enhance the detection sensitivity by squeezing the sample molecules into a smaller volume. Such pre-concentration techniques are also used in conjunction with other separation methods, for instance isotachopheresis (ITP) coupling with capillary zone electrophoresis (CZE).³³⁻³⁶ Although the analytes can be concentrated after such treatment, the quantitative information is lost due to the lack of detector in the pre-treatment stage.

1.2.1.3 Sample Derivation

Sometimes, the sample analytes have to undergo chemical transformation in order to render them to be detectable by the used detectors. For examples, fluorescent reagents were commonly used in bioanalytical application for sample labelling.³⁷⁻³⁹

1.2.2 Sample Manipulation

Two different techniques are widely used for the sample movement inside the integrated devices: hydrodynamic flow and electrodynamic flow.

1.2.2.1 Hydrodynamic Flow for Sample Manipulation

The hydrodynamic flow is a common method to generate liquid flow in miniaturisation by the pressure difference, as it is a cheap, robust and easy-to-control technique. The current miniaturised platform can be easily connected to a syringe or peristaltic pump through tubing or capillaries. Micro-pumps and micro-valves have

also been implemented into microdevices, thus providing a more reliable control. The movement of sample can also be generated simply by the pressure difference inside the microdevice such as sample height or even gravity. Although hydrodynamic flow is easy to implement and well-studied, it has two major drawbacks. First the parabolic profile of liquid it generates will cause band broadening which greatly reduces the analytical resolution.⁴⁰ Secondly, the narrow channel will give a high back-pressure, which dramatically increases the required pressure to propel a fluid through a channel.

1.2.2.2 Electrodynamic Flow for Sample Manipulation

The electrodynamic flow can be described as movement of a liquid due to the presence of an electric field, thus avoids the required high pressure when moving a fluid inside a narrow channel. When electrodynamic flow is applied on miniaturised systems, it depends mostly upon two factors: EOF and electrophoretic mobility. The EOF is generated due to charged inner surface of the microchannel, thus it is mainly determined by the substrate materials and the electrolyte system used, whilst the electrophoretic mobility depends on the charge-to-radius ratio of the sample itself. The EOF velocity (V_{EOF}) can be expressed as:

$$V_{EOF} = \frac{\varepsilon \zeta E}{4\pi\eta}$$

where ε is dielectric constant of the solution, E is applied electric field, ζ is zeta potential and η is buffer viscosity. The direction of EOF is controlled by the inner surface chemistry. If the inner surface produced negatively (positively) charged groups, then the direction of EOF is from the anode to the cathode (from cathode to anode). It will drag the entire liquid bulk towards the cathode (anode). Literature has reported controlling liquid movement by modification of channel inner surface on microchips.⁴¹ Since integration of electrodes onto miniaturised platforms is readily accomplished, the use of electrodynamic flow for controlling the movement of sample

liquid has gained more attention now. The electrophoretic mobility is generally applied for electrophoresis⁴²⁻⁴⁴ and will be discussed later.

1.2.3 Reaction

Both chemical and biochemical reactions can be performed on miniaturised systems with a much smaller volume when compared to conventional instrumentation. Chemical synthesis such as polymerisation has been reported on a miniaturised platform. Due to its fast speed and small reagent consumption, such a device can be used as a testing tool before up-scaling and massive industrial production. Biochemical reactions such as immunoassay,⁴⁵ polymerase chain reaction (PCR),^{46, 47} and DNA hybridisation⁴⁸⁻⁵⁰ have all been well-studied on chip. All the miniaturised biochemical reactions have greatly reduced the samples and reagents consumption, and enable high throughput processing, benefiting from the inherent advantages of μ -TAS.

1.2.4 Separation

1.2.4.1 Electrophoresis

The electrophoretic separation is so far the most favourite separation technique used in miniaturisation, as it avoids the need of high pressure to drive the sample liquid. With geometry, design and adjusting of electric field, the injection and separation of pico-litre samples can be well-controlled without pumps and valves. Microchip electrophoretic separation meets the demands of miniaturisation, automation and integration, therefore it rapidly established as the most active field in μ -TAS areas.⁵¹⁻⁶⁰

When an electric field E is applied to a microchip, the charged particle migrates with an electrophoretic velocity which depends on the applied electric field and its electrophoretic velocity (V_{ep})

$$V_{ep} = \mu_{ep} E$$

In the equation above, μ_{ep} represents electrophoretic mobility, which can be further expressed as:

$$\mu_{ep} = \frac{q}{6\eta\pi r}$$

Thus μ_{ep} is determined by q (solute charge), η (buffer viscosity) and r (solute radius).

With the consideration of EOF inside the channel, the overall velocity (effective velocity) can be expressed as:

$$V_e = V_{ep} + V_{EOF}$$

The charged samples will be separated according to their electrophoretic mobility. Under some circumstance such as gel electrophoretic separation of negatively charged DNA fragments, EOF needs to be eliminated. In microchip gel electrophoresis separation for nucleic acids and proteins, a buffer containing polymer sieving matrix is pre-loaded into the channel before sample injection. After applying an electric field, nucleic acids or protein will be separated according to their individual sizes. Commercial microchip gel electrophoresis instruments for DNA, RNA and protein are also available from several companies. Microchip CE has been applied for genetic analysis including DNA sequencing^{61, 62}, single nucleotide polymorphism (SNP)^{63, 64} and single strand conformation polymorphism (SSCP)⁶⁵ analysis.

1.2.4.2 Chromatography

Due to the high back-pressure inherently associated with the geometry of miniaturised systems, there are less reports of using high pressure driven chromatography in these formats. But a procedure called capillary electrochromatography (CEC) combining of chromatography and electrophoresis has gained more attention.^{66, 67} Like microchip electrophoresis, the samples were driven under an applied electric field, but the channel is pre-stacked or pre-coated with a stationary phase, thus the analytes will be separated according to their individual charge-to-mass ratio and affinity to the

stationary phase as well. These two combined separation mechanisms give high selectivity and high efficiency to CEC and the microfabrication methods make it much easier to implement stationary phase into a microchannel.

1.2.4.3 Other Separation Methods

Some other separation methods have also been applied on miniaturised systems including isoelectric focusing (IEF),⁵⁷⁻⁶⁰ ITP⁶⁸ and etc. Miniaturised IEF is routinely used to separate and characterize proteins and peptide according to their isoelectric point (PI) points. Microchip-based ITP is also used for analysis inorganic or organic ions due to its high loading capacity. Moreover, miniaturised ITP is employed as a pre-concentration technique combining with other separation method to increase the sensitivity.

1.2.5 Detection

The detection techniques for miniaturised system have several special requirements, compared to those for conventional analytical instruments, since the performance of the detectors have great impact on many factors such as limit of detection (LOD), speed, and universality.⁶⁹⁻⁷³ Parameters related to assay detection include;

1. High sensitivity⁷⁴⁻⁷⁶

The detection methods for miniaturised systems should have high sensitivity due to low sample volume ($\mu\text{L} \sim \text{pL}$) and small detection area.

2. Fast response⁷⁷⁻⁸⁰

The detectors for miniaturised systems should have fast responses to the signals since many separations and reactions on miniaturised systems are accomplished in seconds or even less.

3. Integration⁸¹⁻⁸⁸

The detectors have the potential to be integrated onto miniaturised systems, thus allowing a portable analysis platform.

4. Parallelisation⁸⁹⁻⁹¹

The detectors for miniaturised systems should also be able to do parallel detections in order to achieve high throughput analysis.

The current major detection techniques for miniaturised systems are summarised in Figure 1-3.

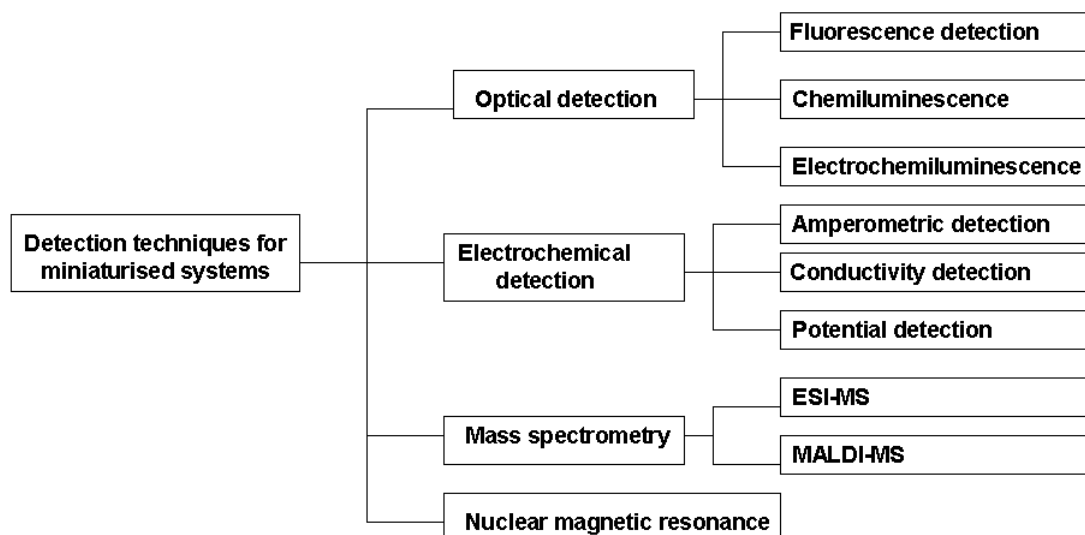


Figure 1-3 Major detection techniques for miniaturised systems

1.2.5.1 Fluorescence Detection

The most popular detection technique for miniaturised devices is laser induced fluorescence (LIF), due to its high sensitivity. A laser beam is focused on the detection spot by lenses, and the excitation source passes its high energy to the sample, thus fluorescence light is emitted and collected by a microscope. After passing through a pinhole and a band-pass filter, its intensity was measured using a photo multiplier tube (PMT) or charge coupled device (CCD) camera. Despite its high sensitivity, one of the main drawbacks for LIF is that the analytes must be fluorescent or can be labelled by fluorescent species. Therefore a vast majority of species can not be detected by this method.

1.2.5.2 Electrochemical Detection

Electrochemical detection can be used as an alternative detection method when optical detection is not a practical option. It can be sub-divided into three techniques including amperometry, conductometry, and potentiometry based on their different mechanisms. In amperometric detection, there are three electrodes: auxiliary, reference and working electrodes. The auxiliary and reference electrodes are used to monitoring the solution potential, while the working electrode detects the analytes. During the detection, the potential between the working and auxiliary electrodes are kept constant. The amperometric detection is based on redox reactions of the analytes generating current at the working electrode. The current can be used to determine the concentration of analyte, as it is proportional to the number of redox reactions. Although the amperometric detection is very sensitive, the contamination of electrodes is a major obstacle impeding further development. By altering the constant potential to constant current, potential detection is achieved, thus the concentration of analyte can be obtained. Conductivity detection serves as a more universal technique, as it can be used for any analyte as long as it has a conductivity difference from the background. A pair of electrodes is generally placed at the end of the microchannel. Contactless electrodes are further developed in order to prevent bubble formation and contamination of electrode surfaces.

1.2.5.3 Chemiluminescence and Electrochemiluminescence Detection

Chemiluminescence (CL) detection is based on emission of light during the chemical reaction, thus its setup is relative simply as it does not require external excitation light resource. CL has a low background noise which gives it a high sensitivity. Electrochemiluminescence (ECL) is another form of CL in which the light-emitting chemiluminescent reaction is effected by electrochemical stimulation. The advantages of CL are preserved, but the ECL detection allows the time and position of the light-emitting reaction to be controlled. For instance, CL and ECL detectors have been employed in miniaturized devices for immunoassay.^{92, 93} For microchip

detection, CL and ECL detection systems offer an inexpensive setup, conferring practicality to the μ -TAS concept of miniaturisation.^{94, 95}

1.2.5.4 Mass Spectrometry

Mass spectrometry (MS) is an essential tool for the characterization of biomolecules, revealing the charge-to-mass ratio of analyte molecules following ionization, and has proven particularly beneficial in the proteomics area. The integration of miniaturised devices and MS has received substantial attention since miniaturised systems have been widely applied to proteomic analysis as novel tools.^{96, 97} Currently, the interface between microsystems and MS is one of the most active areas. The most often used method of ionizing chemical or biological compounds at the interface between separation microsystems and MS is electrospray ionisation. A sharp emitter with low flow rate is normally needed to achieve high ionisation efficiency using a strong electric field between the emitter and MS.⁹⁸

1.2.5.5 Other Detection Methods

Many other detection methods for miniaturised systems have also been reported for their specific applications or unique advantages,⁷³ including Raman spectroscopy, nuclear magnetic resonance (NMR), surface plasmon resonance (SPR). For example, surface-enhanced Raman spectroscopy has been coupled with microfluidic devices for sensitive detection of duplex dye-labelled oligonucleotides.⁹⁹ And a microfluidic chip with an integrated planar microcoil NMR was developed for real-time monitoring samples with volumes of less than a microliter.¹⁰⁰

1.3 Miniaturised Nucleic Acid Analysis

Genetic analysis employing μ -TAS has elicited enormous interest. When the genetic analysis is focused at the single cell level, the inherent dimensions of μ -TAS are suitable for single cell analysis, and μ -TAS probably could find its “killer application” in this field. Because the amount of original cellular matter available for genetic

analysis is often extremely limited and readily lost given the limited availability of homogeneous (extraction-free) assay formats, the amplification of target nucleic acids following careful sample manipulation including separation processes are typically necessary steps. Thus not too surprisingly miniaturised *in vitro* gene amplification, especially PCR, has become synonymous with the development of miniaturisation and microfluidics *per se*.^{46, 47, 101-103} Moreover, miniaturised PCR also gives other advantages such as high thermal cycling speed and low reagent consumption, which benefit from intrinsic high surface-to-volume ratio. But so far, most of the reported miniaturised devices for nucleic acid amplification are stand-alone structures replacing only the role of the conventional PCR thermocycler. The integration of nucleic acid amplification with other functional units such as proximal sample preparation and distal sequence analysis on a single device is broadly accepted as the way forward and starts to emulate the vision of μ -TAS as discussed previously.⁹ Presently, integration of miniaturised PCR is under rapid development, and PCR has been coupled with pre-PCR units such as sample purification and pre-concentration, and post-PCR modules such as capillary gel electrophoresis (CGE) and DNA microarray on single microdevices. The different approaches to integrated gene analysis that encompasses *in-vitro* gene amplification are relatively finite and shown in Figure 1-4.

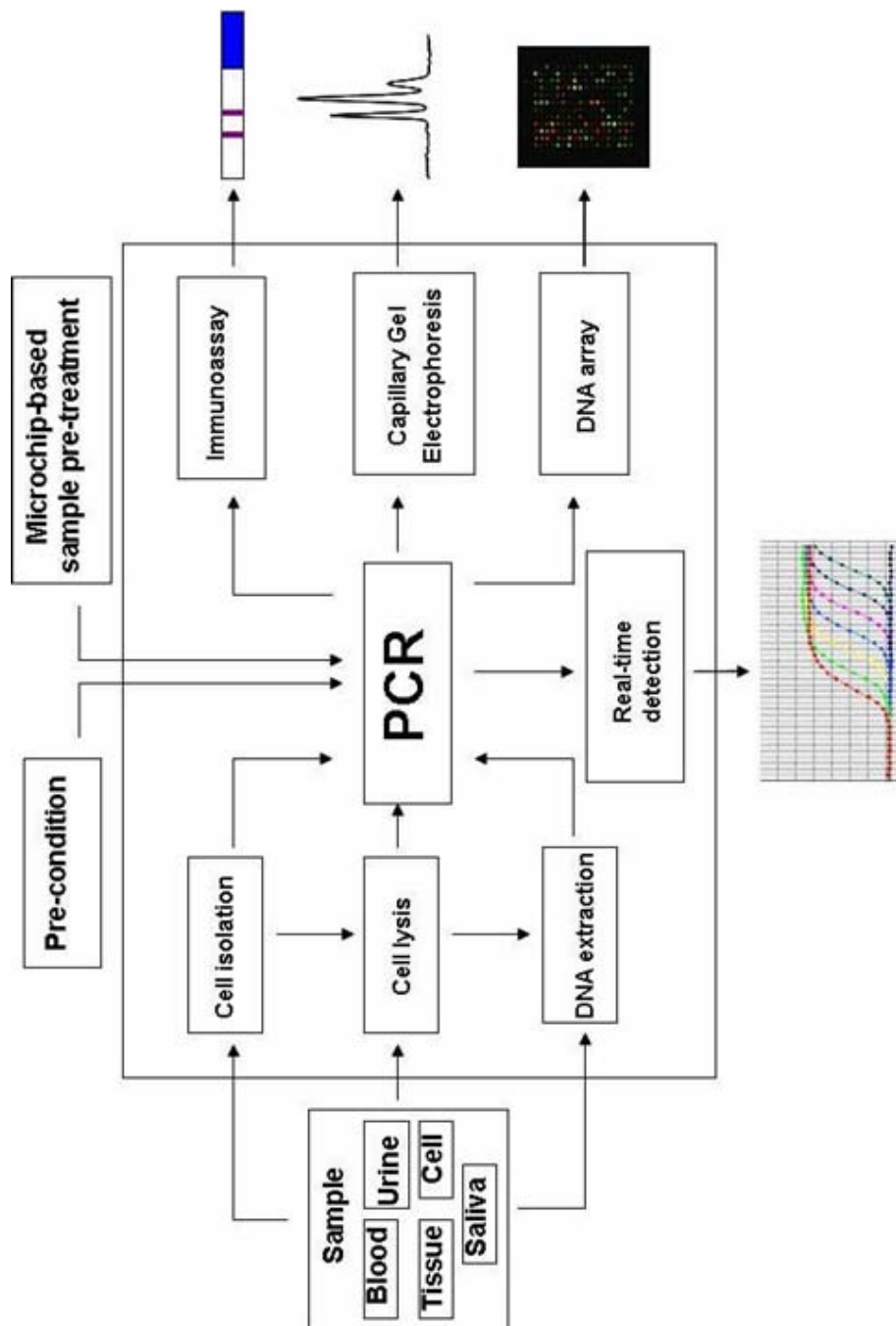


Figure 1-4 Integrated PCR on microfluidic devices

1.3.1 Miniaturised Isotachophoresis (ITP) for Nucleic Acid Purification

As an electrophoretic separation and pre-treatment technique, ITP has been transferred into microchip format or combined with microchip CZE as an on-line pre-concentration technique by a number of researchers.^{36, 104-109} Due to its advantageous features including separation parameters controlled by electrolyte composition and high sample load capacity, ITP has been proved to be a promising tool to improve the inherent limiting ability of μ -TAS to detect extremely low-concentration species.^{33, 34, 110, 111}

In ITP, a volume of analyte is placed between a leading electrolyte (LE) and a terminating electrolyte (TE). The LE is composed of high-mobility ions and so has a higher mobility than the sample ions and the TE. Conversely, the TE is composed of low-mobility ions and so has lower mobility compared to the LE and sample ions. During the electrophoretic separation, analytes in the sample are arranged into discrete bands in order of mobility. The velocity and concentration of these bands are adapted to a value governed by the leading ion. Consequently, both separation and concentration adaptation occur simultaneously (Figure 1-5). The principles and applications of ITP have already been fully described by several earlier reviews.¹¹²⁻¹¹⁵

To date, miniaturised ITP has been used with a wide variety of samples. However, there have been few reported uses of miniaturised ITP involving DNA samples. Although this method has been used as a pre-concentration technique in either ITP-CZE for separation of DNA fragments, none of these reports investigated in detail the behaviour of the ITP stage. It is likely that miniaturised ITP can be used to separate DNA from raw samples which are to undergo PCR reactions. For such a purpose, a suitable electrolyte composition containing appropriate leading and terminating ions is required.

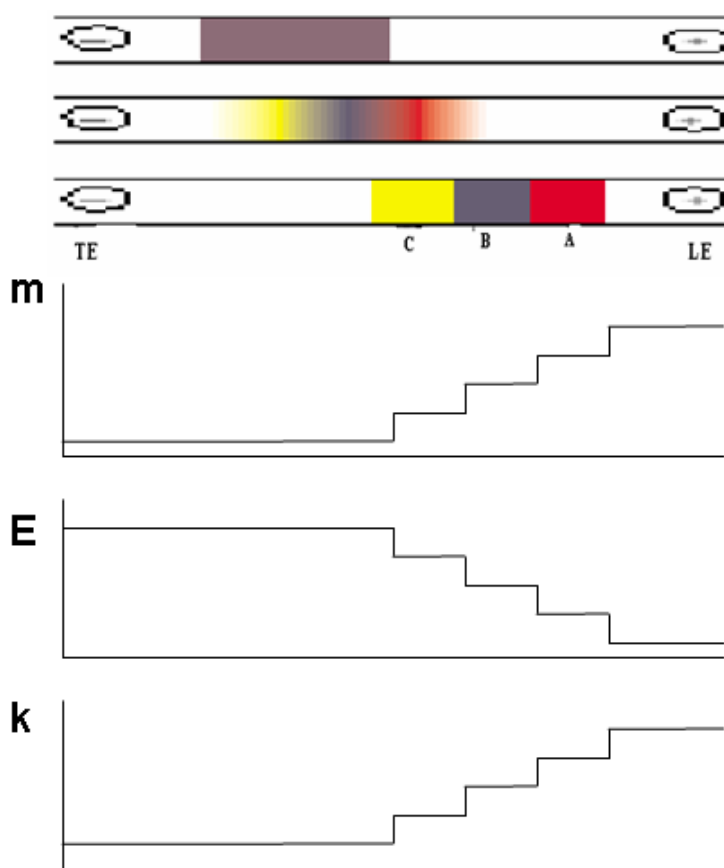


Figure 1-5 Progress of ITP separation and properties of the zones. LE is the leading electrolyte; TE is the terminating electrolyte; A, B and C are sample zones; m is mobility; E is electric field and k is conductivity.

1.3.2 Miniaturised Whole Genome Amplification

1.3.2.1 Whole Genome Amplification

Large quantities of genomic DNA of suitable quality (high molecular weight and purity) for molecular analysis are of critical importance for many applications such as high-throughput genotyping assays, forensic science, embryonic disease diagnosis and most importantly, the long-term DNA sample storage including national and disease-specific DNA archives. However, often the amount of available DNA is insufficient for extensive analyses. This situation is more challenging with the

analysis of single cells where only finite testing can be undertaken. In order to address this problem, several methods for whole genome amplification (WGA) have been developed over the past ten years. The first two WGA methods based on the PCR principle were described in 1992, namely the primer extension PCR (PEP) by Zhang and coworkers,¹¹⁶ and the degenerated oligonucleotide primed PCR (DOP-PCR) by Telenius and collaborators.¹¹⁷ PEP involves a high number of PCR cycles, using *Taq* polymerase and 15 base random primers that anneal at a low stringency temperature. Although the PEP protocol has been improved in different ways (improved-PEP, I-PEP),¹¹⁸ it still results in incomplete genome coverage, failing to amplify certain sequences such as repeats, induces an amplification bias of the order of 10^3 to 10^6 and has a limited efficiency on very small samples (such as single cells).¹¹⁹⁻¹²² Moreover, the use of *Taq* DNA polymerase implies that the maximal product length is about 3 kb. DOP-PCR uses *Taq* polymerase and semi-degenerate oligonucleotides (i.e. CGACTCGAGNNNNNATGTGG) that bind at a low annealing temperature at approximately one million sites in the human genome. The first cycles are followed by a large number of cycles with a higher annealing temperature, allowing only for the amplification of the fragments that were tagged in the first step. DOP-PCR generates, like PEP, fragments that are in average 400-500 bp, with a maximum size of 3 kb. On the other hand, a low input of genomic DNA (less than 1 ng) decreases the fidelity and the genome coverage and increase the likelihood of allele drop out (ADO).¹²³ Thus the main challenge of WGA methods is to obtain balanced and faithful replication of all chromosomal regions without the loss of genomic regions or preferential amplification of genomic loci or alleles.¹²⁴ Recently, a non-PCR-based isothermal method called multiple displacement amplification (MDA) was introduced that is based on the annealing of random hexamers to denatured DNA, followed by strand-displacement synthesis at constant temperature. It has been applied to small genomic DNA samples, leading to the synthesis of high molecular weight DNA with limited sequence representation bias.^{125, 126} Compared to other WGA methods, MDA appears to be most reliable for genotyping since it has the best genomic coverage, lowest sequence related amplification bias and most favourable call rates.^{121, 124, 127-129}

Moreover, MDA is an isothermal amplification process, which avoids the needs for thermocycling.

MDA is an isothermal reaction carried out at 30 °C. It achieves replication of double stranded DNA (dsDNA) in a similar way to the cellular process in which the DNA polymerase invades a replication fork. MDA utilizes a very special DNA polymerase from the bacteriophage Phi29 to extend random hexamer primers. The key to MDA is that the Phi29 DNA polymerase is able to invade the replication fork efficiently without the aid of a helicase. In the MDA reaction, random hexamers anneal to multiple sites along the DNA template and serve as initiation sites for the Phi29 DNA polymerase-mediated replication. As replication proceeds along the template, it reaches the initiation site for the other replication events that are processed in parallel. These DNA strands are displaced, which allows DNA replication to continue. The displaced DNA strands then serve as new templates for random hexamers for initiation of subsequent DNA replication events catalyzed by Phi29 polymerase. This mechanism results in a hyper-branched amplified product during the reaction and enables amplification of a large genome (Figure 1-6). Furthermore, the error rate of Phi 29 DNA polymerase has been estimated to be less than 3×10^{-6} in contrast to 3×10^{-5} for *Taq* DNA polymerase, or 9×10^{-6} for *Taq* polymerase in combination with the *Pwo* polymerase used in high fidelity PCR systems.^{130, 131} The applications of MDA have been carried out in several practical fields which could have a great amount of potential in the future. MDA has been applied to characterize bacteria collected from their natural environment¹³² and even amplify DNA from single bacterial cells to allow genome sequencing.^{133, 134} Amplification of total DNA from human rectum and colon biopsies¹³⁵ and human gallstones¹³⁶ has also been achieved using MDA. In instances where non-human primate genetic resources have been limited, MDA has been applied to a diversity of sample types and was found to be a reliable approach for medical genetic studies,¹³⁷ comparative genetics,¹³⁸ and wildlife forensics¹³⁹ using several genotyping methods.

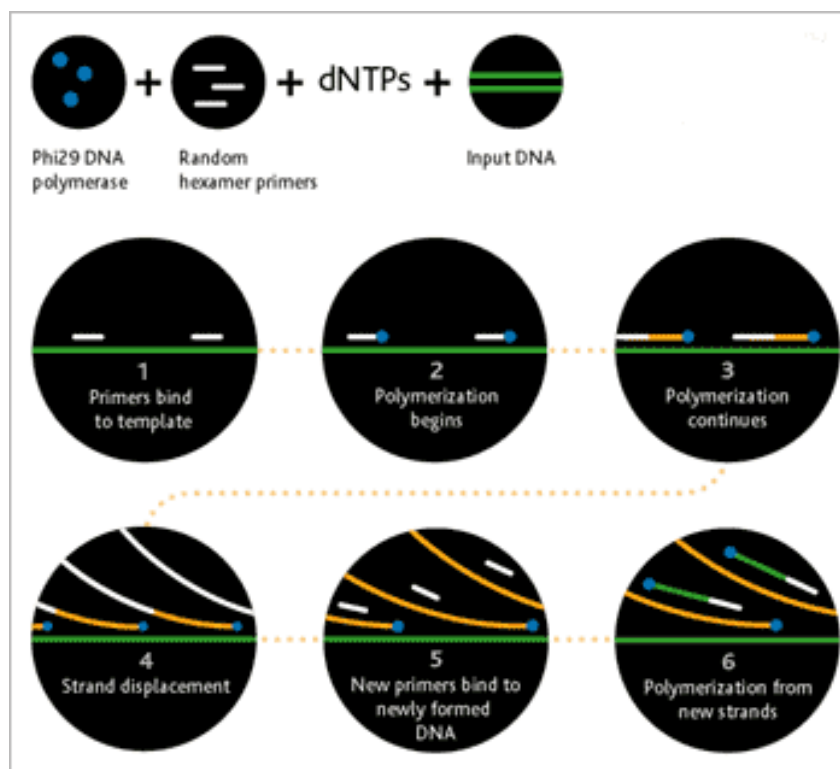


Figure 1-6 MDA reaction mechanism

(http://www5.gelifesciences.com/aptrix/upp01077.nsf/Content/genome_illustra_redirect~genomiphi_work) (From GE healthcare website)

1.3.2.2 WGA on Miniaturised Systems

To date, there has been one reported application of WGA on a microchip, in which DOP-PCR was used for WGA of human genomic DNA on a silicon-glass microchip.¹⁴⁰ The amplified human genomic DNA was then for a locus-specific multiplex PCR in order to detect dystrophin gene exonic deletions causing Duchene/Becker muscular dystrophy. But their results showed the whole genome amplification products obtained by DOP-PCR were only suitable as templates for subsequent PCR with an amplicon size below 250 bp. The limitation is mainly due to the reaction mechanism of DOP-PCR itself. Their study has shown that WGA can be integrated onto the chip format to pre-amplify from limited amounts of whole human genomic DNA to enable further assays.

So far there has been no report of MDA applications in miniaturised systems, although the applications of lab-on-a-chip devices for molecular biology has bloomed in recent years due to advantages in higher sensitivity, lower reagent consumption and integration of different functional units.^{26, 141} For genomic research, DNA sizing, genotyping and on-chip amplification are well studied. Since integration is one of the most important features for μ -TAS, the adaptation of MDA as a sample pre-amplification step will greatly facilitate the multi-parallelised nucleic acid analysis on miniaturised systems, where the limitation of sample amount is a major obstacle, due to the inherent small volume offered by miniaturisation and the low nuclear content of defined small samples. Furthermore, the miniaturised MDA platform has the potential to serve as a sustainable DNA archive, since only a small amount of original DNA sample is needed to establish in essence a perpetual source for genetic studies.

1.3.3 Bidirectional Shunting PCR with Real-time Detection

1.3.3.1 Polymerase Chain Reaction (PCR)

PCR is an *in vitro* technique allowing the enzymatic-catalysed amplification of specific nucleic acid sequences. This method is first introduced by Kary Mullis in 1983 and he was awarded the Nobel Prize for this invention.¹⁴² PCR is one of the most important techniques that revolutionised modern biochemistry and has a tremendous impact on genetics and medical diagnostics. Before its invention, the available amount of a nucleic acid sample was insufficient for universal analysis. With PCR amplification, now minute quantities of nucleic acids, even down to a single DNA molecule can seed analysis.

1.3.3.1.1 Principle

The PCR takes place in three temperature-controlled steps (Figure 1-7).

1. Denaturation: The temperature of the PCR mixture is raised to 94 - 96 °C, where dsDNA is separated into two single strands due to the breaking of the hydrogen bonds between the complementary bases.
2. Annealing: After denaturation, the temperature is then typically lowered to between 50 and 60 °C. Watson-Crick H-bonds can be reformed at this temperature and the single stranded DNA (ssDNA) can hybridize to their complementary strands to reform dsDNA. However, primers consisting of a sequence of about 10-30 bases tend to preferentially anneal to the complementary region on the target DNA, due to their vast excess amounts.
3. Extension: The 3'-end of the hybridized primer is extended along the original DNA template strand by continuous incorporation of complementary nucleotides into the chain, which is catalyzed by the DNA polymerase. Thus, a complementary DNA strand is formed and primer extension is stopped as soon as the complementary DNA strand has been completed. Generally, the speed of extension is 160 bp/s when *Taq* polymerase is used. It has been found that the fidelity of reaction improved at 72 °C. Hence, the temperature is usually set to this value for extension step. And it is also not uncommon to combine the annealing and the extension into one operation called two-step PCR.

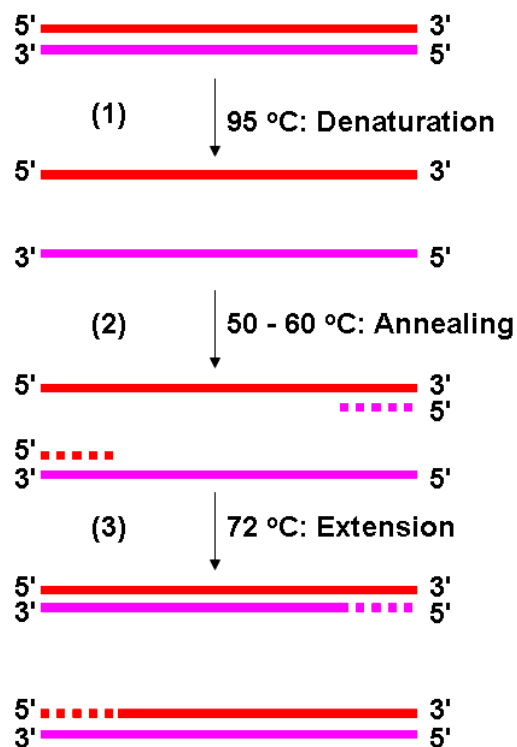


Figure 1-7 The principle of PCR.

The three stages of denaturation, annealing and extension constitute “one cycle”. A typical PCR consists of 25 to 40 such cycles. This procedure of repeated heating and cooling of reaction mixture is commonly referred to as thermocycling. (Figure 1-8) With an extended time for denaturation at the very beginning and for extension at the very end, a typical PCR can be completed within 30 min- 2.5 h. During the reaction, efficient heating and cooling as well as precise temperature control are required. Normally, this can be achieved using Peltier elements, which operate upon resistive heating and semiconductor cooling. Alternatively, heating and/or cooling can also be controlled with air, fluid or irradiation.

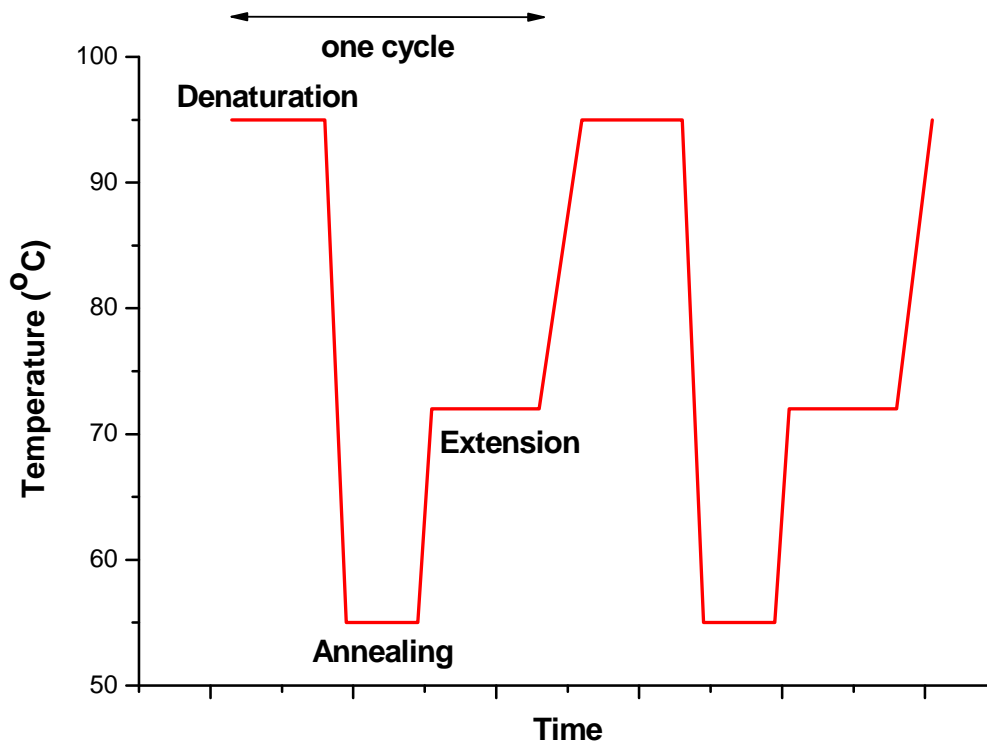


Figure 1-8 The temperature profile of PCR reaction.

In theory, the number of DNA copies is doubled after each cycle, which results in an exponential amplification. The number of DNA molecules at the end of m cycles, N_m , depends on the initial number of DNA copies, N_0 , thus it can be theoretically predicted as:

$$N_m = N_0 \cdot 2^m$$

However, this theoretical number can be never achieved because of limiting factors such as the depletion of reaction components, reaction by products causing negative feedback to the polymerase activity and the enzymatic loss of activity during thermocycling. In practice, the number of DNA molecules can be approximated by the following equation:

$$N_m = N_0 \cdot (1 + x)^m$$

where x is the efficiency of the reaction and can vary between 0 and 1, or expressed as a percentage. For example, with $m = 25$ cycles that starts with a single DNA molecule, $N_0 = 1$, the number of theoretically predicted copies after the end of the

reaction is more than 30 million. Assuming an efficiency of $x = 0.7$, the reaction gives a $\sim 570,000$ -fold amplification.

As the PCR reaction proceeds, a plateau phase is reached and production of amplicons cease. One reason for this is the depletion of the reagents, i.e. the depletion of primers and nucleotides. Furthermore, pyrophosphate released during the reaction acts as a potent inhibitor to the enzyme. Despite being thermostable, the activity of DNA polymerase is also reduced after repeated thermocycling. Another important factor is that the hybridization of longer strands of DNA occurs at higher temperatures than hybridization of a single-stranded DNA (ssDNA) and a primer. More PCR products out-compete the primers for hybridization at later PCR cycles.

1.3.3.1.2 Components for PCR

The PCR mixture normally contains (1) an excess of two primers (oligonucleotides, which are complementary to the ends of the targeted nucleic acid region), (2) the enzyme (DNA polymerase), (3) an excess of the four deoxynucleotide triphosphates (dNTPs), (4) the template DNA and (5) buffer possessing Mg^{2+} which is a co-factor for the DNA polymerase, and also pH stabilising agents.

1. Primers

The primers are short oligonucleotides, which are complementary to the ends of the target sequence. Generally, two primers are used for PCR amplification: a forward primer and a reverse primer (see Figure 1-7). Each hybridise to one of the two strands of the original dsDNA. DNA synthesis always proceeds in the direction from 5' to 3', thus, the first nucleotide to be incorporated reacts with the free 3'-hydroxyl group of the primer. The set of primers has to be designed specifically to ensure that only the targeted sequence will be amplified. The length of the primer is usually 10-30 base pairs (bp). In addition, there should be no intra or inter primer complementarity in order to avoid the formation primer-dimers. The stability of the hybridisation is also important, therefore, the composition is a crucial factor as well as position of bases. In

order to achieve an exponential amplification, the PCR process requires that the two primers are compatible, meaning that they need to work as a pair under similar condition. Particularly, their melting and annealing temperatures should not differ by more than 2 °C and lie between 55 and 80 °C. As can be seen, the design of a primer is a very complex process to ensure the specificity of a PCR reaction. Some primer design softwares (e.g. Primer Express by Applied Biosystems, Oligo by Life Science Software) have been introduced, which has greatly facilitated this arduous task.

2. DNA Polymerase

The role of the polymerase enzyme is to catalyse the synthesis of complementary DNA strands. The most frequently used enzyme originates from a bacterium, *Thermus aquaticus*, which is abbreviated to Taq DNA polymerase. It is a heat-stable enzyme that does not deteriorate or lose its efficiency when the PCR is performed. Apart from being thermostable, the enzyme should also be capable of synthesising long strands of DNA, in other words, having a good polymerisation activity.

3. dNTPs

The four deoxynucleotide triphosphates (dNTPs) including deoxyadenosine triphosphate (dATP), deoxycytidine triphosphate (dCTP), deoxyguanosine triphosphate (dGTP) and thymidine triphosphate (dTTP), are the building blocks (monomers) for DNA synthesis. During the template replication, dNTPs are added to the extending strand according to Watson-Crick base-pairing rule. Once the immobilisation has occurred, the enzyme catalyses the incorporation of the sugar of the dNTP to the backbone of the DNA strand by breaking the diester bond between two phosphorus molecules, namely P_{α} and P_{β} . The energy released by the formation of the pyrophosphate is then used to generate the phosphodiester bond which links the two consecutive nucleotides. The reaction mixture must contain an excess of these dNTPs as they deplete during PCR and usually there should be an equal concentration of each dNTP.

4. Buffer

The buffer is mainly used to maintain optimum conditions for the DNA polymerase, thus its pH and ionic strength is chosen according to the polymerase

used. A typical buffer system has an ionic strength of about 50 mM and consists of Tris-HCl, pH 8.3, with KCl or NaCl. Magnesium ions are crucial for PCR as they are enzymatic co-factors, therefore, MgCl₂ at concentrations between 0.5 and 5 mM, is always added. The Mg²⁺ ions form a soluble complex with DNA and polymerase. Their role is to bring the polymerase and DNA into close proximity and to balance the negative charges on the DNA molecules. In addition, they stimulate the polymerase activity. The concentration of the Mg²⁺ ions is related to both specificity and yield of the reaction. A low concentration leads to poor reaction yields due to the decreased enzymatic activity, while a high concentration results in poor denaturation because dsDNA molecules are stabilised by the Mg²⁺ ions. Furthermore, it indirectly promotes the formation of non-specific products owing to increased annealing of the primers to incorrect sites. Some other additives including glycerine, bovine serum albumin (BSA) are employed in order to stabilise the polymerase or to optimise the primer annealing. Denaturation can also be improved by adding dimethyl sulfoxide (DMSO), formamide or surfactant such as Tween-20. The selection of additives depends heavily on the polymerase used, PCR platform, and individual experiment conditions.

1.3.3.1.3 Real-time PCR

Real-time PCR is also referred as quantitative PCR (QT-PCR). The development of real-time PCR is mainly driven by the obvious demand for quantitative information that cannot be convincingly obtained when using conventional PCR.^{143, 144} Basically, conventional PCR is a qualitative assay answering yes/no questions, with marginal variations in reaction components, thermal cycling conditions, and mispriming events particularly during the early stage of PCR greatly affecting the yield of amplified products. Therefore, it is difficult to attain a consistent relationship between the amount of starting template and absolute amount of amplified product. For better monitoring and obtaining quantitative information, real-time PCR was developed in last decade and soon transformed from an experimental tool into a mainstream scientific technology. Usually a marker (typically a fluorophore) is employed in the

PCR mixture, thus the increase in products after each cycle can be recorded as a stochastic change in marker signal (e.g. fluorescence). Real-time PCR detection provides a more complete picture of the PCR process than measuring the end-point products after a fixed number of cycles. So far, the detection techniques are mainly based on three types of fluorescence detection: dsDNA binding dyes, fluorogenic probes, molecular beacons and scorpion primers.

1. dsDNA Binding Dyes

The dsDNA binding dyes (also called intercalator dyes) are small molecules that fluoresce upon binding to dsDNA. As PCR amplification produces more and more dsDNA molecules, the fluorescence signal increases (Figure 1-9). There are two requirements for a suitable dye: its fluorescence must be negligible and increasing when bound to dsDNA and it must not inhibit PCR. The two most popular intercalator dyes are ethidium bromide and SYBR Green I.^{143, 145} This method is highly sensitive and versatile, as the dyes bind to any dsDNA present with no need for further optimisation. However, such flexibility is also a major drawback because the dyes do not distinguish between specific and non-specific products, and mismatches, and primer-dimers also give fluorescence signals, making it difficult to differentiate them apart.

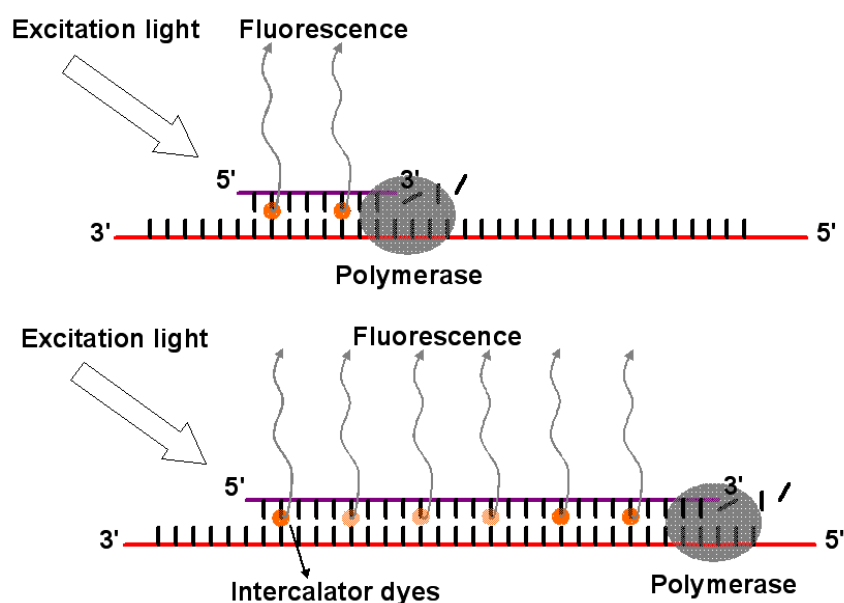


Figure 1-9 Real-time PCR based on dsDNA binding dyes

2. Fluorogenic Probes

The fluorogenic probes (e.g. hydrolysis probes or TaqMan™ probes) are developed in order to enhance the selectivity of real-time PCR.¹⁴⁶ The probe is a short oligonucleotide, which is complementary to a region of the target sequence between the two primers. A fluorescent reporter is attached to the 5' end of the probe, and a quencher to the 3' end. As long as the probe is intact, the proximity of the quencher reduces the fluorescence emitted by the reporter due to a quenching phenomenon known as Fluorescence Resonance Energy Transfer (FRET). The probes are added to the PCR mixture and anneal to the target complementary sequence. At this stage, the fluorescent signal is quenched due to the proximity of reporter and quencher. During the extension step, the polymerase cleaves the reporter from the probe due to its 5' exonuclease activity. As soon as the reporter and quencher are separated, the reporter fluoresces in the reaction mixture (see Figure 1-10).

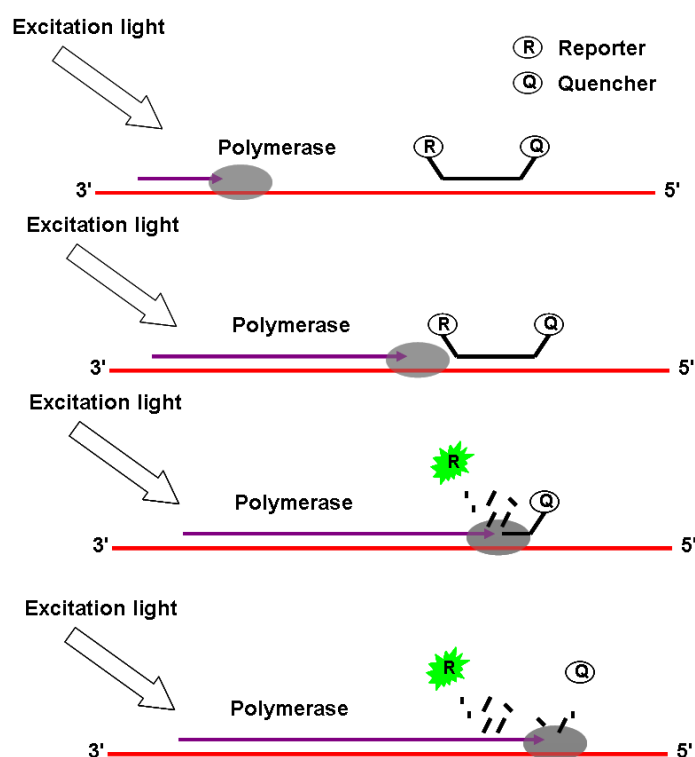


Figure 1-10 Real-time PCR detection based on fluorogenic probes.

The intensity of the reporter fluorescence after each cycle is directly proportional (stochastic) to the number of amplified products. Furthermore, as the probe's sequence is complementary to the part of the target, this method is highly specific with non-specific products not being detected. Multiple probes with different reporters can be used for simultaneous detection of a number of distinct sequences.

3. Molecular Beacons

Molecular Beacons (or conformation probes) consist of a hairpin loop structure, with the loop complementary to a target DNA and the stem formed by the annealing of complementary termini.^{143, 147} A reporter probe is attached to one end of the stem and a quencher to the other. As the stem arms have complementary sequence, they hybridise to each other, causing the fluorescence signal to be quenched by FRET. During the denaturation step, the stem loop is opened. At the annealing temperature, the loop part binds to its target sequence. Once the probe binds to its target, the hairpin is opened and fluorophore and quencher becomes spatially separated from the reporter moiety, resulting in reporter fluorescence. When the temperature is raised to allow primer extension, the Molecular beacons dissociate from their targets and do not interfere with polymerization. A new hybridisation takes place in the annealing step of each cycle, and the intensity of the resulting fluorescence indicates the amount of the accumulated amplicons. (see Figure 1-11) This technique differs from fluorogenic probes because probes are not destroyed so signal stays at a maximum at each cycle. Real-time PCR detection based on Molecular Beacons have been applied to virus detection^{148, 149} and SNP analysis.^{150, 151}

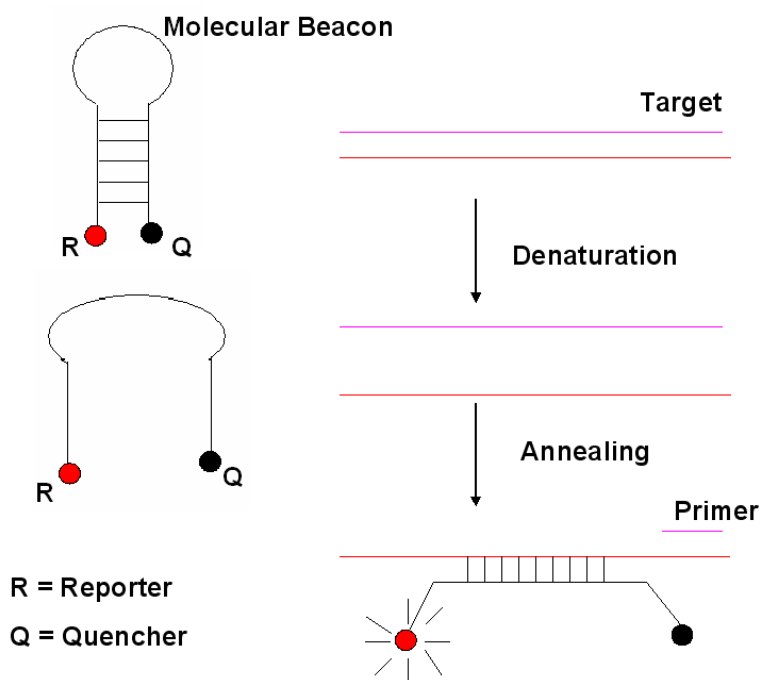


Figure 1-11 Real-time PCR detection based on molecular beacons

4. Scorpion primers

Scorpion primers are an alternative to molecular beacons. A scorpion primer consists of a three-part molecule based on the following structure: [PCR primer] - [blocker molecule] - [molecular beacon]. During the PCR process, the primer hybridises to the target molecule and is then extended. Upon denaturation, the extended-DNA-strand/target hybrid is dissociated and so are the two arms of the stem. Once the temperature goes down for the annealing / extension steps, the loop-part of the molecular beacon anneals to the extended strand and fluorescence is detected. Upon extension the probe is displaced and a drop in the fluorescence signal can be monitored (see Figure 1-12). This detection method is particularly well suited for fast detection systems as it relies on a single-molecule process. Indeed, once the Scorpion primer is extended, the probe and its complementary sequence are on the same strand. A direct consequence is that this proximity provides for a fast hybridization process. Detection with a molecular beacon or a TaqMan™ probe is a multi-molecular reaction and involves the diffusion of at least two molecules, thus increasing detection times.

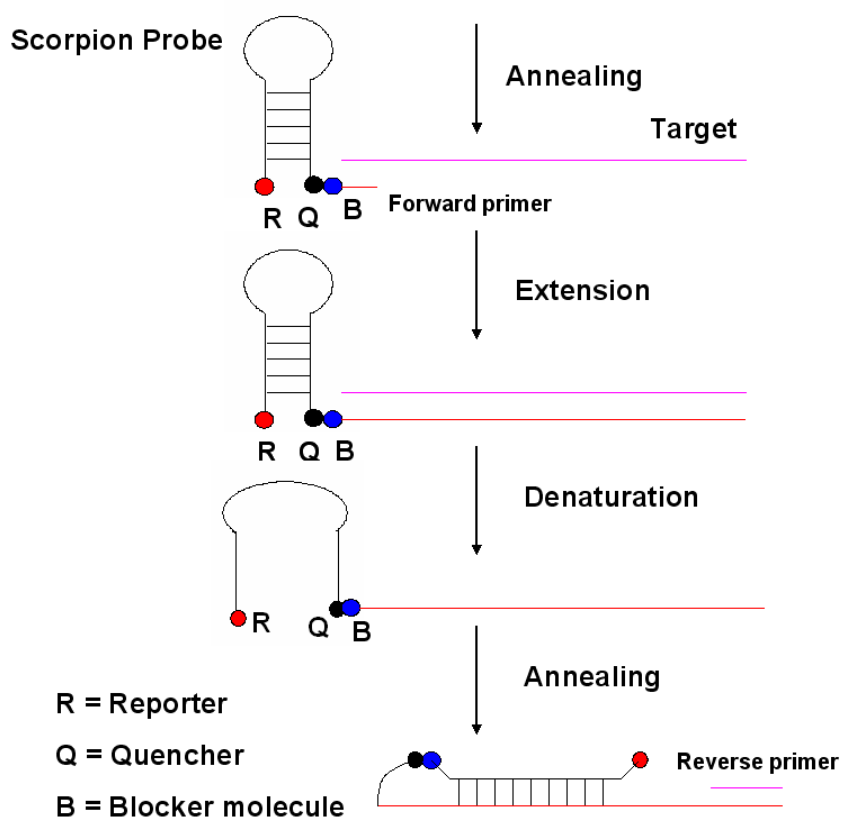


Figure 1-12 Real-time PCR detection based on scorpion primers

1.3.3.2 Miniaturised PCR

PCR has revolutionized the life sciences and remains a ubiquitous enabling nucleic acid analysis tool. Not surprisingly, a host of miniaturised PCR formats have been developed (Figure 1-13)^{47, 102} for many reasons including those that follow.

Miniaturised PCR gives several advantages such as high thermal cycling speed and low reagent consumption, which benefit from intrinsic high surface-to-volume ratio. The comparison of conventional PCR and miniaturised PCR is listed in Table 1-2.

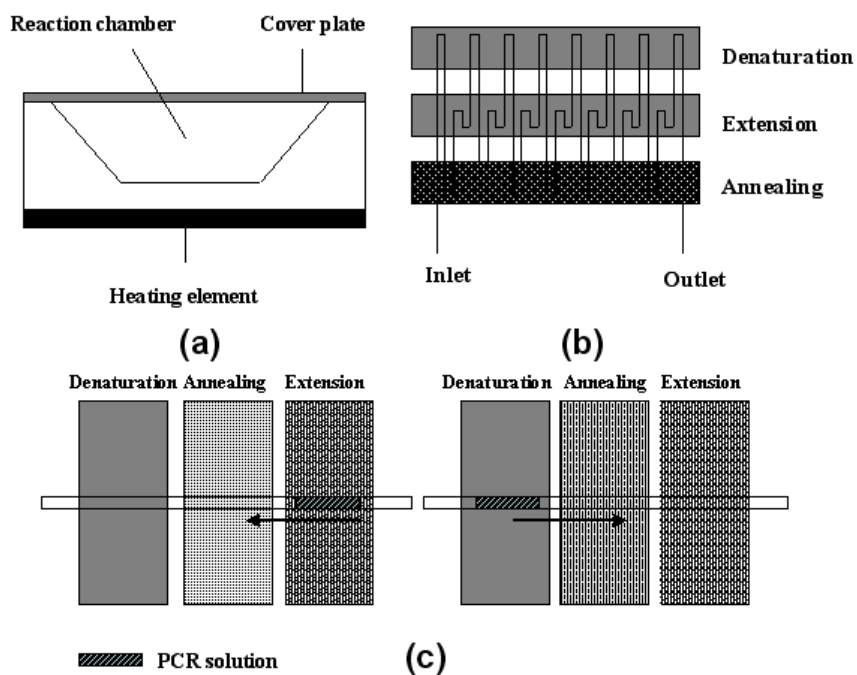


Figure 1-13 (a) Chamber stationary PCR, in a similar manner to conventional PCR but with a relatively small volume; (b) Continuous-flow PCR, samples are thermocycled in a spatial way instead of temporal way; (c) Shunting PCR, a combination of the former two methods with flexibility, high-speed and high-density of reactions.

Table 1-2 Conventional PCR vs. Miniaturised PCR

	Conventional PCR	Miniaturized PCR
Thermal Cycle Time	1-2 h	Mins- 2 h
Required Sample Volume	$\geq 3 \mu\text{L}$	pL - μL
Integrated Sample Preparation	Difficult for automation	Highly possible
Integrated detection	Yes	Yes
Sample throughput	High	Very high
Limit of Detection (LOD)	Single molecule	Single molecule
Instrument Cost	10 – 40 k €	30 k €

Commonly, commercial PCR instruments operate with a stationary, or static, mixture in reaction wells with heat exchange between a thermal block for alternating the temperature. With microchip-based PCR the onus is on thermal isolation to provide a minimal thermal mass for rapid temperature ramping. With the high surface area to volume ratios afforded by microchip cavities this can be achieved in static mode.¹⁵²⁻¹⁵⁵ (see Figure 1-13a) The development of continuous flow mode PCR systems provides an ingenious alternative, with the reaction mixture instead being driven along a microchannel incorporating spatially defined temperature zones.^{156, 157} (see Figure 1-13b) Here the thermal mass is limited to that of the sample volume alone, and temperature ramping is principally dictated by flow velocity. However, this format requires a large device footprint to accommodate all thermal cycles even when a serpentine channel arrangement is used.^{156, 157} In addition, the ratio of residence times in the different temperature zones is dictated by device fabrication, and application diversity becomes greatly limited. Lastly, the massive surface area presented by the microchannel (typically 1 to 2 m in length) causes reagent losses during fluid movement often through reagent surface adsorption and sample fractionation, resulting in efficiency losses that typically lead to complete reaction inhibition.^{156, 157}

To address these drawbacks, several reconfigurations of the continuous flow format have been developed. For example, cycle number flexibility, ease of real-time detection implementation and significant footprint reductions can be achieved using an annular microchannel with literal reagent cycling.^{158, 159} However, like the continuous flow format this approach does not overcome Taylor dispersion produced by the flow parabolic velocity profile and this results in marked temperature dwell time variability. To combat this problem a plug flow can be employed, and has been used within bidirectional flow PCR systems.(see Figure 1-13c). Besides the flexibility of cycle number and dwell time, this format offers the benefit of rapid heat exchange like continuous flow reactors, with the small footprint and moderate surface area to

volume ratio of static microreactors. These bidirectional flow systems have been used for complete thermocycling reactions in minutes.^{160, 161}

So far, real-time PCR has been demonstrated to offer one of the most effective means to quantify the DNA sample by recording the increase in fluorescence resulting from the stochastically associated measurement of fluorescence with increased dsDNA production after each round of thermocycling. Recently, real-time PCR on micro-device has gained much interest. Most of the reports are based on stationary PCR due to its ease of adaptation to internal or external optical detection system.¹⁵²⁻¹⁵⁵ The real-time detection for continuous-flow PCR on chip is difficult, since it needs multiple detectors for use in each channel (each cycle), or the added complexity of a movable detection unit to scan all the channels.¹⁶²

1.4 Research Aims

To succeed with full on-chip genetic analyses, general protocols for biological sample treatment are well-established, which normally involve nucleic acids extraction (e.g. tissue, blood, cell and etc.), analyte amplification (e.g. PCR and RT-PCR) and products analysis (real-time quantitative PCR, slab gel electrophoresis, CGE, DNA array, reporter signal amplification). μ -TAS shows a great capability for assembling different functional units for genetic analysis of various samples or diverse purposes. For current miniaturised PCR systems, several procedures such as sample pre-treatment, delivery, reaction efficiency, and detection sensitivity need simultaneous optimisation, which will greatly facilitate the application of miniaturised systems for use genetic research.

As shown in Figure 1-4, to date, pre-PCR has not been extensively studied and it is difficult to obtain quantitative information of analytes before sending them for subsequent PCR. The quantitative information from pre-PCR is useful for absolute quantification in many fields, where the amounts of specific molecules per cell and

range of molecule numbers across a cell population are both needed for a complete genetic diagnosis.

Although quantitative studies have been reported regarding real-time PCR and post-PCR, the majority of these start with known amounts of nucleic acids. The applications with unknown samples are limited to the qualitative studies due to the uncertainty relating to the amount of nucleic acids entering PCR. Thus, in order to comprehensively realize quantitative studies for genetic-based diagnoses, the functional components that collectively represent an integrated PCR microfluidic device will have to be developed synergistically and in multiple directions, such as; detection units, sample delivery, increasing sensitivity and handling of populations of cells.

Three major issues have to be addressed before quantitative information can be obtained from biological samples using μ -TAS devices.

First, nucleic acid extraction from a complex matrix with quantitative information is required. The first part of my Ph.D. research thesis is to develop a miniaturised ITP device which enables DNA to be isolated and concentrated using a suitable electrolyte system and investigate the behaviour of DNA under the conditions of miniaturised ITP. After that, the performance of miniaturised ITP for nucleic acid purification and concentration will be further tested by using a complex matrix sample including cell lysates.

Secondly, a functional unit pre-amplification for whole genomic DNA is necessary for long-term tracking studies and establishing miniaturised DNA archives. Thus in the second part of my research, miniaturised devices are applied for miniaturised WGA based on the MDA method and the products are used for subsequent genotyping assessments, and with the benefit of reduced contamination risk offered by miniaturisation when compared to conventional WGA applications. In addition, this

approach may offer an enhanced and more cost effective means to maintaining a sustainable DNA archive compared to currently employed procedures.

Lastly, coupling real-time detection with a miniaturised PCR system needs to be further optimised in order to achieve a fast and reliable quantitative analysis. In the third part of my Ph.D. research, a bidirectional shunting miniaturised platform combining advantages of both static and continuous flow PCR is developed, which enables temperature dwell time and cycle number flexibility (see Figure 1-13c). And this platform can be readily adapted to real-time fluorescence detection. Furthermore, such a device has been used for practical applications related to real-world samples such as human genomic DNA.

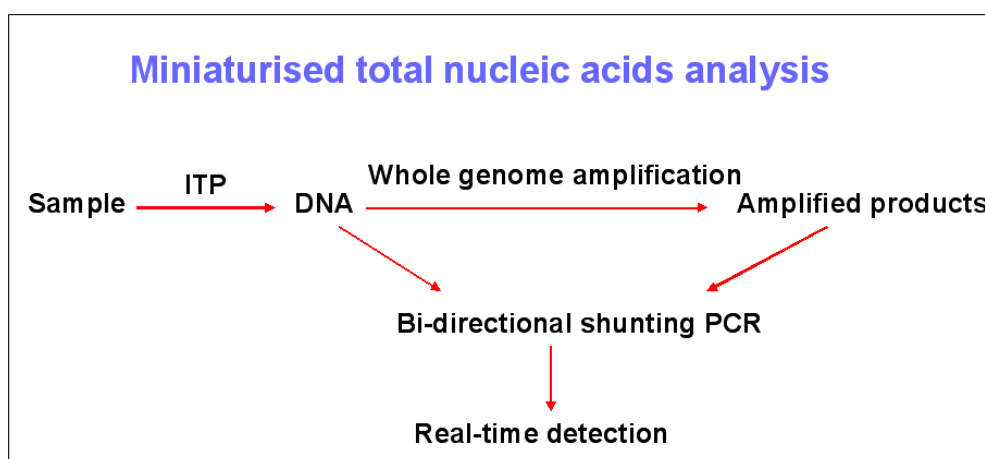


Figure 1-14 Diagram of miniaturised total nucleic acids analysis device

The purpose of my Ph.D. research is to address these three issues by establishing a miniaturised system capable of extracting nucleic acids directly from cell lysates using ITP, MDA pre-amplification of whole genomic DNA and real-time detection of PCR for quantitative information. The three systems developed in this thesis should be adaptable to application in current miniaturised platforms to ultimately form a fully integrated device capable of quantitative nucleic acid analysis. A schematic representation of such a device is shown in Figure 1-14. DNA purification from biological samples by ITP, pre-amplification by whole genome amplification and

subsequent real-time detection of PCR amplified specific gene regions are performed in a seamless and continuous fashion. Such a nucleic acid μ -TAS device will greatly facilitate absolute quantification of nucleic acids for in-vitro diagnostics and point-of-care applications.

The first objective of my research is to use miniaturised ITP for directly pre-concentration of genomic sample from cell lysates with quantitative information for subsequent applications. The set-up will be validated by using pure genomic sample such as salmon sperm DNA and Torula yeast RNA. The qualitative and quantitative information of the analytes should be obtained simultaneously.

The second objective of my research is to amplify the whole human genomic DNA with high fidelity by applying miniaturised microchips. The device should be able of high-throughput processing multiple samples with lower reagent consumption compared to that of conventional methods. The fidelity of amplified products should be checked with real human genomic DNA on different gene regions.

The third objective of my research is to build up a bi-directional flow PCR microreactor combining the advantages of both stationary and continuous-flow miniaturised PCR. The device should be real-time detectable with a comparable performance to conventional machines. In addition, the device should also be easily coupled with the miniaturised system mentioned above to achieve a fully integrated quantitative analysis of human genomic DNA.

Chapter 2

Experimental Section

2.1 Miniaturised ITP for Nucleic Acid Purification

2.1.1 ITP Microchip Fabrication

The miniaturised ITP chip was fabricated by using direct milling of a 78 mm square, 6 mm thick PMMA block as previously reported,¹⁶³ except different configuration of the chip design was made which incorporated a simple straight separation channel and a typical double-T conjunction for sample injection purposes and only one integrated conductivity detector. Briefly described here, the design was created using Mechanical Desktop (Autodesk, San Rafael, CA, USA) and tool paths, for a CAT 3D precision milling machine (Datron, Mühlthal, Germany), computed with Edge-CAM software (Pathtrace, Southfield, MI, USA). Then two slots were milled into the substrate to produce the housing for the integrated conductivity detectors. These slots were cut such that they would be perpendicular to the separation channel, when this was subsequently milled and located in the desired position for the detectors. Access holes were also drilled through the whole thickness of the PMMA block into the ends of these slots. A schematic layout of the device is shown in Figure 2-1. The channels were all 300 μm wide and 200 μm deep. The total length from well A to C was 60 mm. The detector electrodes were positioned 13 mm from well A. The length for double-T area was 2 mm, thus the injected sample volume was 120 nL.

2.1.2 Instrumentation

Sample injection and movement of solution inside the channels was achieved using a hydrodynamic sample transport system, which comprised of a series of reservoirs with associated LFAA1201718H two way solenoid actuated valves (The Lee Company, Westbrook, CT), as shown in Figure 2-1. Valves A and B were connected

to the barrels of a 20 mL disposable plastic syringe while valve C was connected to a 5 mL syringe. Valve D was connected to a waste container. All interconnections were made using 0.8 mm internal diameter fluorinated ethylene-propylene co-polymer (FEP) tubing (The Lee Company, Westbrook, CT). Prior to where these tubes enter the device a small portion of the FEP tubing was replaced by 1.0 mm internal diameter stainless tubing (Superlco, Poole, UK) which acted as the drive electrode for the performing separations. Connections to the valves and the separation device were made using 062 MINSTAC couplings (The Lee Company, Westbrook, CT).

A PS530 high voltage power supply (Standford Research Systems, Sunnyvale, CA, USA) configured to supply negative voltages was used to provide the constant voltage required to drive the separations. The conductivity detector for the microfluidic chip is a development of the previously reported design, which uses capacitive coupling as a low cost method of isolating detector circuitry from the high voltage fields used to drive electroseparations¹⁶³. The design used simple oscillators coupled to the detection electrodes so that the conductance between the electrodes determined the frequency of the oscillation, which formed the basis of the output.

Control of the sample transportation, high voltage power supply and conductivity detector was achieved using LabVIEW software (version 6.1) (National Instruments, Austin, TX, USA) on a standard PC. The hardware interface was achieved using three National Instruments cards controlled using the NIDAQ driver (National Instruments) and programmed using LabVIEW code. The cards used were a PCI-GPIB board for the power supply, a PCI-6601 timing and digital input/output board for the detector and a PCI-6503 digital input/output card for the fluid transportation. A further LabVIEW program was employed for data processing. All of the LabVIEW programmes used were written in-house.

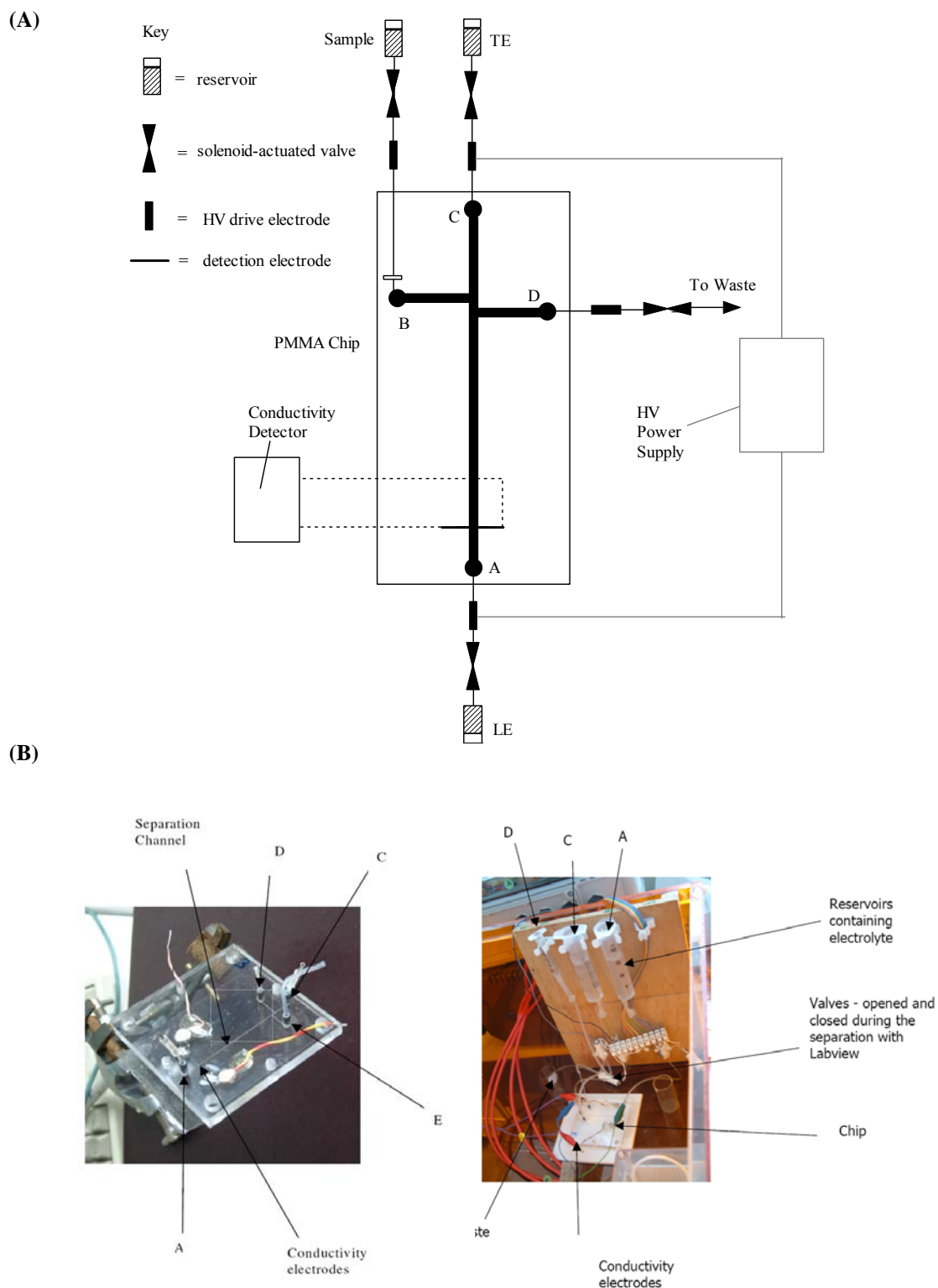


Figure 2-1 (A) Schematic diagram of PMMA ITP microchip. All channels were 300 μm wide and 200 μm deep. (B) (Left): Instrumental setup A: LE buffer, C: TE,

D: sample; (Right): ITP microchip with conductivity detector A: Inlet (LE), C: Inlet (TE), D: Inlet (Sample), E: Outlet (waste).

2.1.3 Separation Conditions

All of the separations performed in this investigation were achieved using the control programme shown in Table 2-1. The system was flushed and the device loaded with leading electrolyte in step 1. Terminating electrolyte was then loaded in step 2. Step 3 injected the sample into the device and filled the separation channel of the double-T section (2 mm in length), thus giving an injection volume of 120 nL. The actual ITP separation was performed in step 4 with a voltage of 1,000 V applied between A and C.

Table 2-1 Separation programme used to carry out miniaturised ITP separation

Step	Time/s	Voltage/V	Valve Status *				Fluid flow path
			A	B	C	D	
1	30	0	○	●	●	○	A → D
2	1	0	●	●	○	○	C → D
3	1	0	●	○	●	○	B → D
4	1000	1000	●	●	●	●	No flow

* ● = closed; ○ = open

2.1.4 Reagents and Materials

The compositions of the electrolytes used in the experiments are given in Table 2-2. The leading electrolyte was produced using chloride acid with Mowiol 40-88 (Aldrich, Gillingham, Dorset, UK) added to suppress electroosmotic flow (EOF). The pH of the leading electrolyte was adjusted using histidine (Aldrich, Gillingham, Dorset, UK). The terminating electrolyte was 2-(N-morpholino)ethanesulfonic acid (MES). DNA samples were prepared using low molecular weight salmon sperm DNA

(Fluka) and RNA samples were prepared from Torula Yeast RNA (Sigma-Aldrich). Bovine serum albumin (BSA) and yeast extract were obtained from Sigma-Aldrich. Samples and electrolyte were prepared using 18 M Ω water (Elga Maxima Ultra Pure, Vivendi Water Systems, High Wycombe, UK).

Table 2-2 Composition of the electrolyte system for the miniaturised ITP separation of nucleic acids

Electrolyte	Leading	Terminating
Ion	HCl	MES
Concentration (mM)	5	10
pH buffer	6.0	-
pH	Histidine	-
Additive	Mowiol 40-88	-
Concentration (g/L)	0.5	-

2.1.5 Yeast Cell Lysis

Cells were grown overnight at 30°C in 10 – 12 mL Yeast Peptone Dextrose (YPD), collected by centrifugation at 2,000 rpm for 5 min and the supernatant was discarded. The cells were then resuspended in 1 mL 1M sorbitol, 0.1 M Na₂EDTA (pH 7.5) and transferred to a 1.5 mL Eppendorf tube. 40 μ l of a 2.5 mg/mL solution of lyticase was added and the tube was incubated at 37°C for 1 h. After centrifuge for 1 min, the supernatant was discarded and the cells were resuspended in 1 mL of 50 mM Tris (pH 7.4), 20 mM Na₂EDTA. 100 μ l 10% sodium dodecyl sulfate (SDS) was added, mixed thoroughly and incubated at 65°C for 30 min. The supernatant was collected and used as yeast cell lysate in further experiments.

2.2 Miniaturised WGA

2.2.1 Microchip Fabrication

The aluminum master mould for microchip fabrication was constructed using micro-machining. The master contained 70 cylinders (2 mm in both diameter and depth) with 4 mm distance between cylinder centres. Poly (dimethylsiloxane) (PDMS) prepolymer and curing reagent (Sylgard 184, Dow Corning) were thoroughly mixed, degassed, and then poured onto the aluminum master mould. After curing at 80 °C for 1 h, the PDMS was peeled off from the master and bound to a glass slide (60 mm × 24 mm × 0.1 mm) following oxygen plasma treatment. The photograph of the microchip array is shown in Figure 2-2.

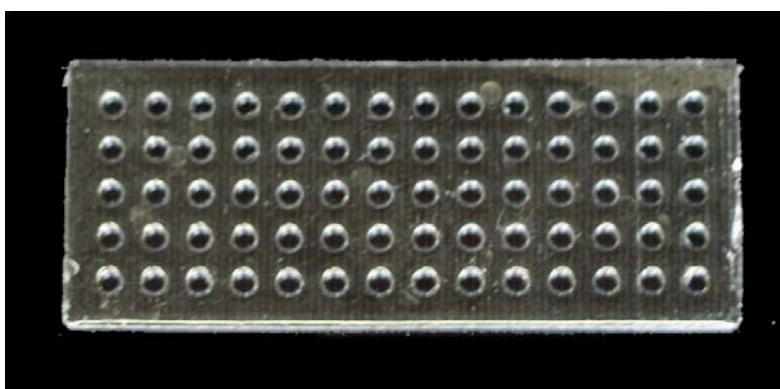


Figure 2-2 Photograph of 70-well PDMS microchip array

2.2.2 Reagents and Materials

Human genomic DNA, TaqMan® Universal Master Mix, and the detection reagent kit for the unique single copy gene RNase P were obtained from Applied Biosystems (Foster City, CA). GenomiPhi V2 DNA Amplification Kit containing sample buffer, reaction buffer and Phi29 DNA polymerase was obtained from GE Healthcare. Dichlorodimethylsilane (DCDMS) was purchased from Fluka.

2.2.3 Microchip Silanisation

The whole PDMS microchip was rinsed with ethanol, pure water and dried under hydrogen gas. Then selected wells were washed with acetone, chloroform, filled with silanisation solution (5% DCDMS in chloroform), incubated for 30 min, and dried under hydrogen gas.

2.2.4 WGA on Microchips

9 μL of sample buffer and 1 μL human genomic DNA were mixed on ice. 9 μL of GenomiPhi reaction buffer and 1 μL of the Phi29 polymerase were added. For both conventional and on-chip real-time WGA monitoring, additionally 0.2 \times SYBR Green I (Invitrogen) was added, gently vortexed and centrifuged. Samples were incubated at 30 $^{\circ}\text{C}$ for 2 h, and then 65 $^{\circ}\text{C}$ for 10 min (to inactivate the Phi29 polymerase) using a conventional thermocycler (Mastercycler 5332, Eppendorf).

For on-chip WGA, 2 μL of sample prepared as above was pipetted and loaded into a well on a PDMS microchip. To prevent the evaporation of the reaction mixture, 2 μL mineral oil was used to cover the reaction well, and a transparent optical cover film was used to further seal the well. The whole chip was incubated on a conventional PCR machine (PTC-200, MJ Research) using the same thermocycling programme used for temperature profiling as noted above.

Conventional WGA real-time monitoring was carried out on an ABI PRISM HT7900 (Applied Biosystems). Fluorescence intensities were collected via the SYBR Green I channel. For on-chip real-time WGA monitoring, the chip was placed on the top of two Peltier elements mounted on a microscope stage. The temperature of the wells for analysis was maintained at 30 $^{\circ}\text{C}$ and fluorescence intensity was measured at 1 minute intervals by manually opening and closing the shutter of a photomultiplier tube (PMT).

For all conventional and on-chip WGA experiments, a no template control (NTC) for each sample is run in parallel by replacing the DNA template with 1 μ L water.

2.2.5 WGA Product Analysis

WGA products amplified conventionally, on PDMS microchip and unamplified human genomic DNA were analysed using standard 0.8% agarose slab gel electrophoresis. The total DNA concentrations of all WGA products were measured with the Nanodrop ND-1000 spectrometer (Nanodrop Technologies).

2.2.6 Real-time Quantitative PCR

Both WGA and unamplified human genomic DNA samples were used as templates for subsequent real-time PCR using the ABI TaqMan[®] RNase P detection reagent kit. The PCR mixture consisted of 1 \times TaqMan[®] Master Mix, 1 \times RNase P primer-probe mix as recommended by the manufacturers. 1 μ L unamplified genomic DNA (1 ng), 1 μ L conventional WGA product and 1 μ L chip WGA product were both amplified from 1 ng human genomic DNA and were used as templates. Loci representation efficiency (WGA product/unamplified DNA) is reported as (loci copy number/mass of WGA products) / (loci copy number/mass of unamplified DNA).

2.2.7 Single-Nucleotide Polymorphisms (SNPs) Analysis

Samples from 8 individuals were genotyped using on-chip amplified and unamplified human genomic DNA by employing two customised TaqMan[®] SNP Genotyping Assays (SNP1: rs2069718, A/G; SNP2: rs13900, C/T, from CIGMR, University of Manchester, UK). 0.5 μ L of a 20 \times mix of primers and probes, 5 μ L of TaqMan[®] master mix, 1 μ L of DNA template and 3.5 μ L water for each reaction were subjected to thermal cycling conditions comprising of 50 $^{\circ}$ C for 2 min and 95 $^{\circ}$ C for 10 min then 40 cycles of 95 $^{\circ}$ C for 15 sec and 60 $^{\circ}$ C for 1 min. Genotypes were obtained by

reading fluorescent signals of the reaction end products on an ABI PRISM 7900HT analyzer.

2.3 Bidirectional Shunting PCR with Real-time Detection

2.3.1 Device Assembly and Operation

A 1.0 mm i.d. glass capillary with a wall thickness of 250 μm was cast within a sheet of PDMS made from 10 parts prepolymer and 1 part curing agent (Sylgard 184, Dow Corning). Critically, the capillary was positioned at one face for direct contact with the heating elements. Two 12 \times 18 mm footprint Peltier elements (QC-17-1.0-3.9M, Quick-Ohm-Küpper & Co. GmbH, Germany) were placed in close contact to the device via 2.5 mm thick aluminium heat sinks. Temperature sensors (AD 590) were mounted on each aluminium block and used with a proportional-integral-derivative (PID) controller for feedback of temperature control. Good thermal contact between the device and heaters was achieved by clamping the elements in a PMMA housing. The bidirectional shunting PCR system is shown in Figure 2-3. For temperature calibration within the capillary a K-type thermocouple (Pt30, TC Ltd) was inserted and measurements were recorded (TC-08, Pico Technology Ltd). The movement of the sample plug was driven by a Kloehn syringe pump, connected via Teflon tubing and controlled using a home-written LabVIEW programme. The temperature zones were stabilized at 95°C for denaturation and 60°C for both primer annealing and extension. The reaction mixture was flanked by mineral oil to form a plug to eliminate evaporation during thermocycling.

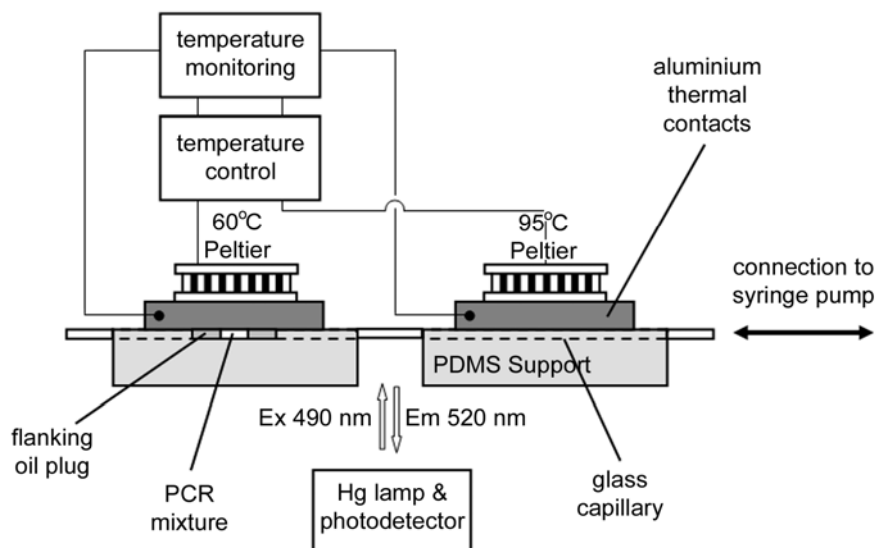


Figure 2-3 Schematic illustration of the bidirectional shunting thermocycling system.

2.3.2 Silanisation

The glass capillary was silanised with dimethyldichlorosilane (DMDCS) according to the protocol described by Obeid *et al.*¹⁵⁷ Briefly, the glass capillary was rinsed with deionised H₂O, washed with acetone and dried under a N₂ stream. The glass capillary was filled with 5% (v/v) DMDCS (Fluka) in chloroform and placed in a desiccator for brief vacuum boiling. The silanisation mixture was removed by evaporation, and the glass capillary was cleaned with a sequence of chloroform, acetone and deionised H₂O, with drying under a N₂ stream. For re-silanisation, additional treating with 10% NaOH for 30 min is performed in order to remove any previous silane monolayer.¹⁶⁴

2.3.3 Silanisation Effect Testing

For testing the silanisation effect, The PCR was based on a RNase P mimic template oligo possessing uracyl moieties (5'-TGGUTGUGAAGACGTCGUUGAACCAACCC-AT ACAUCATCCGCUGGAGCGCTGGAGAGCGAGGAUATGCA-3') and forward primer (5'-TGGTTGTGAAGACGTCGTTGA-3') and reverse primer (5'-TGCATATC-CTCGCTCTCCAGA-3') purchased from Sigma Proligo (Paris, France). The PCR mixture consisted of 1 × TaqMan[®] master mix (Applied Biosystems, Foster City, CA)

containing buffer, dNTPs, modified DNA polymerase from *Thermus aquaticus*, 3.5 mM MgCl₂, 330 nM of each primer and 0.1 ng/μL DNA template. The thermocycling programme consisted of 10 min at 95 °C, followed by 40 cycles of 15 s at 95 °C and 60 s at 60 °C.

2.3.4 Microchip Gel Electrophoresis

Both bidirectional shunting and conventional PCR amplicons were analyzed using the Experion automated electrophoresis system (Bio-Rad Laboratories GmbH, Munich, Germany) following the protocol provided by the manufacturer.

2.3.5 Real-time Detection of Bidirectional Shunting PCR

The whole device was adapted to the Caliper Labchip 42 MDS system equipped with fluorescence detection for real-time detection. The microdevice, aluminium heating sinks and Peltier elements were mounted on the home-made X-Y stage via double-sided tape to ensure a good thermal contact between each other (see Figure 2-4). The PCR mixture (20 μL) consisted of 1 × TaqMan[®] Master Mix, 1 × RNase P primer-probe (FAM) mix (Applied Biosystems, Foster City, USA). Additional 0.1% (v/v) Tween 20, 0.01% (w/v) poly(vinylpyrrolidone) (PVP) and 0.2 μg/μL BSA were added to further protect the reaction from surface inhibitory effects. Different concentrations of human genomic DNA were used as templates. 2 μL of the reaction cocktail prepared above was used in each bidirectional shunting PCR experiment. The PCR reaction mixture was flanked by mineral oil to form a plug to eliminate evaporation during thermocycling. The thermocycling program for bidirectional PCR consists of 10 min hot-start at 95 °C, followed by 40 cycles of 15 s at 95 °C and 30 s at 60 °C. An excitation light (480 nm) was focused on the capillary between two temperature zones. Each time the PCR mixture plug was shunted from 60 °C to 95 °C zone after one cycle, the fluorescence signal was collected and recorded. The performance of bidirectional shunting PCR device was assessed by comparison with the data obtained by a conventional real-time PCR instrument (ABI 7900HT). The

thermocycling condition was the same as above except that 60 s was used at 60 °C for each cycle.

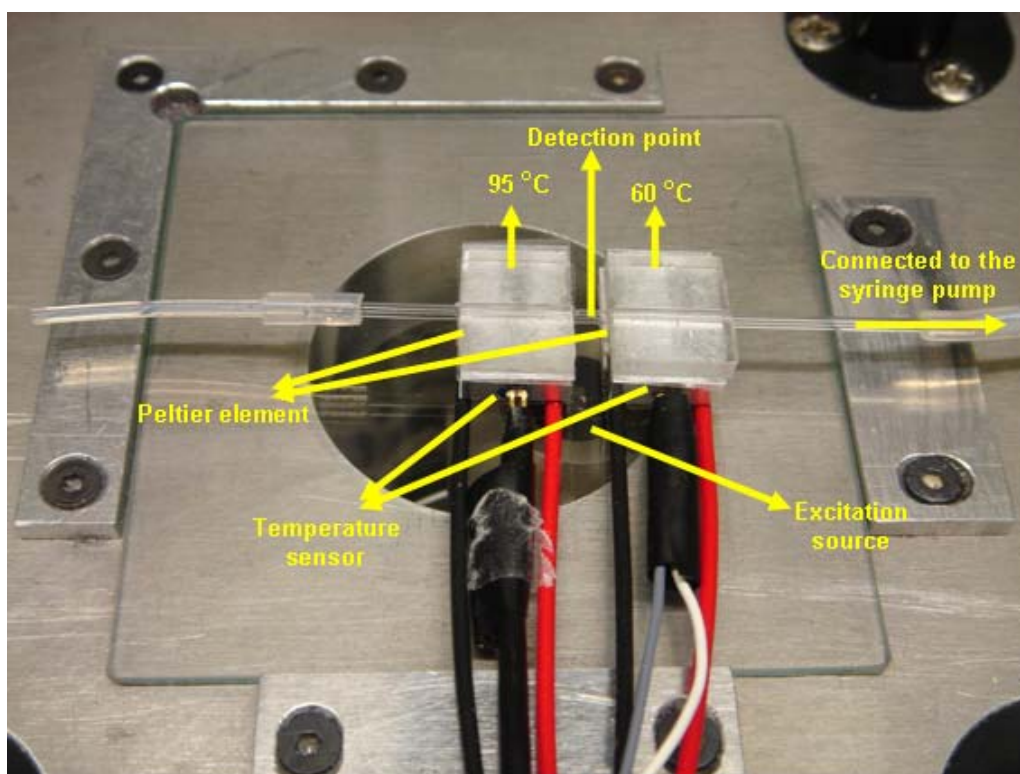


Figure 2-4 Setup of bidirectional shunting PCR with real-time fluorescence detection

Chapter 3

Results and Discussion

3.1 Miniaturised ITP for Nucleic Acid Purification

Isotachopheresis (ITP) is a member of the family of electroseparation techniques. It offers a number of useful features which are not found in capillary zone electrophoresis (CZE).^{165, 166} The most useful of which is the ability to control separation parameters by varying the composition of electrolytes used. The concentration of the leading electrolyte governs the concentration that all of the sample zones adopt, enabling ITP to be used as a method to purify and concentrate dilute samples to pre-determined concentrations. ITP is readily miniaturized and has been used with a wide variety of samples as evidenced a the range of previous applications.¹⁶⁷ However, so far there have been few reported uses of miniaturised ITP involving DNA samples as a pre-concentration method.^{33, 34, 110, 168} Additionally, there has been no report investigating the parameters of nucleic acids separation and concentration on a miniaturised platform.

In this section, we built up a miniaturised ITP system to investigate the isolation and pre-concentration of nucleic acids. An electrolyte system was chosen which enabled nucleic acids to be isolated and concentrated on a microchip device. The developed miniaturised ITP device was subsequently tested for isolation of nucleic acids from crude cell lysates.

3.1.1 Electrolyte System

The focus of this study is to simultaneously achieve extraction and purification of nucleic acids from a complex lysate using miniaturised ITP. In such circumstances, a primary demand is to develop a suitable electrolytic system that allows a pure zone of the particular species of interest (nucleic acids) to be produced by miniaturised ITP.

Fortunately, one of the exploitable features of ITP is the ability to adjust the buffer electrolytes to eliminate interference from other species present in the sample matrix. For example, the number of species can be restricted by using leading electrolytes and terminating electrolytes with a relatively small mobility difference between each other. Conversely, increasing the relative mobilities of these electrolytes also increases the number of species that can be resolved. In order to achieve a pure DNA zone, a leading electrolyte and a terminating electrolyte must be carefully selected with only a relatively small mobility difference between them that is conducive to DNA separation. So far, there has been no reported literature on the behaviour of nucleic acids in miniaturised ITP. Only one report applied free solution ITP as a pre-concentration method for capillary gel electrophoresis (CGE) separation, where DNA presents mobility slightly higher than that of acetate at pH 8.3 and DNA exhibits a constant charge-to-size between pH 6.0 and 8.0. Therefore, We choose 2-(N-morpholino)ethanesulfonic acid (MES) (10 mM) with a slower mobility under the condition of miniaturised ITP. The leading ion selected for miniaturised ITP is chloride, which is a well-known inorganic anion with high mobility, thus it should not cause any interference. Therefore, a leading electrolyte of pH = 6.0 was employed throughout the described experiments, and this pH also minimized potential interference from carbonate that arises from the dissolved atmospheric carbon dioxide. A low concentration (5 mM) of leading electrolyte is employed to avoid any possible precipitation problems. An additive polymer (Mowiol) was added to leading electrolyte suppress the EOF.

3.1.2 Miniaturised ITP for DNA samples

For preliminary experiments, a sample containing 2,500 µg/mL low molecular weight salmon sperm DNA (<2000 bp) was used. The results obtained under previously mentioned experimental conditions are showed in Figure 3-1 and Table 3-1.

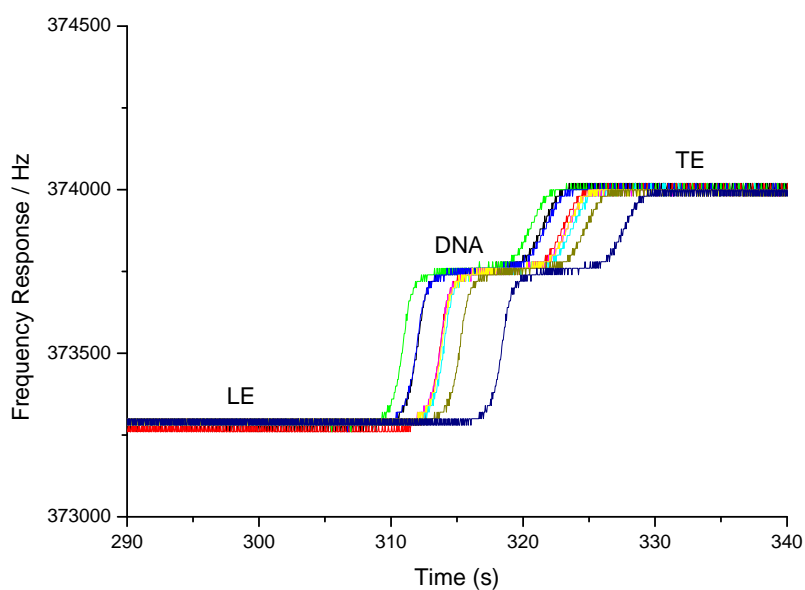


Figure 3-1 Miniaturised ITP separation of salmon sperm DNA (2,500 $\mu\text{g/mL}$), leading electrolyte (LE): 5 mM HCl, 0.5 g/L Mowiol, pH 6.0 (histidine); terminating electrolyte (TE): MES (10 mM).

Table 3-1 Results obtained with salmon sperm DNA (2,500 $\mu\text{g/mL}$)

Replicates	RSH	Zone Length (s)
1	0.642	9.57
2	0.647	9.42
3	0.666	9.67
4	0.661	9.74
5	0.645	9.68
6	0.660	9.65
7	0.662	9.48
8	0.657	9.49
9	0.640	9.30
Average	0.653	9.56
RSD	1.5%	1.5%

RSD = Relative standard deviation

The results showed that DNA produced a sharp zone when subjected to miniaturised ITP, which indicated that all of the DNA fragments were concentrated into a single zone. This is a promising result from a sample preparation perspective, since the choice of buffer electrolytes enable DNA to be concentrated to a predefined concentration of DNA.

We found that the isotachophoretic migration of DNA sample occurred in a reproducible manner. When nine consecutive runs were performed using 2500 µg/mL salmon sperm DNA sample, the relative step height (RSH) as determined by conductivity measurement was 0.653 ± 0.010 SD (See Table 3-1).

In our work, the RSH was calculated as the ratio of the sample step height to the height of the terminating step,

$$RSH = \frac{f_S - f_{LE}}{f_{TE} - f_{LE}}$$

where f_{LE} , f_S and f_{TE} represent the step heights of the LE, sample and TE, respectively.

When conductivity detection was applied in ITP, the step height provided qualitative information about the substances being analyzed. Furthermore, quantitative information could also be acquired from the zone lengths of the samples. The nine repeat runs of the 2,500 µg/mL salmon sperm DNA produced zone lengths \pm SD of 9.56 ± 0.143 s. The low concentration of leading electrolyte (5 mM) also allowed for a relatively fast analysis time. All the runs shown in Figure 3-1 were achieved in less than 6 min.

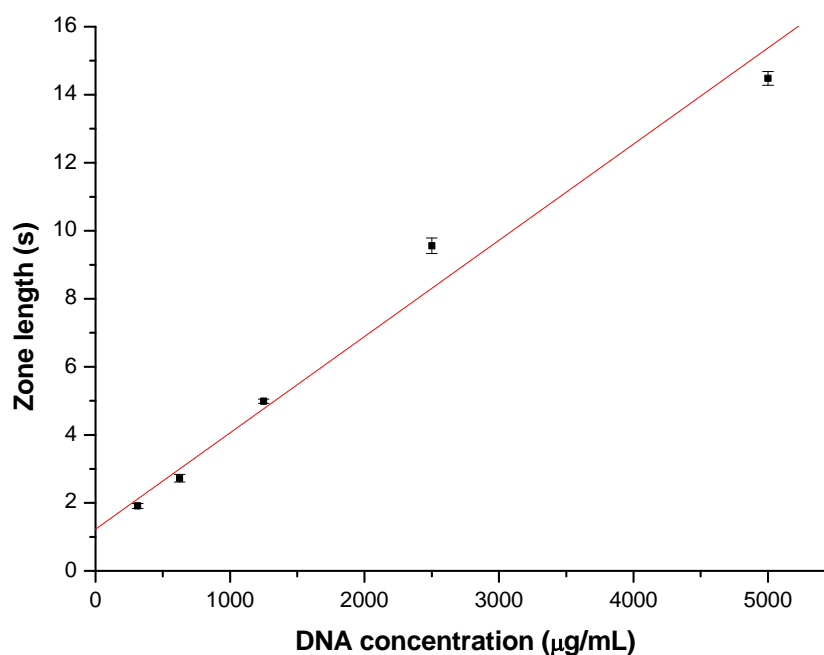


Figure 3-2 Calibration curve of salmon sperm DNA

One of the useful features of ITP which makes it suitable for sample preparation is that the concentration of the sample zones is an isotachophoretic stack of fixed concentration as noted above. This concentration is governed by the choice of the electrolyte buffer combination and approximates that of the leading ion. Thus the zone length of the sample should be proportional to its initial concentration. We investigated the dynamic range of DNA concentration over which the miniaturised ITP can be used. Four replicates runs were performed with each of the samples containing salmon sperm DNA ranging from 312.5 to 5,000 µg/mL. The results were used to check the linearity of the miniaturised ITP system by means of a calibration curve (see Figure 3-2). The parameters of the curve produced using weighted linear regression (Origin 7.0), showed a correlation coefficient of 0.991 with a slope of 0.00283 and an intercept of 1.23. The lowest concentration used in our experiments was not necessarily the limit of detection (LOD), but DNA samples of lower concentration did not give a well-defined step. This is not an issue in our case, because only pure salmon sperm DNA was used. However, for complex lysate

samples, this experiment would be difficult to perform unless a more sensitive LOD was determined. If this challenge was overcome, the miniaturized ITP method would be of great use for sample preparation and purification. Alternative optical detection methods such as UV-absorbance or LIF may offer a more sensitive detection, thus shorter zones could also be determined. But unlike universal conductivity detection, in order to realise the benefits from such an approach, the selection of electrolyte buffer pairs would be restricted since the optical detection method (UV or fluorescence) is a specific detection method that requires the analytes to be UV or fluorescence-detectable. Thus DNA samples can be bracketed by substances which are not detected by UV or fluorescence. Therefore the process can also be used to accurately determine when to move sample from the isotachophoretic stack to extract the required DNA sample for further applications.

3.1.3 Miniaturised ITP for RNA sample

We have also tested the possibility of applying the miniaturised ITP setup for the separation of RNA samples. 2,500 µg/mL Torula Yeast RNA was used as test samples in consecutive 9 runs. The results obtained are shown in Figure 3-3 and Table 3-2. The RNA sample showed a similar property in miniaturised ITP as the salmon sperm DNA sample, indicating that miniaturised ITP can also be employed for RNA preparation and purification. And these consecutive runs also showed good reproducibility for both RSH and zone length.

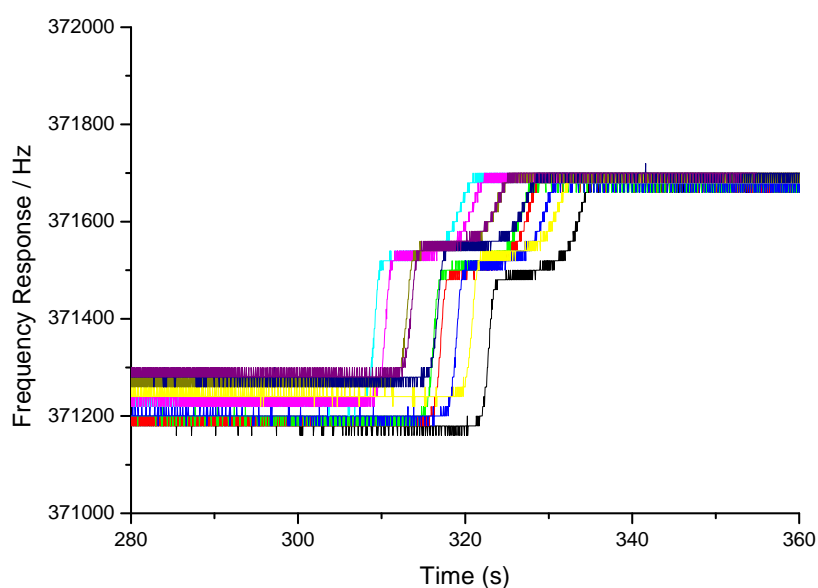


Figure 3-3 Miniaturised ITP separation of salmon sperm DNA (2500 $\mu\text{g/mL}$), leading electrolyte (LE): 5 mM HCl, 0.5 g/L Mowiol, pH 6.0 (histidine); terminating electrolyte (TE): MES (10 mM).

Table 3-2 Results obtained with Torula Yeast RNA (2500 $\mu\text{g/mL}$)

Replicates	RSH	Zone Length (s)
1	0.626	10.89
2	0.640	10.50
3	0.637	10.63
4	0.617	10.67
5	0.652	10.32
6	0.642	10.44
7	0.652	10.40
8	0.659	10.96
9	0.619	10.35
10	0.642	10.27
Average	0.639	10.54
RSD	2.2%	2.3%

3.1.4 Miniaturised ITP for a mixture of DNA and protein

In order to better mimic the real biological samples, which always consist of complex components with different mobility, we used a mixture of salmon sperm DNA and BSA (see Figure 3-4)

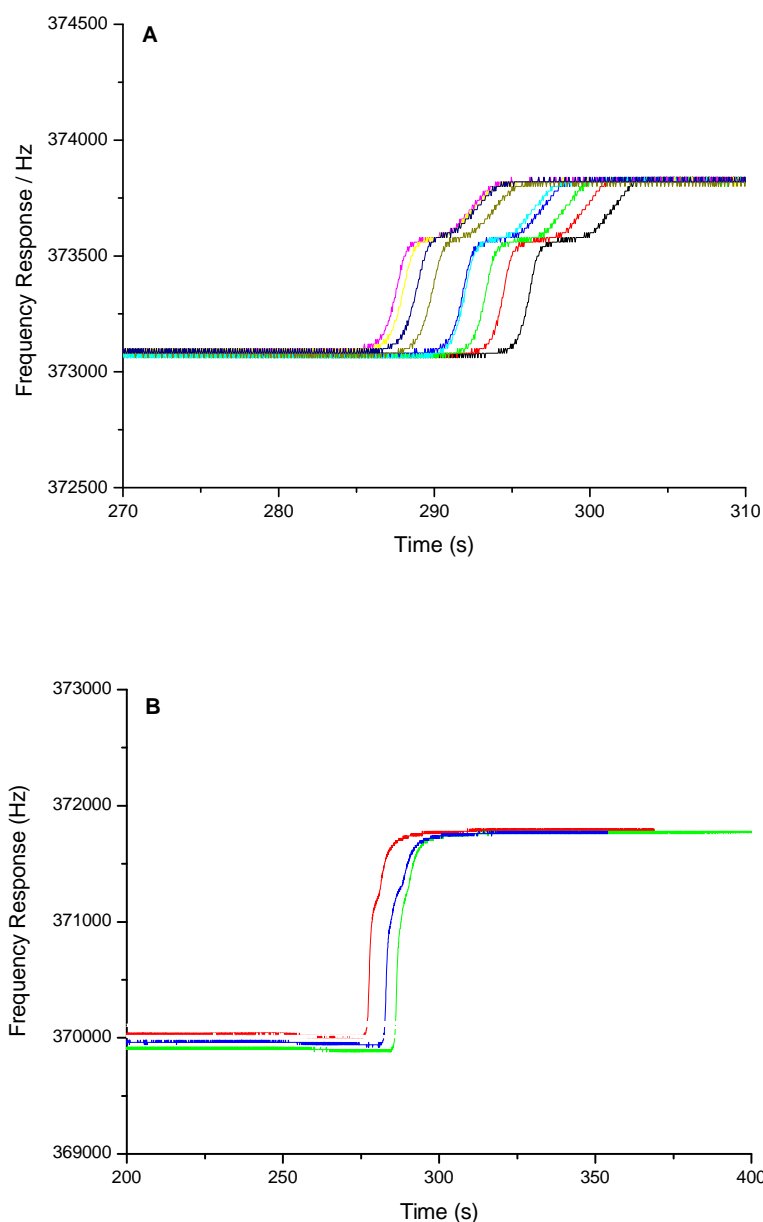


Figure 3-4 Miniaturised ITP separation of (A) mixture of salmon sperm DNA (1250 µg/mL) and BSA (500 µg/mL), and (B) BSA (500 µg/mL). Leading electrolyte (LE): 5 mM HCl, 0.5 g/L Mowiol, pH 6.0 (histidine); Terminating electrolyte (TE): MES (10 mM).

During the isotachophoretic separation, the pH of the whole electrolyte system is believed to be mainly governed by the leading electrolyte. Thus, under the current separation conditions (pH = 6.0), BSA was anticipated to move very slowly, even behind the TE buffer due to its lower effective mobility (PI = 4.7). From Figure 3-4B, we can see that there were no signals related to BSA, which was in agreement with our prediction. The miniaturised ITP separation of salmon sperm DNA from its mixture with BSA showed a similar performance as when BSA was absent, which indicated a good potential for miniaturised ITP to be used to separate and purify DNA from a complex mixture of proteins when adequate pH and electrolyte combinations are selected.

3.1.5 Miniaturised ITP for cell lysates

Cell lysates are a good general starting point for many biological analyses. Nucleic acid extraction from cell lysates is more typically performed either using phenol/chloroform extraction or the specific properties of a membrane from a commercial kit. These methods are expensive, and both of the processes are always labour-intensive and time consuming. Additionally, since the specific nature and content of samples are often varied or even unique if from a solid tissue, standardising sample extraction using conventional sample handling has not been accomplished¹⁶⁹ and may prove elusive in the longer term.⁵⁵ Therefore, sample preparation is a main obstacle for fully integrating miniaturised nucleic acid analysis platforms. There have been few reports of integrated sample preparation for nucleic acids.^{33, 34, 110, 168} From the experiments above, where we found that miniaturised ITP was suited to the purification of nucleic acids from a mixture including protein, we postulate that miniaturised ITP might be an enhanced method for standardising nucleic acid extraction and purification from cell lysates. Since miniaturised ITP was able to present a defined quantity of nucleic acids for subsequent molecular analysis, the output from an assay with a miniaturised ITP front-end has improved quantitative utility because the differences in results reflect analyte copy number rather than discrepancies related to the input of nucleic acid. Thus we also tried using our current

setup for the separation of nucleic acids from crude yeast cell lysates. The process for yeast cell lysis is described in section 2.1.5. The cell lysates were used directly as sample and injected into the miniaturised ITP microchip. The isotachophoregram is shown in Figure 3-5A. For comparison, a yeast extract sample devoid of nucleic acid was also used as sample for miniaturised ITP (Figure 3-5B).

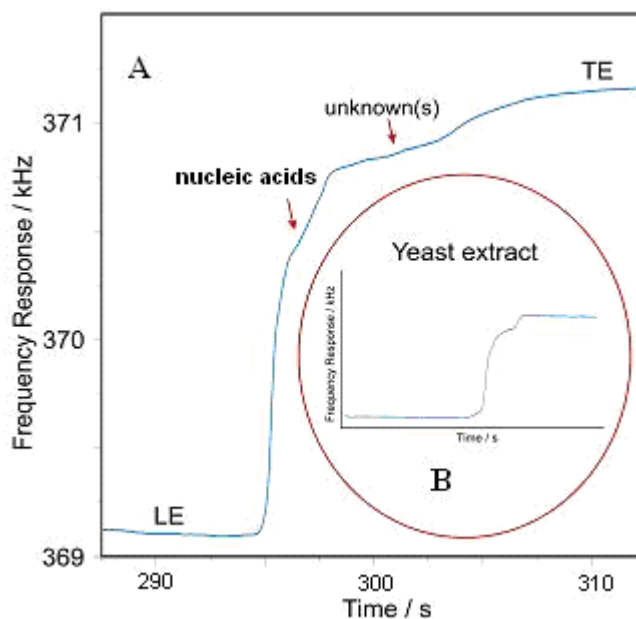


Figure 3-5 Miniaturised ITP separation of yeast cell lysates and (insert) yeast extract, leading electrolyte (LE): 5 mM HCl, 0.5 g/L Mowiol, pH 6.0 (histidine); terminating electrolyte (TE): MES (10 mM).

As can be seen from Figure 3-5, there was a sample zone apparent in the isotachopherogram of yeast cell lysates, which is not found in the isotachopherogram of yeast extract. The RSH of this step was similar to that of salmon sperm DNA obtained before (Figure 3-1), and also to that of yeast RNA (Figure 3-3). Since yeast extract was a mixture of amino acids, peptides, water soluble vitamins and carbohydrates which exist inside the yeast cells, the step that appeared in the isotachopherogram of whole yeast cell lysates probably represented nucleic acids from cell lysates that was removed from the yeast extract. The identification of a specific step for nucleic acids can be achieved by employing other detection

techniques with higher sensitivity, i.e. fluorescence detection using dyes that specifically binds to dsDNA. Fluorescence detection is a well-established detection method for miniaturised nucleic acid analysis (e.g. microchip CGE for DNA sizing), and should not be difficult to adapt it to a miniaturised ITP for nucleic acid identification by slightly changing the configuration of microchannel design and the separation buffer system. Some literatures have already reported miniaturised ITP for DNA pre-concentration for the subsequent DNA sizing detected by fluorescence.^{33, 34}

3.1.6 Conclusions and outlooks

In this section, we have demonstrated the use of miniaturised ITP for the simultaneous isolation and purification of nucleic acids from even crude biological samples. When the nucleic acid samples were subjected to miniaturised ITP, they were found to form homogeneous zones where the length of the sample (zone) related to the initial concentration of the nucleic acid in the sample. This is because the nucleic acid zone has a fixed concentration that is governed by the leading electrolytes. Moreover the separation mechanism of ITP also allows it to remove the unwanted components from the complex matrix. These inherent features make miniaturised ITP a promising tool for nucleic acid extraction and preparation as a functional unit for a μ -TAS device for nucleic acid analysis, particularly for PCR amplification, where the DNA sample preparation is a major obstacle. The reported results indicate that it should be possible to use miniaturised ITP for isolation of nucleic acids from complex matrices such as cell lysis products, once adequate combinations of electrolytes are selected and high sensitivity detection are employed. A defined sample plug (volume) from the ITP channel by using another separation process such as CGE will guarantee the number of molecules of DNA entering subsequent analysis such as an invitro amplification process, including PCR. Only the zone of DNA will be isolated from other species which have different effective mobilities when the sample mixture is separated by ITP. Such a feature can greatly benefit the sample preparation process for PCR, since

the efficiency of PCR, which can be compromised by the presence of inhibitors (e.g. heme, lipids, and protein), will be a constant across sample types. (See Figure 3-6)

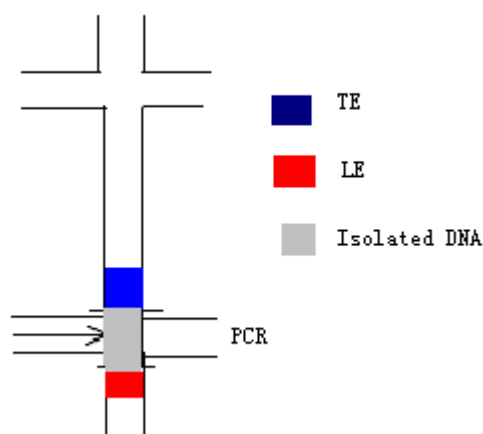


Figure 3-6 Layout of DNA isolation by miniaturised ITP for subsequent PCR

3.2 Miniaturised WGA

For a miniaturised WGA system, several important issues should be taken into consideration, such as the simplicity of thermocycling program, the amplification efficiency, feasibility of real-time detection and the size and fidelity of the amplified products. In this section, we show the results from our miniaturised WGA device, and the important issues mentioned above are discussed. Parallel experiments using conventional instruments for WGA is also performed for comparison.

3.2.1 Denaturation

Although the protocol from the manufacturer recommended an initial denaturation step at 95 °C for the sample mixture, from our study, without this step, the results are equal or even improved compared to those obtained with the denaturation procedure (Figure 3-7), which is in agreement with other reports.^{121, 134} In addition, the omission of the initial denaturation is advantageous for the temperature programming of the microchip-based MDA. Thus we performed both our conventional and on-chip MDA without the initial denature step.

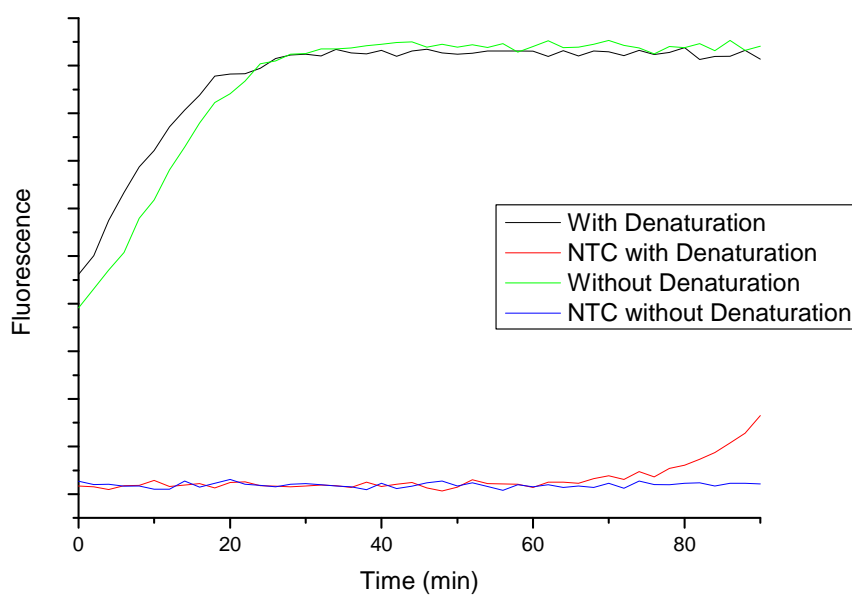


Figure 3-7 Real-time detection of multiple displacement amplification of human genomic DNA using the ABI PRISM HT-7900 machine. 10 ng human genomic DNA as template, $0.1 \times$ SYBR-green I dye. Denaturation: 95 °C for 3 min. Amplification cycle conditions: 30 °C for 90 min, followed by 65 °C for 10 min. Fluorescence intensities were collected via SYBR-green channel every 2 min.

3.2.2 DNA amplification product sizing

The on-chip MDA generated DNA products of 10 kb ~ 40 kb, similar sizes to that of conventional amplified WGA and unamplified genomic DNA, as determined by gel electrophoresis (Figure 3-8). High-molecular-weight amplified DNA products are ideal for DNA library construction and enable genomic sequencing from one or a few cells, in contrast to greater bias in sequence representation of the WGA products obtained using other PCR-based methods where products are only a few hundred base pairs.¹²⁴

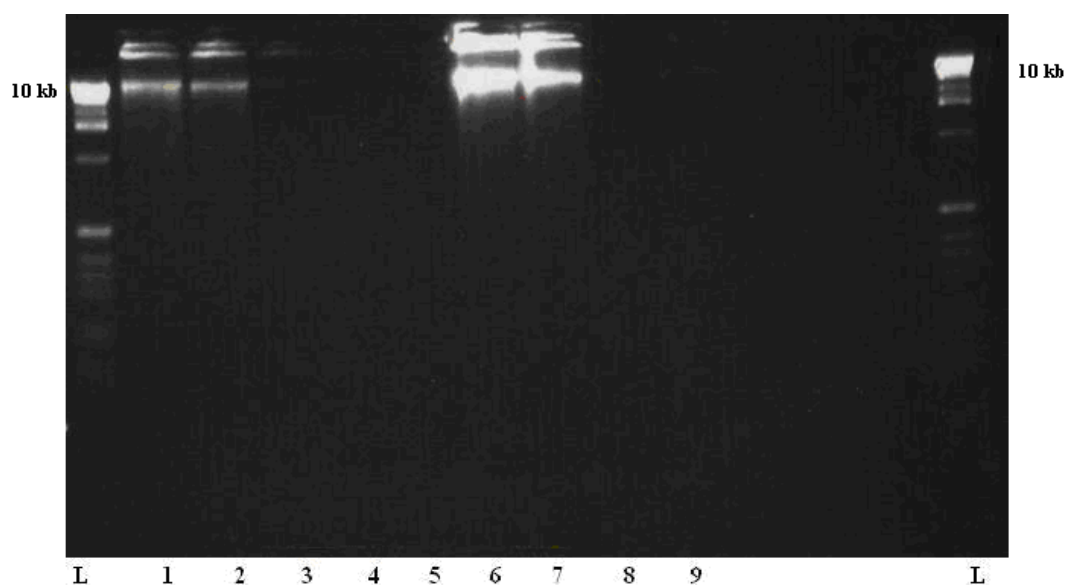
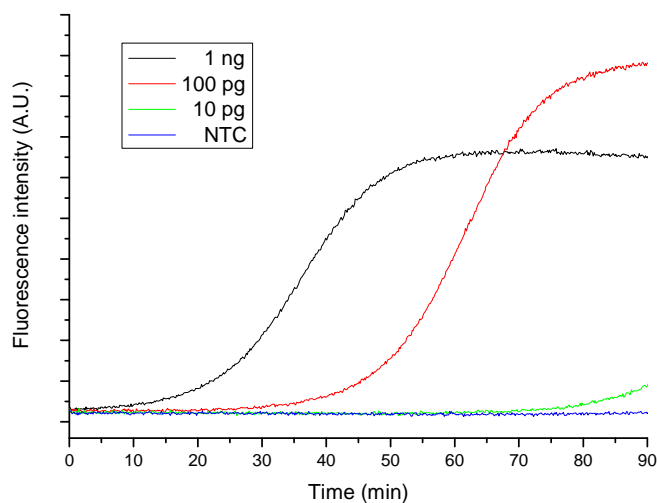


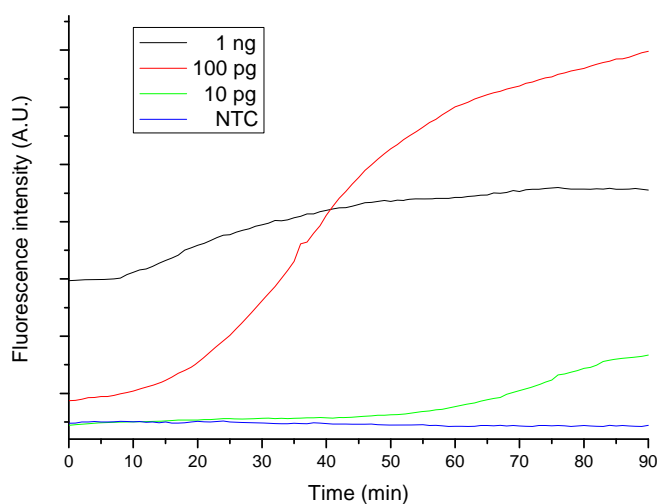
Figure 3-8 Gel electrophoresis analysis of WGA products. Lane L: 1 kb DNA ladder; Lane 1–5: WGA products amplified from the conventional thermocycler with different initial amounts of human genomic DNA. Lane 1: 10 ng; Lane 2: 1 ng; Lane 3: 100 pg, Lane 4: 10 pg; Lane 5: 0; Lane 6-7: WGA products amplified from silanised (Lane 6) and native (Lane 7) PDMS microchip with an initial human genomic DNA amount of 1 ng. Lane 8: NTC WGA product from microchip; Lane 9: unamplified human genomic DNA.

3.2.3 Silanisation effect

Due to surface chemistry, PDMS and glass devices suffer from the adsorption of DNA and enzyme, which is a generally accepted observation in a microchip-based PCR reaction.^{47, 170, 171} Silanisation is a well-established surface modification method to improve DNA amplification efficiency.¹⁵⁶ In our experiment, WGA was performed in both native wells and silanized wells. We observed that the amount of WGA products from native PDMS wells is less than half of that from silanised PDMS wells (see Figure 3-8), which suggests that silanisation is a necessary step to enhance MDA efficiency. Silanised microchips were then used throughout the experiments. (For silanisation effect, also see Section 3.3.3)



(a)



(b)

Figure 3-9 Real-time detection of WGA on (a) conventional real-time PCR machine (ABI PRISM HT 7900) and (b) PDMS microchip.

3.2.4 Real-time monitoring of on-chip MDA

The MDA had an exponential phase like PCR, and the time taken to measurably reach this geometric phase related to the initial template concentration.¹³³ As can be seen from Figure 3-9, the on-chip real-time MDA detection with different initial amount of DNA was in a good agreement with that of the ones performed on conventional

machine. It should be noted, as all conventional PCR, higher concentration of template can cause inhibition to overall amplified products.

3.2.5 Quantitative real-time PCR

The utility of MDA-based WGA products as enriched template for further downstream applications such as real-time PCR was investigated. Compared to unamplified human genomic DNA, the Ct value of chip WGA product was reduced by ~ 8.0 , which corresponds to more than ~ 250 -fold increasing in initial DNA template amount when used as the templates for real-time quantitative PCR detection of RNase P (Figure 3-10). When related to the amplification factor (~ 400 -fold) achieved with conventional WGA, the lower amplification factor (~ 250 -fold) of on-chip WGA is most probably due to the limited reagents (dNTPs and primers) in the 10-fold lower reaction volume, although both started with the same amount of genomic DNA. The specific DNA yields obtained by real-time PCR (chip WGA: 241.6 ± 3.0 ng/ μ L, n = 3; conventional WGA: 428.6 ± 5.4 ng/ μ L, n = 3) and whole DNA concentration by Nanodrop ND 1000 spectrometer (chip WGA: 252.1 ± 3.5 ng/ μ L, n = 3, conventional WGA: 522.0 ± 10.5 ng/ μ L, n = 3) reflect a representation efficiency of 95.8% for on-chip WGA and 82.1% for conventional WGA, respectively. The higher representation efficiency of on-chip WGA product is owing to the reduced reaction volume and the relative high ratio of template in reaction mixture.

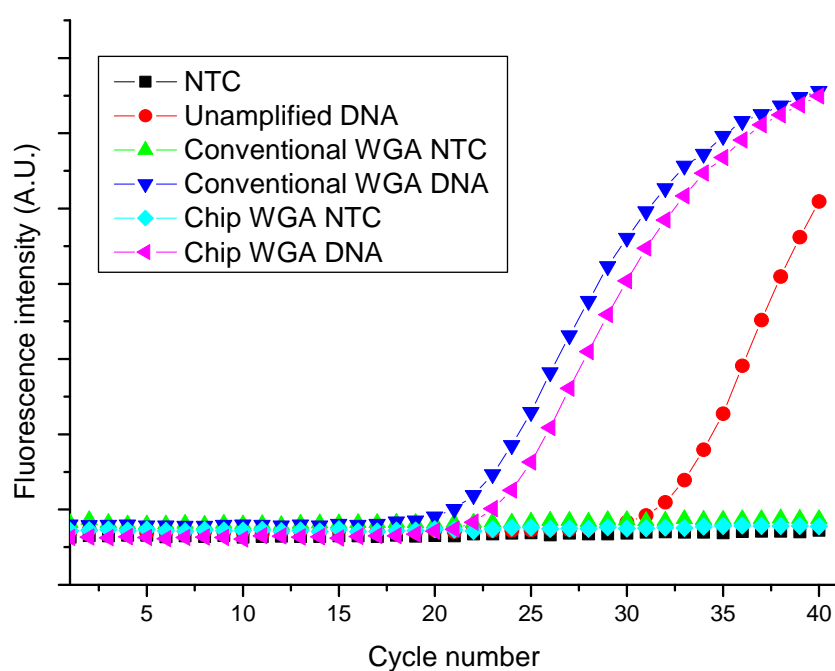


Figure 3-10 Real-time PCR detection of RNase P using 1 μ L template of unamplified genomic DNA (1 ng), 1 μ L conventional WGA product and 1 μ L chip WGA product, respectively. NTC for each sample is run in parallel. Conventional WGA product and chip WGA product are both amplified using 1 ng unamplified genomic DNA as template.

3.2.6 Single-nucleotide polymorphism genotyping

For WGA, the fidelity associated with amplicon synthesis is a critical issue since WGA products must perform similarly to the unamplified genomic samples in subsequent genetic analysis. In this scenario, the sequence information particularly associated with single-nucleotide polymorphisms (SNPs) genotyping presents one of the biggest challenges to WGA. We blind tested samples from both amplified and unamplified genomic DNA from 8 individuals for two SNPs (SNP1: rs2069718, A/G; SNP2: rs13900, C/T). SNP1 was located in the interferon gamma (IFN- γ) gene which is associated with giant cell arthritis (GCA). SNP2 was located in the monocyte chemo-attractant protein (MCP-1) gene which is associated with hepatitis C virus

(HCV) infection. In all 8 cases, on-chip WGA products were correctly genotyped (Table 3-3). It is worthy to note that all the 8 samples and negative control (6 aliquots for each one) were simultaneously amplified on the same chip, indicating that on-chip WGA may offer a high throughput PCR pre-amplification platform for large scale SNP analysis.

Table 3-3 Assays of human genomic samples from 8 individuals for 2 SNPs

Individual	SNP 1	SNP 2
1	A/G	C/C
2	G/G	C/T
3	A/A	C/C
4	G/G	C/T
5	A/G	C/C
6	A/G	C/T
7	G/G	C/T
8	A/G	C/C

3.2.7 Specificity of WGA synthesis

In all experiments for on-chip NTC WGA products, we did not observe any background synthesis and all SNPs analysed showed the correct genotype calling. This was probably due to the reduced reaction volume and increased ratio of template in relation to any reaction components that are responsible or contribute to background.^{172, 173} Therefore, the higher concentration of on-chip amplified DNA and higher representation efficiency of 95.8% compared to 82.1% of conventional WGA can be obtained on miniaturised platforms. This could be a potential advantage of microchip-based MDA for amplifying very small amount of DNA, since the

background synthesis has become a critical issue for MDA reactions,¹⁷⁴ which requires extra screening step to exclude the negative samples.

3.2.7 Conclusions and outlooks

These studies reveal for the first time the use of a microchip device for multiple displacement amplification WGA. The RNase P assay indicated that the level of amplification is approximately 250-fold greater compared to the initial input template genomic DNA when using 2 μ L reaction volume on PDMS microchips. The high representation efficiency of 95.8% reflects a high specificity of the on-chip MDA reaction for amplifying genomic sequences. Moreover, unlike many reports of microfluidic devices in applications related to PCR, where complex thermal control systems are required and only selected regions of DNA samples can be amplified, the use of WGA on-chip has many additional benefits. These relate to a simplified thermal requirement for DNA amplification, the tracking of the reaction, long-term storage and the perpetuation of important patient population cohorts within microfluidic device-based archives.

According to our preliminary experiments, as shown in Figure 3-11, the initial 4 pg human genomic DNA template (equal 1 DNA copy number) has been amplified and verified later with real-time RNase P PCR, indicating that the MDA can be used for amplification of human genomic DNA down to the single copy level.

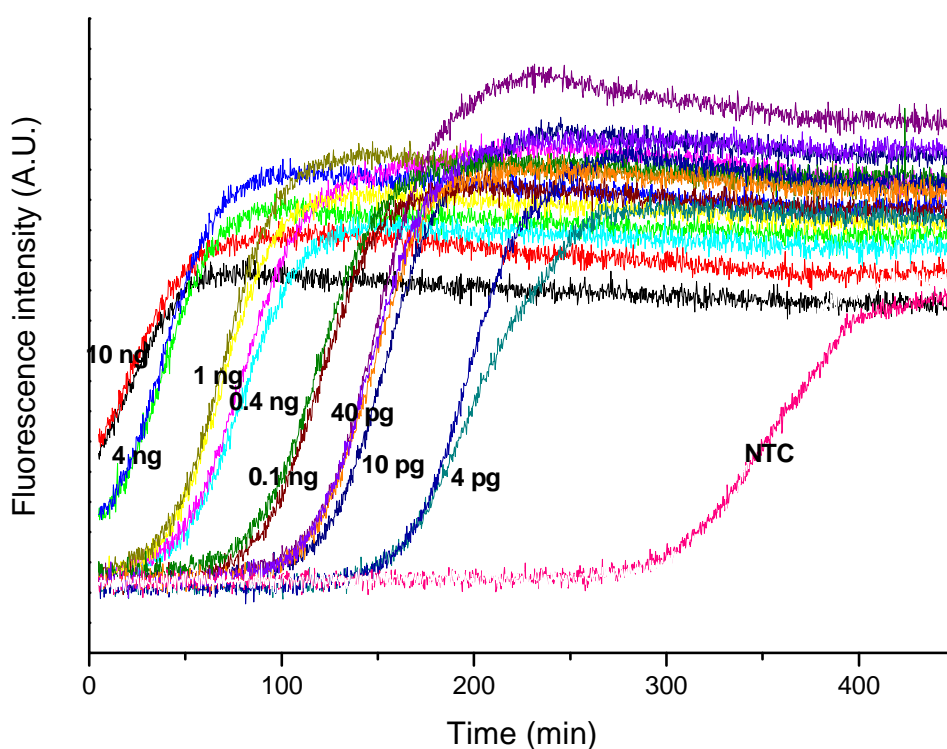


Figure 3-11 Real-time detection of WGA on a conventional real-time PCR machine (ABI PRISM HT 7900) using a series of dilutions from human genomic DNA.

The analyses at single-cell genomic levels will greatly contribute to the understanding of cellular physiopathology, as well as of the evolutionary events acting on single cell genomes. Appropriate areas for application include population genetics, stem cell research, embryology and tissue differentiation, prenatal medicine, detection of early pathological lesions in infections, degenerative and autoimmune diseases.^{133, 137, 175-177} Several problems require the analysis of analysis of individual cells, including preimplantation genetic diagnosis (PGD) for those at risk of transmitting a genetic disorder,^{178, 179} sperm typing for studying recombination rates,¹⁸⁰ and identification of disseminated transformed cells early after surgery of primary tumors.¹⁸¹

Presently, WGA, particularly MDA has become an important and readily available method for genomic studies on single cells due to its unique capability for faithful amplification of tiny quantities of genomic DNA without encountering losses and/or

alteration of the various loci. Moreover, currently there is great interest in single-cell analysis and cell manipulation processes using microfluidic devices. This relates to the small dimensions (10~50 μm) of the channels integrated on the microdevice being similar to those of biological cells, so that they are very suitable for the transport, manipulation and chemical or biochemical treatment of cells.¹⁸²⁻¹⁸⁴ Therefore, the further application of miniaturised WGA devices for single-cell genomic analysis is particularly intriguing. The combination of a miniaturised system and WGA method will greatly facilitate the single cell genomic research, benefiting from the inherent dimensions of miniaturised systems for cell analysis and the ability of WGA amplification of single-copy DNA with extremely high fidelity.

3.3 Bidirectional shunting PCR with real-time detection

3.3.1 Temperature calibration

The actual temperature of the sample plug inside the channel is always not the same as that of the heating block due to temperature losses during thermal transfer, as already described in previous reports.¹⁸⁵⁻¹⁸⁹ Due to the accuracy requirement for temperature control to perform the PCR process, a calibration curve was produced by measuring the temperature of a water plug at the centre of each temperature zone within the shunting apparatus by employing different heating block set temperatures (Figure 3-12). The calibration curve showed that there is a good correlation coefficient between set temperature and the actual temperature ($R = 0.9992$). This correlation is comparable with previous studies.¹⁸⁵⁻¹⁸⁹

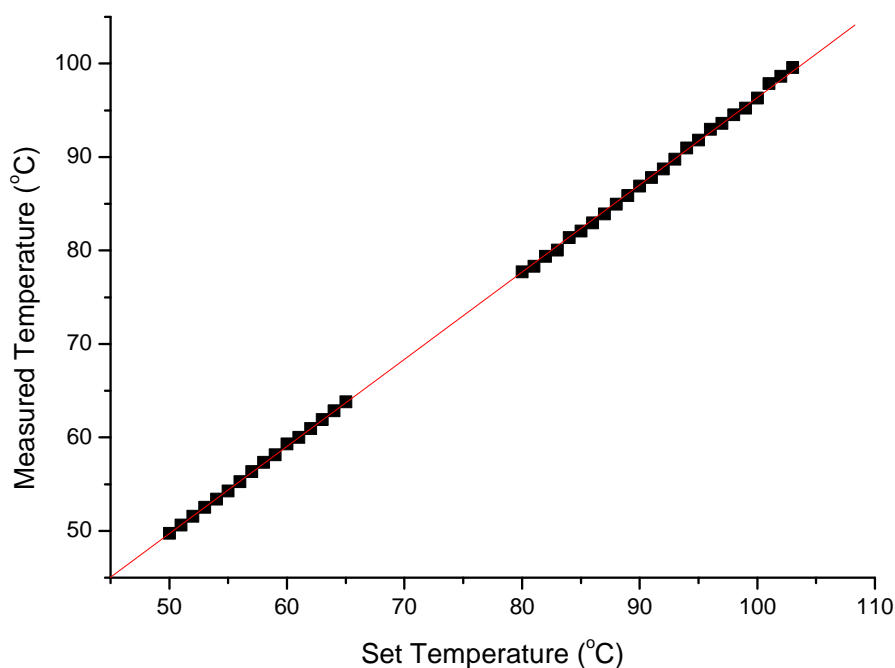


Figure 3-12 Temperature calibration curve of ~ 5 μL water plug in denaturing zone from 80 $^{\circ}\text{C}$ to 105 $^{\circ}\text{C}$ with the other heating block fixed at a set temperature of 61 $^{\circ}\text{C}$, and annealing and extension zone from 50 to 65 $^{\circ}\text{C}$ with the other heating block fixed at a set temperature of 99 $^{\circ}\text{C}$.

Temperature profile along the channel was also recorded by measuring the temperature inside a water plug (~ 5 μL) after it was moved every millimetre along the glass capillary (see Figure 3-13). The temperature profile indicated that the centre of each temperature zone was homogeneous and at a higher temperature, compared to the edges of each zone that possessed a lower temperature due to the thermal loss. A ~ 30 $^{\circ}\text{C}$ drop was found across the 4 mm distance between two temperature zones, which will facilitate the fast thermal exchanging between sample and the miniaturised thermal system.

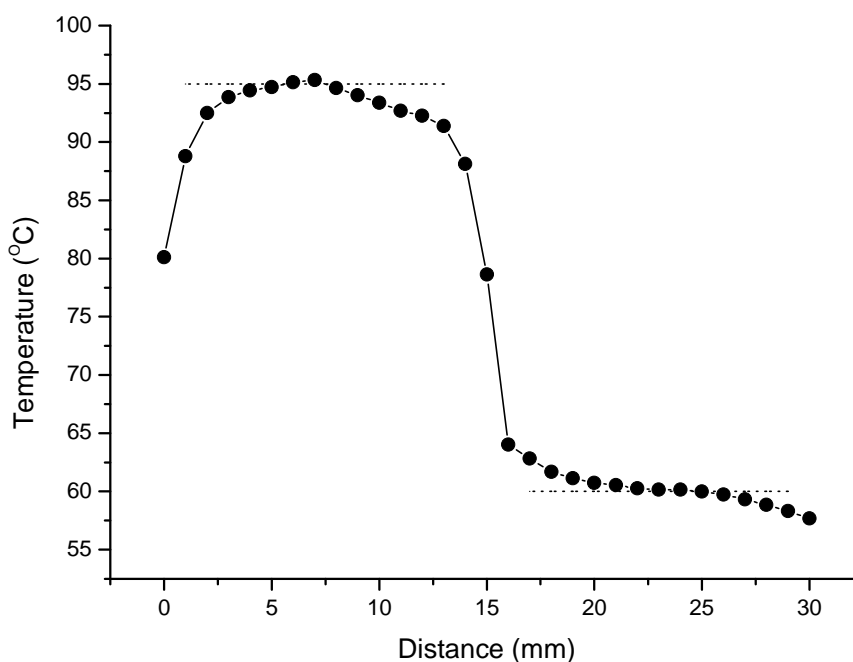


Figure 3-13 Temperature profile of $\sim 5 \mu\text{L}$ water plug moving along the glass capillary over the two temperature zones with the two block temperatures set at 99°C and 61°C , respectively.

3.3.2 Bidirectional Thermocycling

A typical image of bidirectional shunting thermocycling in a glass capillary is shown in Figure 3-14, with image enhancement by using a thermo-sensitive dye (Blue 69°C Slurry, Thermographic Measurements Ltd, UK), which is dark blue when the temperature is below 69°C and becomes transparent when temperature exceeds 69°C . A colour change and precise positioning of the dye plug illustrated our bidirectional shunting device is capable of performing fast thermocycling.

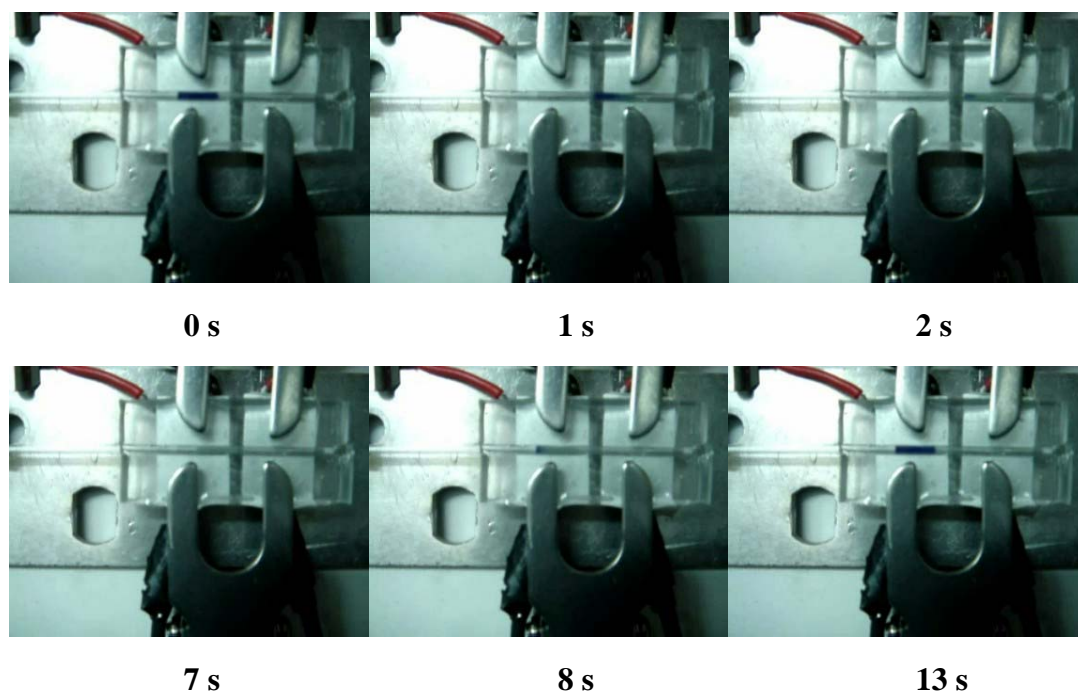
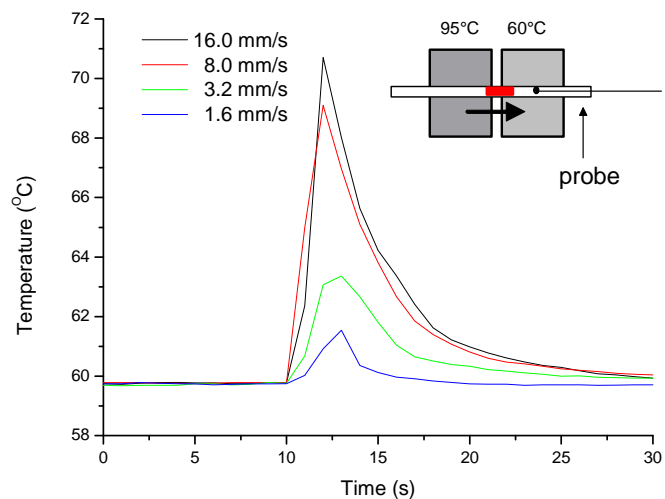


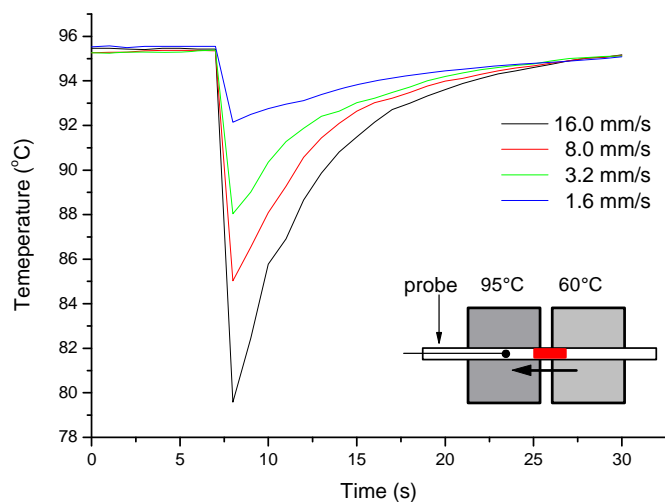
Figure 3-14 Photographs of shunting thermo-sensitive dye (Blue 69 °C Slurry, Thermographic Measurements Ltd, UK) between 95 °C (right) and 60 °C (left) where the dye transitions from colourless to blue respectively, under a velocity of 16 mm s⁻¹.

To determine the temperature transition time for a sample in the shunting apparatus, a thermocouple (thermister) was inserted into the capillary and the temperature offset was used to determine Peltier element temperatures required to achieve the desired 60 °C and 95 °C reaction temperature zones. The design of the shunting PCR apparatus places Peltier elements in close contact via aluminium heat sinks that aid temperature stability. However, these do not represent an infinite thermal mass and the arrival of the liquid causes transient temperature perturbations. The extent of perturbation is influenced by transport velocity, and is shown in Figure 3-15 for liquid samples arriving at the 60°C zone (a) and the 95°C (b) for velocities ranging from 16.0 mm s⁻¹ to 1.6 mm s⁻¹. High velocities do not enable sufficient heat exchange during transport between temperature zones and result in $\geq 10^\circ\text{C}$ temperature corruption requiring ~ 10 s before desirable reaction temperatures are attained. Operating at the lower 1.6 mm s⁻¹ velocity does not cause significant perturbation, and with a zone-to-zone transport time of 10 s. Considering the turbulence inside an oil-sample-oil sandwiched plug that

may caused by high shunting velocity, all our bidirectional shunting PCR experiments were performed using 1.6 mm s^{-1} velocity.



(a)



(b)

Figure 3-15 Temperature perturbations caused by the transport of a $5 \mu\text{L}$ water plug moving from $95 \text{ }^\circ\text{C}$ to $60 \text{ }^\circ\text{C}$ (a) and from $60 \text{ }^\circ\text{C}$ to $95 \text{ }^\circ\text{C}$ (b) for flow velocities ranging from 16.0 mm s^{-1} to 1.6 mm s^{-1} .

The thermal mass of the plug at these relatively milli-scale dimensions and a cylindrical reaction system both retard heat exchange. A flat and shallow channel is greatly preferred when heat transfer behaviour is considered;

$$Q = \kappa A(T^\circ C) / d$$

where Q is the heat transfer, κ is the thermal conductivity, A the temperature exchange area and d the thickness of the interface. With miniaturisation to a 100 nL reaction volume of 1 mm in length within a channel 100 μm deep and 1 mm width vastly improved heat exchange can be achieved for rapid thermal ramping and with a faster reaction times. With the envisaged extraordinarily fast temperature responses higher reaction selectivity and thus sensitivity was predicted. However, this study highlighted the inhibitory effects of the entire internal surface area, and requirements for further advances in reaction protection are anticipated.

3.3.3 Silanisation surface modification

The high surface area to volume ratios and non-polypropylene materials of miniaturised PCR are well known to cause reaction fouling by sequestering the activity of *Taq* polymerase and other reaction components. Previous studies in this Ph.D study (see Section 3.2.3) demonstrated the important enabling contribution that can be made by silanisation. With static mode reactors this problem can be considerably ameliorated by coating the chamber surfaces with hydrophobic silanes, typically methylated chlorosilanes.¹⁹⁰ The silanisation of continuous flow microchannels only partially promotes PCR effectiveness, with moderate amplicon yields from high template inputs.¹⁵⁷ In these examples, the reagents are mobilized along a microchannel of considerable length, such that the complete surface area that the small volume of reagents is exposed to throughout the reaction is enormous (often 2 metres in length). The surface area is greatly reduced with the bidirectional millifluidic device and the use of a glass capillary provides the preferred SiO_x surface environment. However, silanisation of the capillary with DMDCS to present a

hydrophobic surface with a 1 μL sessile water droplet contact angle of $\sim 105^\circ$ was insufficient to prevent reaction inhibition.

Chemical additives are commonly used to improve reaction efficiency and reduce reaction inhibition. Protein adsorption on silica surfaces can be inhibited using PVP.^{191, 192} The use of high molecular weight PVP at a concentration of 0.4% has been used for the dynamic (*i.e.* during the reaction) passivation of surfaces to enable efficient PCR in a PDMS microreactor. However, higher concentrations resulted in reaction inhibition. In this study, 0.01% PVP was used to obtain modest reaction efficiency (22% relative to the positive control) in a silanised capillary. Both dynamic and static passivation with BSA is a popular choice to render surfaces PCR-compatible.^{157, 193} By the further addition of 0.2 $\mu\text{g } \mu\text{L}^{-1}$ BSA as well as 0.1% (v/v) Tween 20, amplification of the RNase P mimic template was found to be 84% as efficient when compared to the conventional thermocycling instrument. Use of these additives in isolation was not effective, indicating the requirement for using the additives in concert.

Successive shuttling PCR reactions fail as the silane monolayer is disrupted by thermocycling temperatures in the presence of the reaction buffer, and re-silanisation is required to restore biocompatibility prior to subsequent runs.^{164, 190} These reports are corroborated by our duplicated results which are documented in Figure 3-16a. Here amplicons produced using a conventional thermocycler are compared with those produced by bidirectional flow PCR with a fresh silane layer and those without re-silanisation following a prior PCR run.

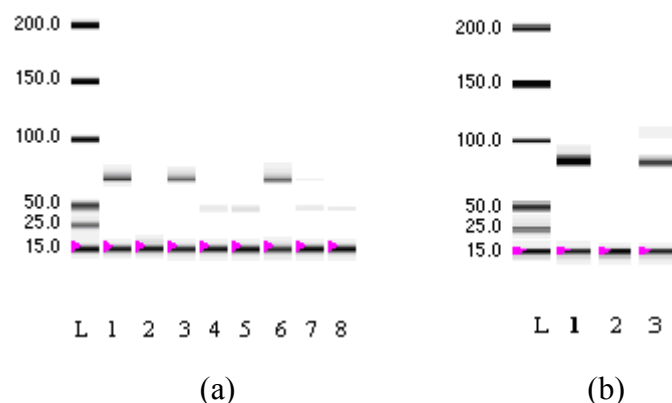


Figure 3-16 Microchip gel electrophoresis images. (a) Silanisation effect on shunting PCR products: Lane L: DNA ladder; Lane 1: positive control; Lane 2: No template control (NTC); Lane 3-5: shunting PCR on silanised chip used once then reused a second and third time respectively; Lane 6-8: shunting PCR on a re-silanised chip used once and then reused a second and third time respectively. (b) PCR products of human genomic DNA. Lane L: DNA Ladder; Lane 1; positive control; Lane 2: NTC, Lane 3: shunting PCR product.

3.3.4 Real-time PCR of human genomic DNA

We evaluated the ability to achieve bidirectional microfluidic amplification from real-world human genomic template inputs. The size of the RNase P PCR product was defined by microchip gel electrophoresis, which is the same as the product obtained from commercial PCR instrument (see Figure 3-16b).

Real-time PCR on the bidirectional shunting device was performed for detection of RNase P using a series of diluted human genomic DNA template (24000, 2400, 240, and 24 copies number). Sequences for the RNase P primers are shown in section 2.3.3. A parallel experiment was performed using conventional real-time machine (ABI 7900 HT). The raw data from our experiments consisted of 40 spikes in fluorescence intensity, corresponding to the passing of sample plug at the fixed detection point after the extension stage. At the beginning, the spikes in fluorescence intensity are due to the scattering of light from the boundary of sample plug and

mineral oil. The increasing in fluorescence intensity later on is mainly due to the increasing of released FAM dye, which corresponds to the formation of RNase P products as the PCR proceeds (see Figure 3-17).

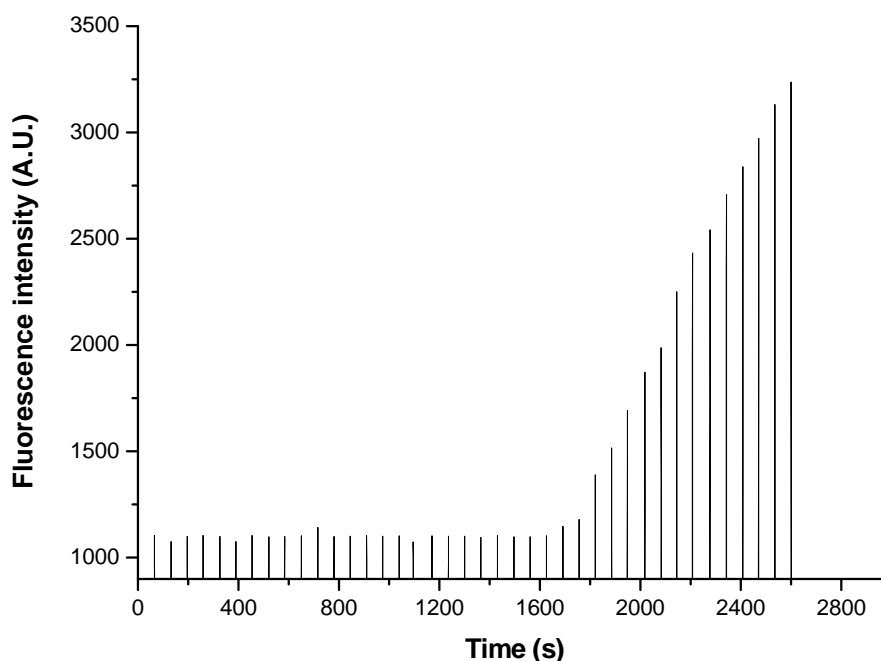


Figure 3-17 Real-time fluorescence detection of bidirectional shunting PCR using 2400 copies number human genomic DNA as template. The thermocycling program consisted of 10 min at 95 °C, followed by 40 cycles of 15 s at 95 °C zone and 60 s at 60 °C zone. The shunting velocity for sample plug is 1.6 mm s⁻¹.

In order to check whether our system was suitable for Ct determination and practical application for quantification of unknown sample, the peak height of each spike was normalized to the individual background and then plotted, as shown in Figure 3-18. For each curve, a baseline and a line for the exponential stage were drawn using linear fit function (OriginPro 7.0). The Ct value of each curve was defined as the intercept of these lines. The Ct values obtained by both conventional machine and bidirectional shunting PCR using different starting human genomic DNA template were plotted in Figure 3-19 for comparison.

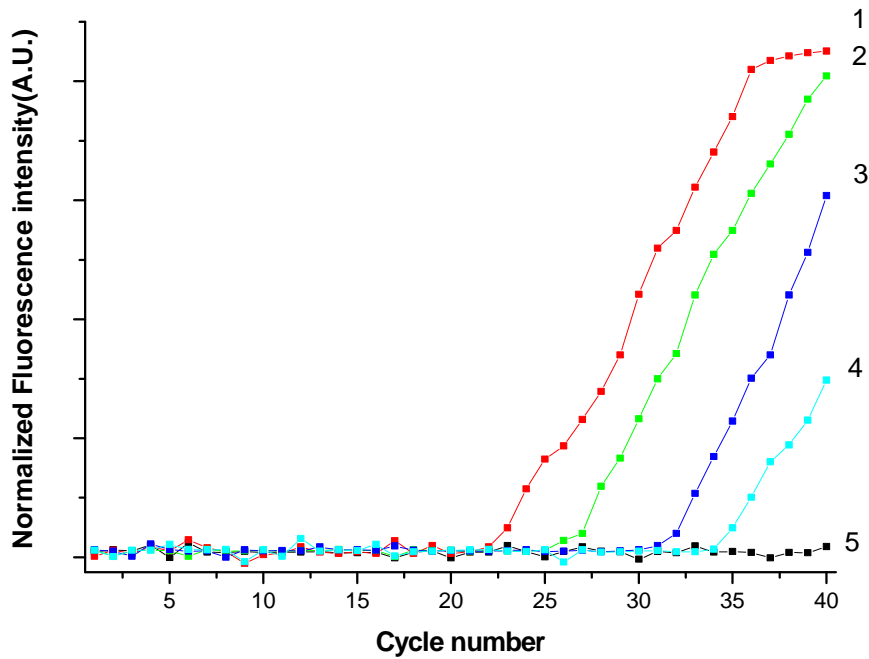


Figure 3-18 Real-time PCR on bidirectional shunting device for detection of RNase P using a human genomic DNA dilution series. 1-5 represent copies number of 24000, 2400, 240, 24 and NTC respectively.

In practice, the concentration of DNA molecules at the threshold can be approximated by the following equation:

$$C_T = C_0 \times (1 + x)^{C_t}$$

Where C_T and C_0 represent the concentration of PCR products after t cycles and initial concentration respectively, and x is the efficiency of the PCR reaction. Equation 2 can be written in another way as

$$C_t = - [\text{Log}(1 + x)]^{-1} \cdot (\text{Log}C_0 + \text{Log} C_T)$$

Since the concentration that achieve threshold level is always constant, Eq. (2) can be further written as

$$C_t = m \text{Log}C_0 + b$$

where $m = - [\text{Log}(1 + x)]^{-1}$ and $b = - [\text{Log}(1 + x)]^{-1} \cdot \text{Log } C_T$, thus C_t value is proportional to the logarithm of initial DNA template concentration. Linear regression of the C_t vs. $\text{Log} C_0$ yields a slope of m of -3.51 for the conventional instrument and -4.04 for the bidirectional shunting PCR reactor. These values can be used to calculate the PCR efficiency x :¹⁵²

$$x = 10^{-1/m} - 1$$

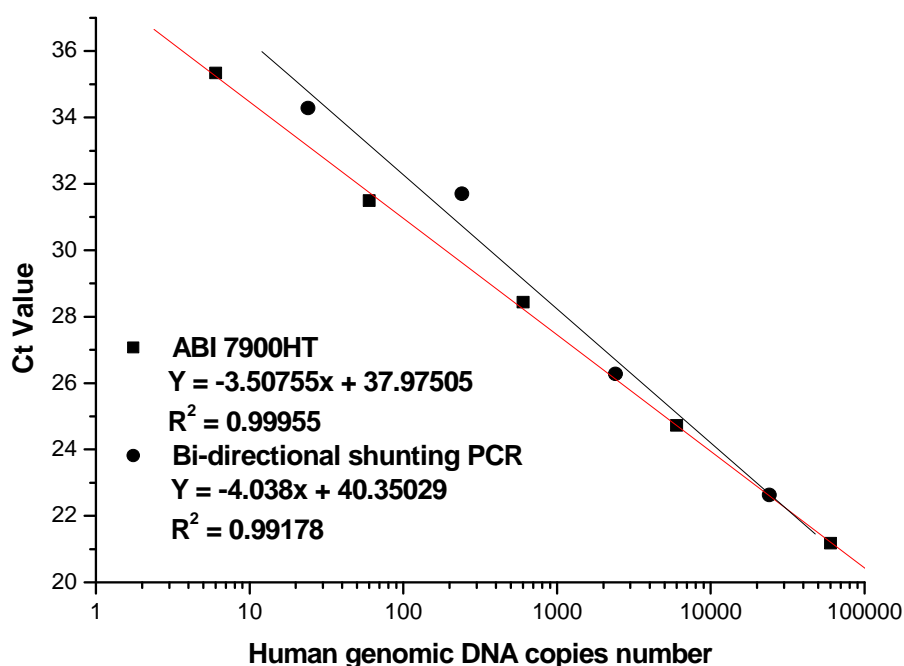


Figure 3-19 C_t value vs the logarithm of the initial DNA copies number using conventional real-time PCR instrument (ABI 7900HT) and bidirectional shunting PCR, respectively.

Following the equation for calculation of real-time PCR efficiency mentioned above, the PCR reaction efficiency was calculated to be 92.7% and 77.0% for conventional instrument and bidirectional shunting PCR, respectively. The correlation coefficient for bidirectional shunting PCR was 0.998, indicating that real-time detection data provided accurate information of the initial DNA template concentrations, together with a high dynamic range of five orders of magnitude.

The efficiency of bidirectional shunting PCR was about ~15% lower than that of the conventional machine, which is mainly due to the high surface-to-volume ratio and surface inhibition during silanisation and dynamic coating. With further scaling-down and optimization of the device such as changes to channel dimension, better surface-to-volume ratio and improved surface modification, the total running time can be expected to be greatly reduced, and the PCR efficiency improved to hopefully reach single gene/transcript copy number level detection.

3.3.5 Conclusions and outlooks

A novel method for fast DNA amplification with bidirectional shunting of an aqueous reaction plug through two different fixed temperature zones has been demonstrated in this chapter. The presented device combines the advantages of both stationary and continuous-flow PCR, offering rapid heat exchange for fast temperature ramping, and the flexibility of cycle ramping and reaction vessel characteristics for use with most thermocycling applications. The total reaction time can be readily reduced by using miniaturisation in the micrometer scale, which is well-developed. Real-time monitoring of successful RNase P amplification of human genomic DNA down to ~24 copies has been achieved after hydrophobic surface modification and the use of chemical additives. The current milli-scale device is ripe for miniaturisation for ultra-fast processing times and quantitative nucleic acids analysis. Furthermore, the features of our device such as small size, automation and ease of sample manipulation makes itself ready to be integrated into miniaturised nucleic acid analyses.

Another key aspect of miniaturization is the ability to undertake reactions in parallel. This is important for many reasons including the co-amplification of a standard curve for comparative target copy quantification, and enhanced reproducibility seen with use of batch runs. Many laboratory-based applications require high throughput capabilities. For example, multilayer soft lithography was used for 72 RT-PCRs,¹⁹⁴ which was shortly followed by a massively parallel (14,112 simultaneous reactions)

format for the multi-gene analysis of environmental bacteria.¹⁹⁵ As demonstrated by Frey *et al* with a 10 channel system, the linear channel of the bidirectional reactor can also readily be parallelized.¹⁹⁶ For laboratory based implementation the key driver will be to standardize interfaces for compatibility with existing fluid handling and optical detection formats.

The current device can also be easily coupled with previously described miniaturised ITP and WGA to form a fully integrated device (see Section 1-4). The nucleic acid samples can be purified, pre-concentrated, amplified and detected in a seamless channel with capability of sample-in, answer-out, which ultimately can serve as a prototype for point-of-care devices. (see Figure 1-14)

Chapter 4

Conclusions

This thesis reports the findings of three miniaturised systems for nucleic acids purification and pre-concentration, whole genomic DNA amplification and real-time detection of bidirectional shunting PCR.

The first miniaturised system employs isotachopheresis (ITP) for nucleic acid pre-treatment. When the nucleic acid samples are subjected to miniaturised ITP, they were found to form homogeneous zones whose length related to the initial concentrations. This is because these ITP derived nucleic acid zone has a fixed concentration governed by the concentration of buffer electrolytes. Moreover the separation mechanism of ITP also allows the removal of unwanted components from a complex matrix through Careful selection of leading and trailing buffer ion mobility. The concentrating effect of miniaturised ITP was wholly apparent for both DNA and total RNA. These inherent features make miniaturised ITP a promising tool for nucleic acid extraction and preparation as a functional unit for a μ -TAS device for nucleic acid analysis, particularly for PCR amplification, where the DNA sample preparation is a major obstacle. Current results and know how indicate that it should be possible to use miniaturised ITP system for isolation of nucleic acids from complex matrices such as cell lysis products, once adequate electrolytes are selected and high sensitivity detection is employed.

The second miniaturised system reveals for the first time the use of a microchip device for multiple displacement amplification WGA. The RNase P assay indicated that the level of amplification produces close to approximately 250-fold increase compared to the initial input template genomic DNA when using 2 μ L reaction volume on PDMS microchips. The high representation efficiency of 95.8% reflects a high specificity of the on-chip multiple displacement amplification of genomic

sequences. Unlike many reports of microfluidic devices in applications of PCR, the use of WGA on-chip has a great many additional benefits that relate to the tracking, long-term storage and the perpetuation of samples from important patient and population cohorts. The fidelity of the polymerase appears to be maintained and is extremely high as suggested by the perfect analysis score of SNPs which reflect the actual sequences unveiled by conventional SNP-based PCRs.

For the third miniaturised system, a novel method for fast DNA amplification with bidirectional shunting of a reaction plug through different temperature zones has been demonstrated. The presented device combines the advantages of both stationary and continuous-flow PCR, offering rapid heat exchange for fast temperature ramping, and flexibility of cycle characteristics (including dwell time, change of temperature, online monitoring of fluorescence) for use with all thermocycling applications. Real-time monitoring of successful RNase P amplification of human genomic DNA down to ~24 copies has been achieved after hydrophobic surface modification and the use of chemical additives. The current milli-scale device is ripe for further miniaturisation for ultra-fast processing times and quantitative nucleic acids analysis. Furthermore, the features of our device such as small size, automation and ease of sample manipulation make it readily suited to integration into miniaturised nucleic acid analysis platforms. Another key aspect of miniaturisation is the ability to undertake reactions in parallel. When compared to typically convoluted-channel PCR devices, our linear channel as used for the bidirectional reactor can be more readily parallelized. For laboratory based implementation the key step will be to standardize interfaces for compatibility with existing fluid handling and optical detection formats.

The current three miniaturised systems are ready for integration into total nucleic acid analysis microfluidic devices, where genomic DNA purification from biological samples by ITP, pre-amplification by whole genome amplification and subsequent real-time detection of PCR amplified specific gene regions are performed in a seamless and continuous fashion (see Figure 1-14). Such a nucleic acid μ -TAS device

will greatly facilitate absolute quantification of nucleic acids for in-vitro diagnostics and point-of-care applications.

References

- (1) Manz, A.; Miyahara, Y.; Miura, J.; Watanabe, Y.; Miyagi, H.; Sato, K. *Sensors and Actuators B-Chemical* **1990**, *1*, 249-255.
- (2) Manz, A.; Harrison, D. J.; Verpoorte, E. M. J.; Fettinger, J. C.; Paulus, A.; Ludi, H.; Widmer, H. M. *Journal of Chromatography* **1992**, *593*, 253-258.
- (3) Manz, A.; Verpoorte, E.; Effenhauser, C. S.; Burggraf, N.; Raymond, D. E.; Harrison, D. J.; Widmer, H. M. *Hrc-Journal of High Resolution Chromatography* **1993**, *16*, 433-436.
- (4) Manz, A.; Verpoorte, E.; Effenhauser, C. S.; Burggraf, N.; Raymond, D. E.; Widmer, H. M. *Fresenius Journal of Analytical Chemistry* **1994**, *348*, 567-571.
- (5) Manz, A.; Harrison, D. J.; Verpoorte, E.; Widmer, H. M. *Advances in Chromatography* **1993**, *33*, 1-66.
- (6) Harrison, D. J.; Fluri, K.; Seiler, K.; Fan, Z. H.; Effenhauser, C. S.; Manz, A. *Science* **1993**, *261*, 895-897.
- (7) Harrison, D. J.; Glavina, P. G.; Manz, A. *Sensors and Actuators B-Chemical* **1993**, *10*, 107-116.
- (8) Manz, A.; Effenhauser, C. S.; Burggraf, N.; Harrison, D. J.; Seiler, K.; Fluri, K. *Journal of Micromechanics and Microengineering* **1994**, *4*, 257-265.
- (9) Manz, A.; Effenhauser, C. S.; Burggraf, N.; Verpoorte, E.; Raymond, D. E.; Widmer, H. M. *Analisis* **1994**, *22*, M25-M28.
- (10) Jacobson, S. C.; Hergenroder, R.; Koutny, L. B.; Warmack, R. J.; Ramsey, J. M. *Analytical Chemistry* **1994**, *66*, 1107.
- (11) Woolley, A. T.; Mathies, R. A. *Analytical Chemistry* **1995**, *68*, 4081.
- (12) Woolley, A. T.; Hadley, D.; Landre, P.; deMello, A. J.; Mathies, R. A.; Northrup, M. A. *Analytical Chemistry* **1996**, *69*, 1355.
- (13) Li, P. C. H.; Harrison, D. J. *Analytical Chemistry* **1997**, *69*, 1564-1568.
- (14) McCormick, R. M.; Nelson, R. J.; Alonso-Amigo, M. G.; Benvegna, D. J.; Hooper, H. H. *Analytical Chemistry* **1997**, *69*, 2626.

- (15) Duffy, D. C.; McDonald, J. C.; Schueller, O. J. A.; Whitesides, G. M. *Anal. Chem.* **1998**, *70*, 4974-4984.
- (16) Roberts, M. A.; Rossier, J. S.; Bercier, P.; Girault, H. *Analytical Chemistry* **1997**, *69*, 2035.
- (17) Kopp, M. U.; de Mello, A. J.; Manz, A. *Science* **1998**, *280*, 1046-1048.
- (18) Woolley, A. T.; Lao, K.; Glazer, A. N.; Mathies, R. A. *Analytical Chemistry* **1998**, *71*, 566.
- (19) Medintz, I.; Wong, W. W.; Berti, L.; Shiow, L.; Tom, J.; Scherer, J.; Sensabaugh, G.; Mathies, R. A. *Genome Research* **2001**, *11*, 413.
- (20) Emrich, C. A.; Tian, H.; Medintz, I. L.; Mathies, R. A. *Analytical Chemistry* **2002**, *74*, 5092.
- (21) Unger, M. A.; Chou, H. P.; Thorsen, T.; Scherer, A.; Quake, S. R. *Science* **2000**, *288*, 113-116.
- (22) Easley, C. J.; Karlinsey, J. M.; Bienvenue, J. M.; Legendre, L. A.; Roper, M. G.; Feldman, S. H.; Hughes, M. A.; Hewlett, E. L.; Merkel, T. J.; Ferrance, J. P.; Landers, J. P. *Proc Natl Acad Sci U S A* **2006**, *103*, 19272-19277.
- (23) Auroux, P. A.; Iossifidis, D.; Reyes, D. R.; Manz, A. *Anal Chem* **2002**, *74*, 2637-2652.
- (24) Reyes, D. R.; Iossifidis, D.; Auroux, P. A.; Manz, A. *Anal Chem* **2002**, *74*, 2623-2636.
- (25) Vilkner, T.; Janasek, D.; Manz, A. *Anal Chem* **2004**, *76*, 3373-3385.
- (26) Dittrich, P. S.; Tachikawa, K.; Manz, A. *Anal Chem* **2006**, *78*, 3887-3908.
- (27) Sia, S. K.; Whitesides, G. M. *Electrophoresis* **2003**, *24*, 3563-3576.
- (28) McDonald, J. C.; Whitesides, G. M. *Acc Chem Res* **2002**, *35*, 491-499.
- (29) McDonald, J. C.; Duffy, D. C.; Anderson, J. R.; Chiu, D. T.; Wu, H.; Schueller, O. J.; Whitesides, G. M. *Electrophoresis* **2000**, *21*, 27-40.
- (30) Erickson, D.; Li, D. Q. *Analytica Chimica Acta* **2004**, *507*, 11-26.
- (31) Ng, J. M. K.; Gitlin, I.; Stroock, A. D.; Whitesides, G. M. *Electrophoresis* **2002**, *23*, 3461-3473.
- (32) Lichtenberg, J.; de Rooij, N. F.; Verpoorte, E. *Talanta* **2002**, *56*, 233-266.

- (33) Wainright, A.; Williams, S. J.; Ciambrone, G.; Xue, Q. F.; Wei, J.; Harris, D. *Journal of Chromatography A* **2002**, *979*, 69-80.
- (34) Wainright, A.; Nguyen, U. T.; Bjornson, T.; Boone, T. D. *Electrophoresis* **2003**, *24*, 3784-3792.
- (35) Grass, B.; Hergenroder, R.; Neyer, A.; Siepe, D. *Journal of Separation Science* **2002**, *25*, 135-140.
- (36) Grass, B.; Neyer, A.; Johnck, M.; Siepe, D.; Eisenbeiss, F.; Weber, G.; Hergenroder, R. *Sensors and Actuators B-Chemical* **2001**, *72*, 249-258.
- (37) Underberg, W. J.; Waterval, J. C. *Electrophoresis* **2002**, *23*, 3922-3933.
- (38) Waterval, J. C.; Lingeman, H.; Bult, A.; Underberg, W. J. *Electrophoresis* **2000**, *21*, 4029-4045.
- (39) Bardelmeijer, H. A.; Waterval, J. C.; Lingeman, H.; van't Hof, R.; Bult, A.; Underberg, W. J. *Electrophoresis* **1997**, *18*, 2214-2227.
- (40) Pittman, J. L.; Gessner, H. J.; Frederick, K. A.; Raby, E. M.; Batts, J. B.; Gilman, S. D. *Anal Chem* **2003**, *75*, 3531-3538.
- (41) Effenhauser, C. S.; Manz, A.; Widmer, H. M. *Analytical Chemistry* **1995**, *67*, 2284-2287.
- (42) Righetti, P. G.; Gelfi, C.; D'Acunto, M. R. *Electrophoresis* **2002**, *23*, 1361-1374.
- (43) Osbourn, D. M.; Weiss, D. J.; Lunte, C. E. *Electrophoresis* **2000**, *21*, 2768-2779.
- (44) Fritz, J. S. *J Chromatogr A* **2000**, *884*, 261-275.
- (45) Lion, N.; Rohner, T. C.; Dayon, L.; Arnaud, I. L.; Damoc, E.; Youhnovski, N.; Wu, Z. Y.; Roussel, C.; Josserand, J.; Jensen, H.; Rossier, J. S.; Przybylski, M.; Girault, H. H. *Electrophoresis* **2003**, *24*, 3533-3562.
- (46) Zhang, C. S.; Xu, J. L.; Ma, W. L.; Zheng, W. L. *Biotechnology Advances* **2006**, *24*, 243-284.
- (47) Auroux, P. A.; Koc, Y.; deMello, A.; Manz, A.; Day, P. J. R. *Lab on a Chip* **2004**, *4*, 534-546.
- (48) Szantai, E.; Guttman, A. *Electrophoresis* **2006**, *27*, 4896-4903.

- (49) Situma, C.; Hashimoto, M.; Soper, S. A. *Biomolecular Engineering* **2006**, *23*, 213-231.
- (50) Mastrangelo, C. H.; Burns, M. A.; Burke, D. T. *Proceedings of the Ieee* **1998**, *86*, 1769-1787.
- (51) Chen, L.; Ren, J. C. *Combinatorial Chemistry & High Throughput Screening* **2004**, *7*, 29-43.
- (52) Taddeo, B.; Esclatine, A.; Zhang, W.; Roizman, B. *Journal of Virology* **2003**, *77*, 6178.
- (53) Khandurina, J.; Guttman, A. *Journal of Chromatography A* **2002**, *943*, 159-183.
- (54) Liu, S. R.; Guttman, A. *Trac-Trends in Analytical Chemistry* **2004**, *23*, 422-431.
- (55) Verpoorte, E. *Electrophoresis* **2002**, *23*, 677-712.
- (56) Lacher, N. A.; Garrison, K. E.; Martin, R. S.; Lunte, S. M. *Electrophoresis* **2001**, *22*, 2526-2536.
- (57) Dolnik, V. *Electrophoresis* **2006**, *27*, 126-141.
- (58) Dolnik, V.; Liu, S. R. *Journal of Separation Science* **2005**, *28*, 1994-2009.
- (59) Shi, X. Q.; Liang, H.; Fan, J. *Chinese Journal of Analytical Chemistry* **2005**, *33*, 735-739.
- (60) Kasicka, V. *Electrophoresis* **2001**, *22*, 4139-4162.
- (61) Woolley, A. T.; Mathies, R. A. *Anal Chem* **1995**, *67*, 3676-3680.
- (62) Paegel, B. M.; Emrich, C. A.; Wedemayer, G. J.; Scherer, J. R.; Mathies, R. A. *Proc Natl Acad Sci U S A* **2002**, *99*, 574-579.
- (63) Woolley, A. T.; Sensabaugh, G. F.; Mathies, R. A. *Anal Chem* **1997**, *69*, 2181-2186.
- (64) Medintz, I.; Wong, W. W.; Sensabaugh, G.; Mathies, R. A. *Electrophoresis* **2000**, *21*, 2352-2358.
- (65) Tian, H.; Emrich, C. A.; Scherer, J. R.; Mathies, R. A.; Andersen, P. S.; Larsen, L. A.; Christiansen, M. *Electrophoresis* **2005**, *26*, 1834-1842.

- (66) Stachowiak, T. B.; Svec, F.; Frechet, J. M. J. *Journal of Chromatography A* **2004**, *1044*, 97-111.
- (67) Bandilla, D.; Skinner, C. D. *Journal of Chromatography A* **2004**, *1044*, 113-129.
- (68) Chen, L.; Prest, J. E.; Fielden, P. R.; Goddard, N. J.; Manz, A.; Day, P. J. R. *Lab on a Chip* **2006**, *6*, 474-487.
- (69) Mogensen, K. B.; Klank, H.; Kutter, J. P. *Electrophoresis* **2004**, *25*, 3498-3512.
- (70) Vandaveer, W. R.; Pasas-Farmer, S. A.; Fischer, D. J.; Frankenfeld, C. N.; Lunte, S. M. *Electrophoresis* **2004**, *25*, 3528-3549.
- (71) Uchiyama, K.; Nakajima, H.; Hobo, T. *Analytical and Bioanalytical Chemistry* **2004**, *379*, 375-382.
- (72) Gotz, S.; Karst, U. *Analytical and Bioanalytical Chemistry* **2007**, *387*, 183-192.
- (73) Viskari, P. J.; Landers, J. P. *Electrophoresis* **2006**, *27*, 1797-1810.
- (74) Cesaro-Tadic, S.; Dernick, G.; Juncker, D.; Buurman, G.; Kropshofer, H.; Michel, B.; Fattinger, C.; Delamarque, E. *Lab Chip* **2004**, *4*, 563-569.
- (75) Ueno, Y.; Tate, A.; Niwa, O.; Zhou, H. S.; Yamada, T.; Honma, I. *Anal Bioanal Chem* **2005**, *382*, 804-809.
- (76) Wang, S. L.; Fan, X. F.; Xu, Z. R.; Fang, Z. L. *Electrophoresis* **2005**, *26*, 3602-3608.
- (77) Lee, S.; Choi, J.; Chen, L.; Park, B.; Kyong, J. B.; Seong, G. H.; Choo, J.; Lee, Y.; Shin, K. H.; Lee, E. K.; Joo, S. W.; Lee, K. H. *Anal Chim Acta* **2007**, *590*, 139-144.
- (78) Jung, J.; Chen, L.; Lee, S.; Kim, S.; Seong, G. H.; Choo, J.; Lee, E. K.; Oh, C. H.; Lee, S. *Anal Bioanal Chem* **2007**, *387*, 2609-2615.
- (79) Liu, J.; Williams, B. A.; Gwartz, R. M.; Wold, B. J.; Quake, S. *Angew Chem Int Ed Engl* **2006**, *45*, 3618-3623.
- (80) Studer, V.; Pepin, A.; Chen, Y.; Ajdari, A. *Analyst* **2004**, *129*, 944-949.
- (81) Liu, R. H. *Conf Proc IEEE Eng Med Biol Soc* **2004**, *7*, 5394.

- (82) Lee, S. H.; Lee, C. S.; Kim, B. G.; Kim, Y. K. *Biomed Microdevices* **2007**.
- (83) Ramsey, J. D.; Collins, G. E. *Anal Chem* **2005**, *77*, 6664-6670.
- (84) Dittrich, P. S.; Schwille, P. *Anal Chem* **2003**, *75*, 5767-5774.
- (85) Jiang, Y.; Wang, P. C.; Locascio, L. E.; Lee, C. S. *Anal Chem* **2001**, *73*, 2048-2053.
- (86) Gustafsson, M.; Hirschberg, D.; Palmberg, C.; Jornvall, H.; Bergman, T. *Anal Chem* **2004**, *76*, 345-350.
- (87) Kamei, T.; Paegel, B. M.; Scherer, J. R.; Skelley, A. M.; Street, R. A.; Mathies, R. A. *Anal Chem* **2003**, *75*, 5300-5305.
- (88) Roman, G. T.; Kennedy, R. T. *J Chromatogr A* **2007**, *1168*, 170-188; discussion 169.
- (89) Du, W. B.; Fang, Q.; He, Q. H.; Fang, Z. L. *Anal Chem* **2005**, *77*, 1330-1337.
- (90) Young, S. M.; Curry, M. S.; Ransom, J. T.; Ballesteros, J. A.; Prossnitz, E. R.; Sklar, L. A.; Edwards, B. S. *J Biomol Screen* **2004**, *9*, 103-111.
- (91) Kartalov, E. P.; Zhong, J. F.; Scherer, A.; Quake, S. R.; Taylor, C. R.; Anderson, W. F. *Biotechniques* **2006**, *40*, 85-90.
- (92) Yakovleva, J.; Davidsson, R.; Lobanova, A.; Bengtsson, M.; Eremin, S.; Laurell, T.; Emneus, J. *Anal Chem* **2002**, *74*, 2994-3004.
- (93) Lv, Y.; Zhang, Z.; Chen, F. *Analyst* **2002**, *127*, 1176-1179.
- (94) Yan, J.; Yang, X.; Wang, E. *Anal Bioanal Chem* **2005**, *381*, 48-50.
- (95) Schwarz, M. A.; Hauser, P. C. *Lab Chip* **2001**, *1*, 1-6.
- (96) Koster, S.; Verpoorte, E. *Lab Chip* **2007**, *7*, 1394-1412.
- (97) Fortier, M. H.; Bonneil, E.; Goodley, P.; Thibault, P. *Anal Chem* **2005**, *77*, 1631-1640.
- (98) Sung, W. C.; Makamba, H.; Chen, S. H. *Electrophoresis* **2005**, *26*, 1783-1791.
- (99) Park, T.; Lee, S.; Seong, G. H.; Choo, J.; Lee, E. K.; Kim, Y. S.; Ji, W. H.; Hwang, S. Y.; Gweon, D. G.; Lee, S. *Lab Chip* **2005**, *5*, 437-442.
- (100) Wensink, H.; Benito-Lopez, F.; Hermes, D. C.; Verboom, W.; Gardeniers, H. J.; Reinhoudt, D. N.; van den Berg, A. *Lab Chip* **2005**, *5*, 280-284.

- (101) Kricka, L. J.; Wilding, P. *Analytical And Bioanalytical Chemistry* **2003**, *377*, 820-825.
- (102) Roper, M. G.; Easley, C. J.; Landers, J. P. *Analytical Chemistry* **2005**, *77*, 3887-3893.
- (103) Day, P. J. *Expert Rev Mol Diagn* **2006**, *6*, 23-28.
- (104) Olvecka, E.; Masar, M.; Kaniansky, D.; Johnck, M.; Stanislawski, B. *Electrophoresis* **2001**, *22*, 3347-3353.
- (105) Prest, J. E.; Baldock, S. J.; Fielden, P. R.; Goddard, N. J.; Brown, B. J. T. *Analyst* **2002**, *127*, 1413-1419.
- (106) Baldock, S. J.; Fielden, P. R.; Goddard, N. J.; Prest, J. E.; Brown, B. J. T. *Journal of Chromatography A* **2003**, *990*, 11-22.
- (107) Prest, J. E.; Baldock, S. J.; Fielden, P. R.; Goddard, N. J.; Brown, B. J. T. *Journal of Chromatography A* **2003**, *990*, 325-334.
- (108) Kriikku, P.; Grass, B.; Hokkanen, A.; Stuns, I.; Siren, H. *Electrophoresis* **2004**, *25*, 1687-1694.
- (109) Prest, J. E.; Baldock, S. J.; Fielden, P. R.; Goddard, N. J.; Kalimeri, K.; Brown, B. J. T.; Zraggen, M. *Journal of Chromatography A* **2004**, *1047*, 289-298.
- (110) Xu, Z. Q.; Hirokawa, T.; Nishine, T.; Arai, A. *Journal of Chromatography A* **2003**, *990*, 53-61.
- (111) Vreeland, W. N.; Williams, S. J.; Barron, A. E.; Sassi, A. P. *Analytical Chemistry* **2003**, *75*, 3059-3065.
- (112) Kaniansky, D.; Masar, M.; Bodor, R.; Zuborova, M.; Olvecka, E.; Johnck, M.; Stanislawski, B. *Electrophoresis* **2003**, *24*, 2208-2227.
- (113) Gebauer, P.; Bocek, P. *Electrophoresis* **1997**, *18*, 2154-2161.
- (114) Gebauer, P.; Bocek, P. *Electrophoresis* **2000**, *21*, 3898-3904.
- (115) Gebauer, P.; Bocek, P. *Electrophoresis* **2002**, *23*, 3858-3864.
- (116) Zhang, L.; Cui, X.; Schmitt, K.; Hubert, R.; Navidi, W.; Arnheim, N. *Proc Natl Acad Sci U S A* **1992**, *89*, 5847-5851.

- (117) Telenius, H.; Carter, N. P.; Bebb, C. E.; Nordenskjold, M.; Ponder, B. A.; Tunnacliffe, A. *Genomics* **1992**, *13*, 718-725.
- (118) Dietmaier, W.; Hartmann, A.; Wallinger, S.; Heinmoller, E.; Kerner, T.; Endl, E.; Jauch, K. W.; Hofstadter, F.; Ruschoff, J. *Am J Pathol* **1999**, *154*, 83-95.
- (119) Xu, K.; Tang, Y.; Grifo, J. A.; Rosenwaks, Z.; Cohen, J. *Hum Reprod* **1993**, *8*, 2206-2210.
- (120) Sermon, K.; Lissens, W.; Joris, H.; Van Steirteghem, A.; Liebaers, I. *Mol Hum Reprod* **1996**, *2*, 209-212.
- (121) Dean, F. B.; Hosono, S.; Fang, L.; Wu, X.; Faruqi, A. F.; Bray-Ward, P.; Sun, Z.; Zong, Q.; Du, Y.; Du, J.; Driscoll, M.; Song, W.; Kingsmore, S. F.; Egholm, M.; Lasken, R. S. *Proc Natl Acad Sci U S A* **2002**, *99*, 5261-5266.
- (122) Jiao, Z. X.; Zhuang, G. L.; Zhou, C. Q.; Shu, Y. M.; Liang, X. Y.; Li, J.; Zhang, M. F.; Deng, M. F. *Zhonghua Yi Xue Za Zhi* **2003**, *83*, 298-301.
- (123) Kittler, R.; Stoneking, M.; Kayser, M. *Anal Biochem* **2002**, *300*, 237-244.
- (124) Lovmar, L.; Syvanen, A. C. *Hum Mutat* **2006**, *27*, 603-614.
- (125) Hawkins, T. L.; Detter, J. C.; Richardson, P. M. *Curr Opin Biotechnol* **2002**, *13*, 65-67.
- (126) Hughes, S.; Arneson, N.; Done, S.; Squire, J. *Prog Biophys Mol Biol* **2005**, *88*, 173-189.
- (127) Hosono, S.; Faruqi, A. F.; Dean, F. B.; Du, Y.; Sun, Z.; Wu, X.; Du, J.; Kingsmore, S. F.; Egholm, M.; Lasken, R. S. *Genome Res* **2003**, *13*, 954-964.
- (128) Yan, J.; Feng, J.; Hosono, S.; Sommer, S. S. *Biotechniques* **2004**, *37*, 136-138, 140-133.
- (129) Bergen, A. W.; Haque, K. A.; Qi, Y.; Beerman, M. B.; Garcia-Closas, M.; Rothman, N.; Chanock, S. J. *Hum Mutat* **2005**, *26*, 262-270.
- (130) Esteban, J. A.; Salas, M.; Blanco, L. *J Biol Chem* **1993**, *268*, 2719-2726.
- (131) Nelson, J. R.; Cai, Y. C.; Giesler, T. L.; Farchaus, J. W.; Sundaram, S. T.; Ortiz-Rivera, M.; Hosta, L. P.; Hewitt, P. L.; Mamone, J. A.; Palaniappan, C.; Fuller, C. W. *Biotechniques* **2002**, *Suppl*, 44-47.

- (132) Gonzalez, J. M.; Portillo, M. C.; Saiz-Jimenez, C. *Environ Microbiol* **2005**, *7*, 1024-1028.
- (133) Zhang, K.; Martiny, A. C.; Reppas, N. B.; Barry, K. W.; Malek, J.; Chisholm, S. W.; Church, G. M. *Nat Biotechnol* **2006**, *24*, 680-686.
- (134) Spits, C.; Le Caignec, C.; De Rycke, M.; Van Haute, L.; Van Steirteghem, A.; Liebaers, I.; Sermon, K. *Hum Mutat* **2006**, *27*, 496-503.
- (135) Monstein, H. J.; Olsson, C.; Nilsson, I.; Grahn, N.; Benoni, C.; Ahrne, S. *J Microbiol Methods* **2005**, *63*, 239-247.
- (136) Nilsson, I.; Shabo, I.; Svanvik, J.; Monstein, H. J. *Helicobacter* **2005**, *10*, 592-600.
- (137) Coskun, S.; Alsmadi, O. *Prenat Diagn* **2007**, *27*, 297-302.
- (138) Carret, C. K.; Horrocks, P.; Konfortov, B.; Winzeler, E.; Qureshi, M.; Newbold, C.; Ivens, A. *Mol Biochem Parasitol* **2005**, *144*, 177-186.
- (139) Jane, Ka, J. E.; Grassman, L. I.; Derr, J. N.; Honeycutt, R. L.; Eiadthong, W.; Tewes, M. E. *Wildlife Society Bulletin* **2006**, *34*, 1134-1141.
- (140) Cheng, J.; Waters, L. C.; Fortina, P.; Hvichia, G.; Jacobson, S. C.; Ramsey, J. M.; Kricka, L. J.; Wilding, P. *Anal Biochem* **1998**, *257*, 101-106.
- (141) Auroux, P. A.; Koc, Y.; deMello, A.; Manz, A.; Day, P. J. *Lab Chip* **2004**, *4*, 534-546.
- (142) Saiki, R. K.; Bugawan, T. L.; Horn, G. T.; Mullis, K. B.; Erlich, H. A. *Nature* **1986**, *324*, 163-166.
- (143) Arya, M.; Shergill, I. S.; Williamson, M.; Gommersall, L.; Arya, N.; Patel, H. R. *Expert Rev Mol Diagn* **2005**, *5*, 209-219.
- (144) Kaltenboeck, B.; Wang, C. *Adv Clin Chem* **2005**, *40*, 219-259.
- (145) Schefe, J. H.; Lehmann, K. E.; Buschmann, I. R.; Unger, T.; Funke-Kaiser, H. *J Mol Med* **2006**, *84*, 901-910.
- (146) Suzuki, N.; Yoshida, A.; Nakano, Y. *Clin Med Res* **2005**, *3*, 176-185.
- (147) Belak, S. *Acta Vet Hung* **2005**, *53*, 113-124.
- (148) Lewin, S. R.; Vesanen, M.; Kostrikis, L.; Hurley, A.; Duran, M.; Zhang, L.; Ho, D. D.; Markowitz, M. *J Virol* **1999**, *73*, 6099-6103.

- (149) Jebbink, J.; Bai, X.; Rogers, B. B.; Dawson, D. B.; Scheuermann, R. H.; Domiati-Saad, R. *J Mol Diagn* **2003**, *5*, 15-20.
- (150) Mhlanga, M. M.; Malmberg, L. *Methods* **2001**, *25*, 463-471.
- (151) Pierce, K. E.; Rice, J. E.; Sanchez, J. A.; Brenner, C.; Wangh, L. J. *Mol Hum Reprod* **2000**, *6*, 1155-1164.
- (152) Wang, Z.; Sekulovic, A.; Kutter, J. P.; Bang, D. D.; Wolff, A. *Electrophoresis* **2006**, *27*, 5051-5058.
- (153) Cady, N. C.; Stelick, S.; Kunnavakkam, M. V.; Batt, C. A. *Sensors And Actuators B-Chemical* **2005**, *107*, 332-341.
- (154) Xiang, Q.; Xu, B.; Fu, R.; Li, D. *Biomedical Microdevices* **2005**, *7*, 273-279.
- (155) Hu, G. Q.; Xiang, Q.; Fu, R.; Xu, B.; Venditti, R.; Li, D. Q. *Analytica Chimica Acta* **2006**, *557*, 146-151.
- (156) Kopp, M. U.; Mello, A. J.; Manz, A. *Science* **1998**, *280*, 1046-1048.
- (157) Obeid, P. J.; Christopoulos, T. K.; Crabtree, H. J.; Backhouse, C. J. *Anal Chem* **2003**, *75*, 288-295.
- (158) West, J.; Karamata, B.; Lillis, B.; Gleeson, J. P.; Alderman, J.; Collins, J. K.; Lane, W.; Mathewson, A.; Berney, H. *Lab Chip* **2002**, *2*, 224-230.
- (159) Liu, J.; Enzelberger, M.; Quake, S. *Electrophoresis* **2002**, *23*, 1531-1536.
- (160) Frey, O.; Bonneick, S.; Hierlemann, A.; Lichtenberg, J. *Biomed Microdevices* **2007**.
- (161) Chiou, J.; Matsudaira, P.; Sonin, A.; Ehrlich, D. *Anal Chem* **2001**, *73*, 2018-2021.
- (162) Nakayama, T.; Kurosawa, Y.; Furui, S.; Kerman, K.; Kobayashi, M.; Rao, S. R.; Yonezawa, Y.; Nakano, K.; Hino, A.; Yamamura, S.; Takamura, Y.; Tamiya, E. *Anal Bioanal Chem* **2006**, *386*, 1327-1333.
- (163) Prest, J. E.; Baldock, S. J.; Fielden, P. R.; Goddard, N. J.; Brown, B. J. *Analyst* **2003**, *128*, 1131-1136.
- (164) Prakash, R.; Kaler, K. *Microfluidics And Nanofluidics* **2007**, *3*, 177-187.
- (165) Gebauer, P.; Bocek, P. *Electrophoresis* **2002**, *23*, 3858-3864.
- (166) Gebauer, P.; Bocek, P. *Electrophoresis* **2000**, *21*, 3898-3904.

- (167) Chen, L.; Prest, J. E.; Fielden, P. R.; Goddard, N. J.; Manz, A.; Day, P. J. *Lab Chip* **2006**, *6*, 474-487.
- (168) Xu, Z. Q.; Nishine, T.; Arai, A.; Hirokawa, T. *Electrophoresis* **2004**, *25*, 3875-3881.
- (169) de Mello, A. J.; Beard, N. *Lab on a Chip* **2003**, *3*, 11n-19n.
- (170) Zhang, C.; Xu, J.; Ma, W.; Zheng, W. *Biotechnology Advances* **2006**, *24*, 243.
- (171) Kricka, L. J.; Wilding, P. *Analytical and Bioanalytical Chemistry* **2003**, 377, 820.
- (172) Hutchison, C. A., 3rd; Smith, H. O.; Pfannkoch, C.; Venter, J. C. *Proc Natl Acad Sci U S A* **2005**, *102*, 17332-17336.
- (173) Hutchison, C. A., 3rd; Venter, J. C. *Nat Biotechnol* **2006**, *24*, 657-658.
- (174) Lasken, R. S.; Stockwell, T. B. *BMC Biotechnol* **2007**, *7*, 19.
- (175) Hanson, E. K.; Ballantyne, J. *Anal Biochem* **2005**, *346*, 246-257.
- (176) Panelli, S.; Damiani, G.; Espen, L.; Micheli, G.; Sgaramella, V. *Gene* **2006**, *372*, 1-7.
- (177) Spits, C.; Le Caignec, C.; De Rycke, M.; Van Haute, L.; Van Steirteghem, A.; Liebaers, I.; Sermon, K. *Nat Protoc* **2006**, *1*, 1965-1970.
- (178) Schowalter, K. V.; Fredrickson, J.; Thornhill, A. R. *Methods Mol Med* **2007**, *132*, 87-99.
- (179) Hellani, A.; Coskun, S.; Benkhalifa, M.; Tbakhi, A.; Sakati, N.; Al-Odaib, A.; Ozand, P. *Mol Hum Reprod* **2004**, *10*, 847-852.
- (180) Jiang, Z.; Zhang, X.; Deka, R.; Jin, L. *Nucleic Acids Res* **2005**, *33*, e91.
- (181) Gangnus, R.; Langer, S.; Breit, E.; Pantel, K.; Speicher, M. R. *Clin Cancer Res* **2004**, *10*, 3457-3464.
- (182) Andersson, H.; van den Berg, A. *Sensors and Actuators B-Chemical* **2003**, *92*, 315-325.
- (183) Sims, C. E.; Allbritton, N. L. *Lab Chip* **2007**, *7*, 423-440.
- (184) El-Ali, J.; Sorger, P. K.; Jensen, K. F. *Nature* **2006**, *442*, 403-411.
- (185) Roper, M. G.; Easley, C. J.; Legendre, L. A.; Humphrey, J. A.; Landers, J. P. *Anal Chem* **2007**, *79*, 1294-1300.

- (186) Seger-Sauli, U.; Panayiotou, M.; Schnydrig, S.; Jordan, M.; Renaud, P. *Electrophoresis* **2005**, *26*, 2239-2246.
- (187) de Mello, A. J.; Habgood, M.; Lancaster, N. L.; Welton, T.; Wootton, R. C. *Lab Chip* **2004**, *4*, 417-419.
- (188) Mao, H.; Yang, T.; Cremer, P. S. *J Am Chem Soc* **2002**, *124*, 4432-4435.
- (189) Ross, D.; Gaitan, M.; Locascio, L. E. *Anal Chem* **2001**, *73*, 4117-4123.
- (190) Felbel, J.; Bieber, I.; Pipper, J.; Kohler, J. M. *Chemical Engineering Journal* **2004**, *101*, 333-338.
- (191) Robinson, S.; Williams, P. A. *Langmuir* **2002**, *18*, 8743-8748.
- (192) Giordano, B. C.; Copeland, E. R.; Landers, J. P. *Electrophoresis* **2001**, *22*, 334-340.
- (193) Koh, C. G.; Tan, W.; Zhao, M. Q.; Ricco, A. J.; Fan, Z. H. *Analytical Chemistry* **2003**, *75*, 4591-4598.
- (194) Marcus, J. S.; Anderson, W. F.; Quake, S. R. *Analytical Chemistry* **2006**, *78*, 956-958.
- (195) Ottesen, E. A.; Hong, J. W.; Quake, S. R.; Leadbetter, J. R. *Science* **2006**, *314*, 1464-1467.
- (196) Frey, O.; Bonneick, S.; Hierlemann, A.; Lichtenberg, J. *Biomed Microdevices* **2007**, *9*, 711-718.

Acknowledgments

There are so many people I need to thank for helping me get through the most challenging period in my life.

I would like to express my gratitude to my supervisors, Prof. Dr. Andreas Manz and Prof. Dr. Philip Day for giving me the opportunity to do my Ph.D. study here and providing all the supports that I need. They always bring up some great ideas and make sure that I am on the right track.

I would like to thank Dr. Jonathan West for his helpful suggestion and helping with language polishing. Additionally, I would like to thank Dr. Norbert Jakubowski, Rolf Brandt, Beate Boebersen for helping me accustomed to German environment. I also would like to thank Ingo Feldmann for helpful discussion, helping me finding reagents and equipments, and being my photographer.

I am grateful to Dr. Aleksandra, Polatajko, Dr. Petra Dittrich, Dr. Dirk Janasek, Lindsay Maccoux, Melissa Mariani, Jean-Philippe Frimat, Venkatachalam Arunachalam, Ying Cai, Helke Reinhardt, Sebastian Lohse, Claus Schumann for their helpful discussions.

I would like to thank Prof. Peter Fielden, Dr. Prest Jeff and Dr. Sara Baldock from University of Manchester for providing the access to their facilities and useful suggestions regarding ITP work.

I want to thank my wife Han Lu for her unconditional support. She always make me sure that there's a delicious meal and a sweet home after hard working.

Lastly, I thank my parents for their support for the past twenty-eight years.

Curriculum Vitae

Name: Lin Chen

Gender: Male

Year and place of birth: 1978, Shanghai, P.R. China.

Address: Dessauer Str. 28, 44263, Dortmund.

Tel: 0049-231-1392145; **Fax:** 0049-231-1392120

E-mail: chenlin119@yahoo.com

Languages: Chinese (native), English (fluent), German (limited)

Education

Ph.D. **Biochemical Engineering** (2004.06 – 2007.09)

University of Dortmund, Germany

Advisor: Prof. Andreas Manz and Prof. Philip J. Day

M. Eng. **Applied Chemistry** (2001.09 – 2004.03)

College of Chemistry and Chemical Engineering

Shanghai Jiao Tong University, Shanghai, P.R. China

Advisor: Prof. Jicun Ren

B. Eng. **Applied Chemistry** (1997.09 – 2001.06)

College of Chemistry and Chemical Engineering

Shanghai Jiao Tong University, Shanghai, P.R. China

Advisor: Prof. Qinghua Meng and Prof. Deying Huang